An Investigation of the Morphological and Mechanical Properties of Cancellous Bone in Rheumatoid Arthritis and Osteoarthritis of the Hip.

by

Anke Breckon

Submitted to the University of Cape Town in partial fulfilment of the requirements for the degree of Master of Science in Medicine, in Biomedical Sciences.

June 1993

I, Anke Breckon hereby declare that the work on which this thesis is based is my original work (except where acknowledgements indicate otherwise) and that neither the whole work nor any part of it has been, is being or is to be submitted for another degree in this or any other University.

I empower the university to reproduce for the purpose of research either the whole or any portion of the contents in any manner whatsoever.

Signed .....

SIGNATURE

30 June 1993 .....

DATE

ABSTRACT

Disease and aging are known to affect the mechanical properties and morphology of cancellous bone. Rheumatoid Arthritis is believed to be associated with generalised osteoporosis and periarticular bone rarefaction. Osteoarthritis of the Hip is believed to be associated with densification of the cancellous bone. The aim of this study was to determine the properties and mechanical relationships of cancellous bone for these two conditions, both of which frequently require joint replacement surgery.

Femoral heads obtained during Total Hip Replacement Arthroplasty for RA and OA were used. The sample included 10 female RA, 12 female and 10 male OA femoral heads. Morphological and mechanical parameters of bone specimens from the principal weight bearing region of these femoral heads were investigated. The experimental techniques included Dual Energy X-Ray Absorptiometry, Compression Testing and Morphometry using an Automated Image Analysis System. A number of variables were measured for each specimen, including: Apparent and Bone Mineral Density, Strength, Young's Modulus and Strain Energy Density. The trabecular thickness, spacing and surface area density were also measured in the subchondral region and in the region of the compressive trabeculae, of each femoral head.

Compressive strength and Young's Modulus demonstrated strong power relationships with both apparent and bone mineral densities. The structure of the cancellous bone was not uniform throughout the femoral heads, the degree of structural orientation was found to increase from the subchondral region to the compressive trabeculae. This phenomenon was found to affect the above mentioned relationships. Strain Energy Density also correlated positively with apparent density. Gender was found to have an effect on the mean values found for the densities and

mechanical properties, the values were always greater in males than in females (in the OA group). However the mean body mass of the male group was significantly greater than that of the female group. Morphometry revealed that **Osteoarthritis** of the Hip is not necessarily associated with very dense cancellous bone in all individuals. The Trabecular Bone Volume Fraction in the subchondral region differed greatly between patients. In certain individuals the subchondral bone was very dense and well connected, in others the bone in this region was of a very low density, with thin, poorly connected trabeculae. A small group of individuals had subchondral bone of intermediate density. **Rheumatoid Arthritis** was associated with very dense bone with an irregular structure in the subchondral region, suggesting collapse and remodelling of the bone. In the region of the principal compressive trabeculae the results varied greatly in RA, indicating that some individuals within this group had an inadequate bone structure in this region; evidence that this condition can be associated with osteoporosis.

Knowledge of the ranges and mean values of the mechanical and morphological variables measured in this study, and the exact nature of their inter-relationships will allow better understanding and prediction of bone properties in Rheumatoid Arhtritis and Osteoarthritis of the Hip. Qualitative interpretation of the results may be of value to clinicians involved in the management of patients with these conditions, while bioengineers involved in endoprosthesis research may be interested in the quantitative aspects of our findings.

ACKNOWLEDGEMENTS

I would like to express my sincere gratitude to:

Mr A. Spirakis and Professor I.D. Learmonth for supervision and guidance throughout this project.

Prof. T. Sewell and Mr D. Gerneke for assistance with the Image Analysis System.

Prof. G. Nurick for assistance and guidance with the mechanical testing of the bone cubes.

Mrs M. Levey for the many hours spent preparing the bone specimens for the making of microscope sections.

Mrs D. Choice for her assistance with Dual Energy X-Ray Absorptiometry.

Dr M L. Thompson for her help and guidance in doing the statistical analysis of the results, and Dr R. Bridger for his help in analysing the results of the preliminary experiment.

Mr M. Price for his assistance in the construction of the jigs and various parts used in the experiments.

Dr C. Breckon for his assistance with compression testing of the bone cubes.

Sr F. Schreuder for her help in collecting the femoral heads post Total Hip Replacement Surgery.

TABLE OF CONTENTS

		Page
ABSTRACT		iii
ACKNOWLEDGEMENTS		v
TABLE OF CONTENTS		vi
LIST OF ILLUSTRATIONS		ix
LIST OF TABLES		xiv
GLOSSARY		xv
NOMENCLATURE		xvii
CHAPTER 1: INTRODUCTION		
1.1	The Problem and Rationale for the Study	1
CHAPTER 2: BACKGROUND		
2.1	Anatomy of the Hip Joint and Proximal Femur	4
2.2	Hip Joint : Movements and Forces	8
2.3	Rheumatoid and Osteoarthritis of the Hip	11
CHAPTER 3: REVIEW OF RELATED LITERATURE		
3.1	Background: Cancellous Bone Structure and Properties	14
3.2	The Mechanical Testing of Cancellous Bone	18
3.3	Radiographic Techniques used to predict bone properties	24
3.4	Morphometry of cancellous bone.	26
CHAPTER 4: THE EXPERIMENTAL PROCEDURE		
4.1	Overview and Flowchart of the Experimental Methodology	31

4.2 Collection and Preservation of the Femoral Heads 32

4.3 Preparation of the Specimens 32

4.4 Bone Mineral Density 36

4.5 Prediction of Ultimate Strength 38

4.6 Compression Testing 40

4.7 Apparent Density 45

4.8 Cancellous Bone Structure 46

4.9 Cancellous Bone Morphology 50

4.9.1 Preparation of Microscope Slides 50

4.9.2 Image Analysis and Stereology 51

CHAPTER 5: RESULTS: THE MECHANICAL PROPERTIES

5.1 The Results in General 56

5.2 Relationships between Apparent Density, BMD and the Mechanical Properties. 63

5.2.1 Apparent Density and Bone Mineral Density 66

5.2.2 Apparent Density and the Mechanical Properties 67

5.2.3 BMD and the Mechanical Properties 73

5.2.4 Relationships between the Mechanical Properties 77

5.3 Summary 79

CHAPTER 6: RESULTS: CANCELLOUS BONE MORPHOLOGY

6.1 Subchondral Bone 81

6.2 Compressive Trabeculae 82

6.3 Relationships between the Morphological Parameters 83

6.4 Qualitative Assessment of Cancellous Bone 87

CHAPTER 7: DISCUSSION 93

CHAPTER 8: CONCLUSIONS AND RECOMMENDATIONS 104

APPENDIX A: Bone Remodelling Physiology in RA and OA. 108

APPENDIX B: Patient History Proforma. 113

APPENDIX C: Details of Preliminary Experiment Relating BMD to Strength. 114

APPENDIX D: Method for the Preparation of Undecalcified Cancellous Bone Sections. 117

APPENDIX E: Procedure used for Image Analysis. 119

APPENDIX F: Experimental Results. 120

APPENDIX G: Results of the Morphometric Analysis. 127

APPENDIX H: Scatterplots of the Raw Data. 130

REFERENCES 134

LIST OF ILLUSTRATIONS

Fig. 2.1 Schematic drawing of the Hip Joint, anterior view (Frankel and Nordin 1989) 4

Fig. 2.2 Schematic drawing showing the Arrangement of the Trabeculae in the Proximal Femur. (Whitehouse and Dyson 1974) 5

Fig. 2.3 Schematic representation of the layers constituting the femoral head. (Mow et al. 1974) 6

Fig. 2.4 Angular Relationships between the Femoral Neck and Shaft. 7
- **a** The Neck - to - Shaft angle.
- **b** The angle of anteversion.

Fig. 2.5 Compressive Stress on the femoral head during upright standing. (Pauwels 1980) 9

Fig. 2.6 Diagram to illustrate the forces acting on the hip joint during single leg stance. (Pauwels 1980) 10

Fig. 3.1 Compressive Stress-Strain Curve for wet Cancellous bone (Gibson 1985) 16

Fig. 3.2 The relationship between average stiffness and the number of loading cycles. (Linde et al.1987) 21

Fig. 3.3 The Hologic QDR-1000 X-Ray Bone Densitometer. 25

Fig. 4.1 Bone cubes that would be used for mechanical testing. 35

Fig. 4.2 Printout from the QDR-1000 X-Ray Absorptiometer. 37

Fig. 4.3 A Typical Compression Test Recording. 42

Fig. 4.4 A Typical Stress-Strain Curve. 44

Fig. 5.1 The mean values found for Blocks 1-8 in OA (males and females) 59
- **a** Mean Apparent Densities
- **b** Mean Strengths
- **c** Mean Young's Moduli
- **d** Mean Strain Energy Densities

Fig.5.2 The mean values found in RA (females) 61
a Mean Apparent Densities
b Mean Strengths
c Mean Young's Moduli
d Mean Strain Energy Densities

Fig. 5.3a Apparent Density vs BMD in OA Bone. 66
b Apparent Density vs BMD in RA Bone. 67

Fig. 5.4a Scatterplot of Strength vs Apparent Density in OA Bone. 67
b Scatterplot of Strength vs Apparent Density in RA Bone. 68
c Strength vs Apparent Density after log transformation, for OA Bone. 69
d Strength vs Apparent Density after log transformation, for RA Bone. 70

Fig. 5.5a Young's Modulus vs Apparent Density, in OA Bone. 71
b Young's Modulus vs Apparent Density, in RA Bone. 71

Fig. 5.6a Strain Energy Density vs Apparent Density, in OA Bone. 72
b Strain Energy Density vs Apparent Density, in RA Bone. 73

Fig. 5.7a Scatterplot of Strength vs BMD, in OA Bone. 73
b Scatterplot of Strength vs BMD, in RA Bone. 74
c Strength vs BMD after log transformation, in OA Bone. 74
d Strength vs BMD after log transformation, in RA Bone. 75

Fig. 5.8a Young's Modulus vs BMD, in OA Bone. 76
b Young's Modulus vs BMD, in OA Bone. 76

Fig. 5.9a Young's Modulus vs Strength, in OA Bone. 77
b Young's modulus vs Strength, in RA Bone. 78

Fig. 5.10a Strain Energy Density vs Strength, in OA Bone. 78
b Strain Energy Density vs Strength, in RA Bone. 79

Fig. 6.1 Surface Area Density vs Trabecular Bone Volume in the Subchondral Region. 83

Fig. 6.2 Surface Area Density vs Trabecular Bone Volume in the region of the Principal Compressive Trabeculae. 84

Fig. 6.3 Mean Trabecular Thickness vs Trabecular Bone Volume in the Subchondral Region. 84

Fig. 6.4 Mean Trabecular Thickness vs Trabecular Bone Volume in the region of the Principal Compressive Trabeculae. 85

Fig. 6.5 Marrow Space Width vs Trabecular Bone Volume in the region of the Principal Compressive Trabeculae. 85

Fig. H1 Young's Modulus vs Apparent Density in OA Bone. 130

Fig. H2 Young's Modulus vs Apparent Density in RA Bone. 130

Fig. H3 Strain Energy Density vs Apparent Density in OA Bone. 131

Fig. H4 Strain Energy Density vs Apparent Density in RA Bone. 131

Fig. H5 Young's Modulus vs BMD in OA Bone. 131

Fig. H6 Young's Modulus vs BMD in RA Bone. 132

Fig. H7 Young's Modulus vs Strength in OA Bone. 132

Fig. H8 Young's Modulus vs Strength in RA Bone. 132

Fig. H9 Strain Energy Density vs Strength in OA Bone. 133

Fig. H10 Strain Energy Density vs Strength in RA Bone. 133

LIST OF PHOTOGRAPHS

Photo 4.1	Jigs used to prepare the specimens	33
Photo 4.2	Three bone slices	33
Photo 4.3	Columns of bone removed from each slice	34
Photo 4.4	The two blocks of bone to be used for morphometry	34
Photo 4.5	Cutting the bone cubes for Mechanical Testing	35
Photo 4.6	Finishing off the bone cubes	35
Photo 4.7	The Hologic QDR-1000 X-Ray Bone Densitometer.	36
Photo 4.8	Perspex container used for DEXA	37
Photo 4.9	INSTRON Universal Testing Instrument	40
Photo 4.10	Close-up view showing the experimental set-up	41
Photo 4.11	The equiaxed structure of cancellous bone seen in the subchondral region.	47
Photo 4.12	Partially oriented cancellous bone	47
Photo 4.13	Cylindrical arrangement of cancellous bone	48
Photo 4.14	Rods and plates structure.	48
Photo 4.15	Jung Polycut 5000 Microtome.	50
Photo 4.16	A bone section stained with Toluidine Blue.	51
Photo 4.17	The Joyce Loebl Image Analysis System.	52
Photo 6.1	Subchondral cancellous bone showing very dense area.	87
Photo 6.2	X-Ray showing features typical of Hypertrophic OA.	88
Photo 6.3	Subchondral cancellous bone showing very low density bone.	89
Photo 6.4	X-Ray showing features typical of Atrophic OA.	89
Photo 6.5	Subchondral cancellous bone from Case 11.	90
Photo 6.6	X-Ray of a Normotrophic Hip.	90

Photo 6.7 RA subchondral cancellous bone. 91

Photo 6.8 X-Ray showing a hip joint with RA. 92

LIST OF TABLES

Table 3.1 The relationship between Young's Modulus and Apparent Density for Cancellous Bone. 15

Table 3.2 The relationship between Young's Modulus and Apparent Density. 15

Table 3.3 Summary of the studies aimed at determining the Mechanical properties of Cancellous Bone. 19

Table 3.4 Bone Histomorphometric Data for Males and Females, Comparing RA vs Normals. (Mellish et al.(1987)) 28

Table 3.5 Summary of studies that measured cancellous bone morphometry in the proximal femur. 29

Table 5.1 Mean Ages and Masses of Subjects. 57

Table 5.2 Mean values for the Apparent Density, BMD and Mechanical Properties. 58

Table 5.3 Summary of the relationships for OA and RA bone. 80

Table 5.4 The ranges and mean values found for the variables. 80

Table 6.1 Cancellous bone morphology in the Subchondral Region. 81

Table 6.2 Cancellous bone morphology in the Compressive Trabeculae. 82

Table A Cytokines found in Rheumatoid Arthritis. 111

Table C Results obtained from the preliminary experiment. 115

Table F Experimental Results. 120

Table G Results of the Morphometric Analysis. 127

GLOSSARY

Anisotropic : A medium in which certain physical properties are different in different directions.

Anterior : Situated in front of or in the forward part of the organ.

Apparent Density : The hydrated tissue mass, divided by the total volume of the bone specimen, following the removal of marrow fat.

Arthroplasty : A surgical operation to make a moveable joint.

Bone Mineral Density : The mineral content of the bone specimen, divided by the bulk volume of the specimen.

Coxarthrosis : Osteoarthritis of the hip joint.

Eburnated : exposed subchondral bone which has become dense and polished, following cartilage degeneration.

Elastic Modulus : Ratio of the stress applied to a specimen, to the strain produced.

Hounsfield Units : The units in which density (x - ray attenuation), is reported in Computed Tomography scans.

Hyperostosis : Excessive bone formation, or bone hypertrophy.

Isotropic : A medium in which the physical properties are independent of direction.

Lateral : Denotes a position farther from the midline of a body or a structure.

Medial : Closer to the midline of a body or structure.

Posterior : The back part, or surface of a body.

Relative Density : The apparent density of a specimen divided by the density of the material making up the actual structure.

Ultimate Strength :The stress measured at the first peak of the stress-strain curve.

Stress : Applied force divided by the cross-sectional area of the specimen.

Strain : Change in length divided by the original length of the specimen.

Strain Rate : The rate at which the strain occurs in a specimen.

Strain Energy Density : The energy absorbed by the specimen during the compression test, calculated from the area beneath the stress-strain curve (up to ultimate strength).

NOMENCLATURE

C	: Celsius
cm	: centimetres
g	: grams
kVp	: kilovolt peak
N	: Newton
MPa	: Megapascal
mm	: millimetres
E	: Young's Modulus or stiffness
R	: the sample Pearson product - moment correlation coefficient.
R^2	: the estimated proportion of variance in Y, attributable to X (the square of the correlation coefficient)
TBV%	: Trabecular Bone Volume
S_V	: Surface Area Density
MTW	: Mean Trabecular Width
MTPT	: Mean Trabecular Plate Thickness
ρ	: apparent density
σ	: stress
σ_{ult}	: ultimate stress or strength
ε	: strain
σ^2	: the population variance
μ**m**	: micron (10^{-6} m)

CHAPTER 1

INTRODUCTION

1.1 THE PROBLEM AND THE RATIONALE FOR THE STUDY

Cancellous bone is a highly specialised cellular material, situated at the ends of long bones. The function of the trabeculae is to act as a shock absorber and to transmit the stresses from the articular surfaces to the shafts of the bones. Cancellous bone plays an important role in maintaining the integrity of the joints, but also falls victim to afflictions of the joints. Conditions in which cancellous bone is affected include Osteoarthritis of the large joints, Rheumatoid Arthritis, Perthes disease, Avascular Necrosis and Osteoporosis.

Osteoarthritis of the **hip joint** occurs in up to 40% of the population over the age of 60 (Bentley 1987). Although there is still controversy about the pathogenesis involved in this condition the end result is cartilage degradation and evidence of bone remodelling. The bone changes are believed to involve thickening of the trabeculae and increased connectivity, resulting in stiffening of the cancellous bone (Radin & Rose 1986). **Rheumatoid Arthritis** is an auto-immune inflammatory disease, characterised by persistent inflammation of the synovium, local destruction of joint structures and a variety of systemic manifestations. R.A. is believed to be associated with an increased bone turnover rate with a preponderance of resorption over formation, resulting in rarefaction of the cancellous bone (Bogoch 1988). Both these conditions are very debilitating, often affecting people in the prime of life when they could be very productive members of society, and they often necessitate Joint Replacement Arthroplasty.

However, even joint replacement arthroplasty can be complicated by changes in the cancellous bone architecture in the immediate vicinity of the implants.

These complications may be due to:

1. Inadequate quality of the bone in which the prosthesis is implanted due to the underlying pathology, and / or wear debris induced osteolysis.
2. Altered stress state as a result of the implantation of the prosthetic components.
3. The adaptive remodelling capacity of the trabecular bone, which is not fully predictable.

To perfect joint replacement procedures researchers use computer based modelling techniques which allow experimentation with different implant materials and design features. The aims of such studies are to investigate the mechanical parameters affecting Total Joint Replacement Procedures. One of the crucial factors in such investigations is the accurate determination of the mechanical properties of normal and diseased bone. Furthermore, the cancellous bone from femoral heads that have been removed for OA is used for bone grafting in Primary and Revision Arthroplasty Surgery, to repair bony defects. For these reasons it has become increasingly important to advance the understanding of the mechanics of cancellous bone.

A number of studies have been done on cancellous bone from various anatomical locations, which have provided a great deal of knowledge about the mechanical properties of **"normal"** cancellous bone. There is widespread agreement that apparent density is the best predictor of the modulus of elasticity and strength (Carter and Hayes 1976, Rice et al.1988, Gibson 1985), but it does not completely explain the mechanical behaviour of cancellous bone. One also needs to account for the organisation of the material components (Goldstein 1987). Gibson (1985) stated that cancellous bone may occur in different structural patterns and Cowin et al.(1989) investigated the varying degrees of textural symmetry found in cancellous bone. Research has also been done on quantifying the trabecular architecture, namely trabecular thickness and spacing (Whitehouse 1974, Whitehouse and Dyson 1974, Parfitt et al. 1983).

In this study, a number of established techniques were applied to cancellous bone from the femoral heads of OA and RA sufferers who had undergone Total Hip Replacement Arthroplasty. Dual Energy X-Ray Absorptiometry (DEXA) was used to determine the bone mineral density. Mechanical Testing was used to determine Young's Modulus, strength and strain energy density of the cancellous bone. The apparent density of the bone was also measured. Morphometric parameters including trabecular thickness and spacing were determined for the subchondral region and the region of the principal compressive trabeculae, using an Automated Image Analysis System. Information about these parameters and their inter-relationships would:

1. Provide information about the quality of the peri-articular cancellous bone in these two conditions.
2. Show the distribution of the bone changes from the subchondral cancellous bone to the deeper compressive trabeculae in both conditions.
3. Contribute to the understanding of cancellous bone mechanics.

This may help clinicians in their management of these patients, in the planning of osteotomies, and the timing of joint replacement surgery. It may assist those involved in endoprosthesis design who require disease specific information regarding cancellous bone's composition, organisation and mechanical behaviour. Finally it is hoped that this study will also provide some insight into the different morphological subgroups of OA Hip which can be identified radiologically (Solomon 1984).

CHAPTER 2

BACKGROUND

2.1 ANATOMY OF THE HIP JOINT AND PROXIMAL FEMUR

The hip joint is a relatively stable ball and socket joint, in which the acetabulum of the pelvis forms the concave component and the femoral head forms the convex component (Fig. 2.1).

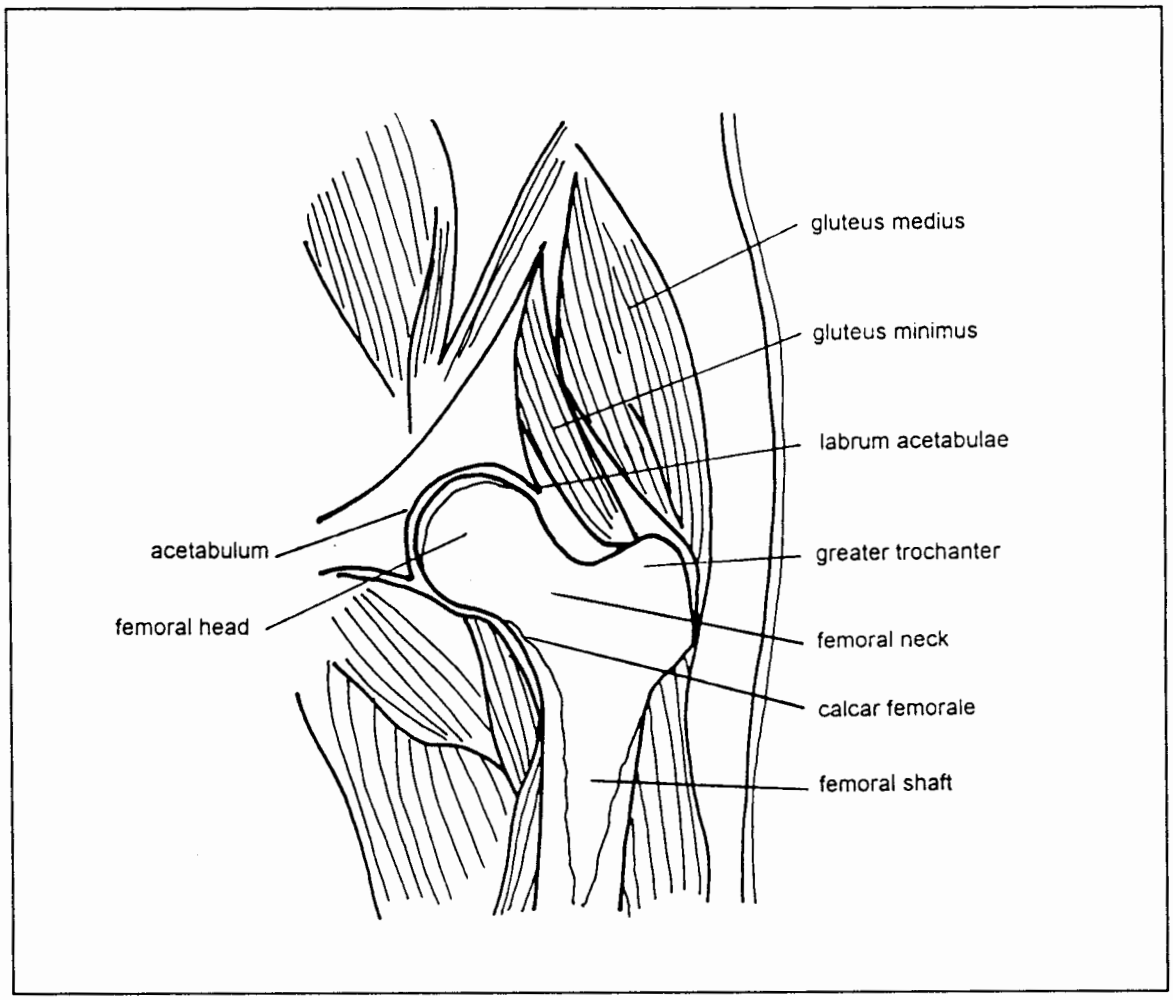

Fig. 2.1 Schematic drawing of the Hip Joint, anterior view. (Adapted from Frankel and Nordin 1989)

The femoral head is connected to the acetabulum by the ligamentum teres, which inserts into the fovea capitus, a shallow depression situated centrally on the medial

aspect of the femoral head. The joint is further stabilised by a fibrous joint capsule. The femoral head forms two thirds of a sphere and is covered in articular cartilage, which is thickest on the central and medial surface, thinning out towards the periphery.

The femoral head is connected to the shaft of the femur by the femoral neck. The femoral neck consists of the calcar femorale, a thick plate of cortical bone which forms the distal anchorage of the medial (compression) group of trabeculae. Stresses from the acetabulum are transferred to the shaft of the femur chiefly through this column of strongly constructed cancellous bone. The lateral (tension) group of trabeculae arises from the lateral femoral cortex and curves upwards and medially to merge with the compression trabeculae in the femoral head (Fig. 2.2).

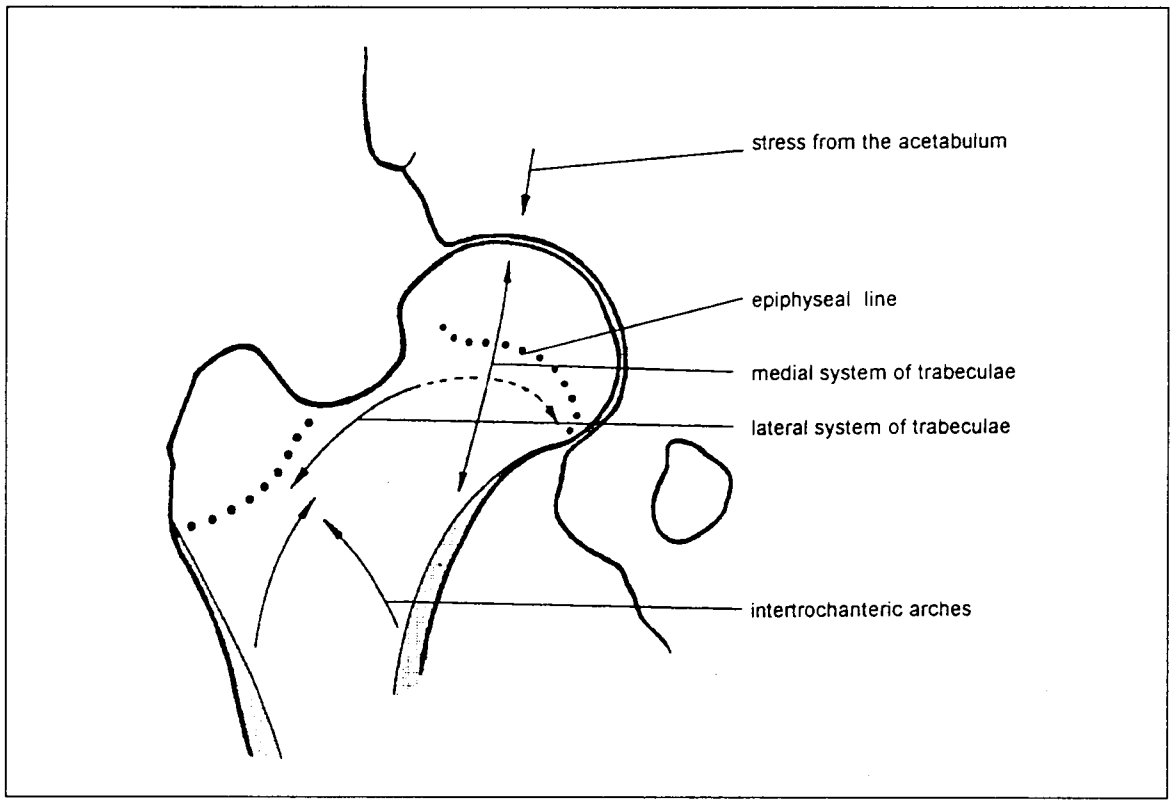

Fig. 2.2 Schematic drawing showing the Arrangement of the Trabeculae in the proximal femur. (Adapted from Whitehouse and Dyson 1974)

At a more detailed level, the femoral head consists of a layer of **articular cartilage**, the **subchondral plate** and **cancellous bone** (Fig. 2.3).

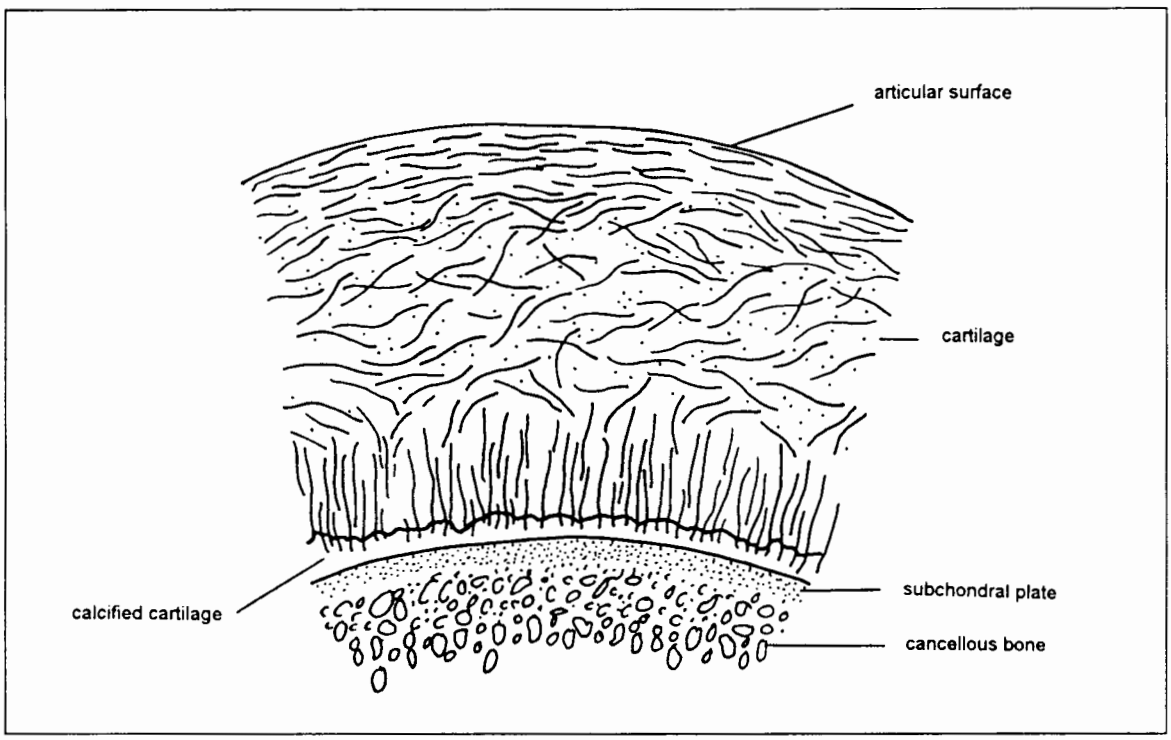

Fig. 2.3 Schematic representation of the layers constituting the femoral head. (Adapted from Mow et al. 1974)

The articular cartilage has two functions: to distribute the joint loads over as wide an area as possible, thus decreasing the stresses experienced by the contacting joint surfaces (Askew and Mow 1978); and secondly, to allow relative movement of the opposing joint surfaces with minimal friction and wear (Armstrong and Mow 1980). The cartilage is anchored to the subchondral plate which is a very thin layer of bone (0.5-1mm thick). It is the **role of the cancellous bone**, which forms a three dimensional lattice work of plates and rods, **to absorb shock and transfer stresses** to the femoral shaft, the **articular cartilage is too thin to fulfil this role** (Radin and Rose 1986).

The femoral neck has two angular relationships with the femoral shaft that are important to maintain good hip joint function.

1. The **Neck-to-Shaft Angle** , which allows for freedom of motion at the hip joint because it offsets the femoral shaft from the pelvis laterally, Fig. 2.4a. This angle is about 125 ° in most adults (Nordin and Frankel 1989).
2. The **Angle of Anteversion,** which is drawn as a projection of the long axis of the femoral head and the transverse axis of the femoral condyles, Fig.2.4b. This angle is approximately 12° in adults (Nordin and Frankel 1989).

Fig. 2.4 Angular relationships between the femoral neck and the femoral shaft. (Adapted from Frankel and Nordin 1989)

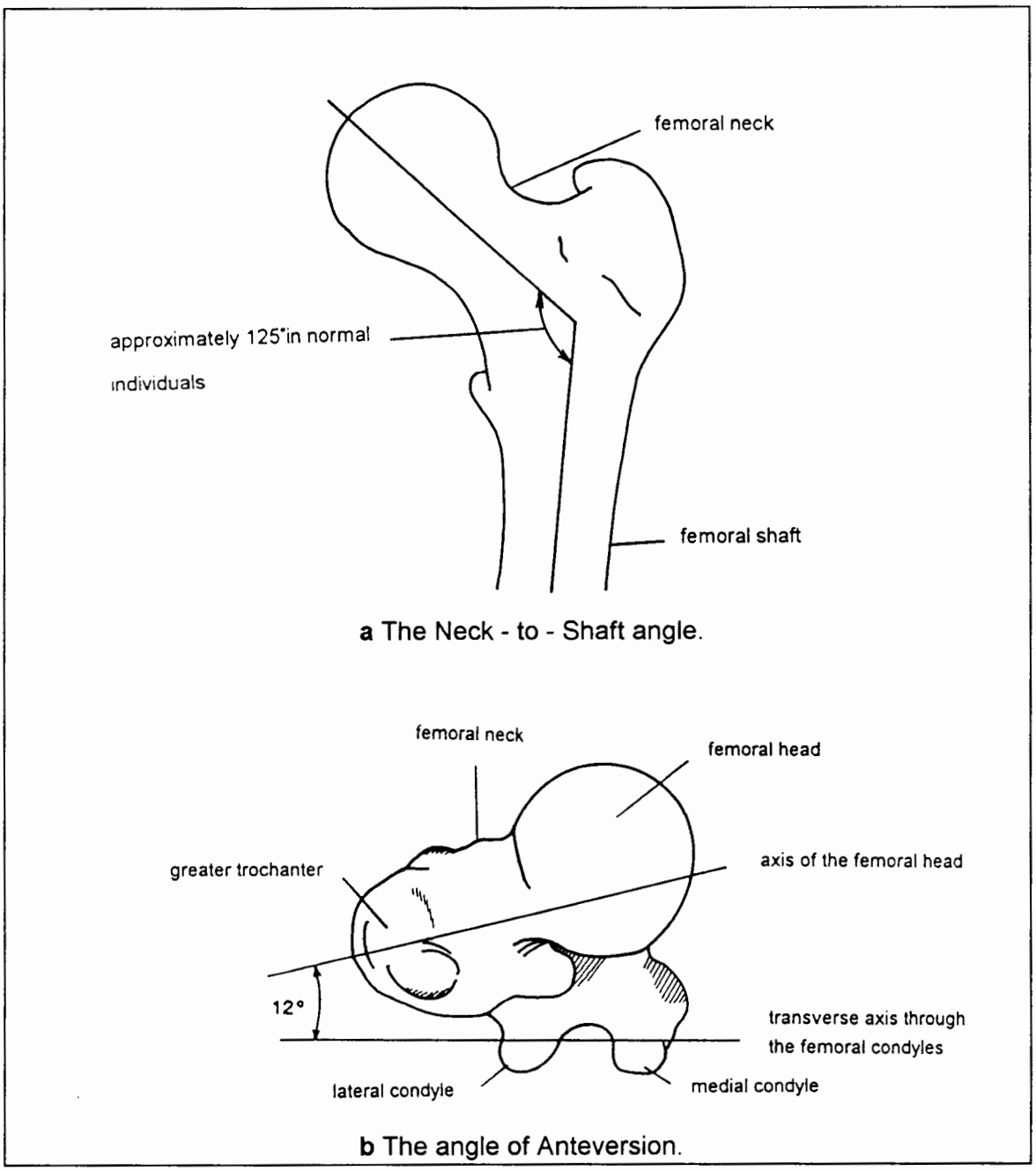

If these two angular relationships are not within the normal range, then the range of motion at the hip joint may be reduced or the force relationships about the joint may be altered, predisposing the person to a degenerative hip disorder.

2.2 HIP JOINT: MOVEMENTS AND FORCES

Hip joint motion takes place in all three planes,

- flexion and extension (140°- 0- 15°) occurs in the sagittal plane.
- abduction and adduction (30° -0 -25 °) occurs in the frontal plane.
- internal and external rotation (70°-0 -90°) occurs in the transverse plane.

However during normal gait only a small range of motion is used. Murray (1967) found that only 40° flexion to 5° extension occurred at the hip joint during normal gait. Johnston and Smidt (1969) who measured hip joint motion in the frontal and transverse planes during normal gait, found that approximately 5° of adduction and abduction occurred, and about 5° of internal and external rotation occurred during normal gait. With ageing and diseases such as RA and OA the ranges of motion in all three planes are usually significantly reduced, the net result is that a smaller area of the articular surfaces will be used excessively.

Bone is known to respond to its stress environment (Wolff's Law), thus it is necessary for us to consider the magnitude and direction of the forces acting at the hip joint, as these determine the structure and properties of the bone in the proximal femur.

When a subject is standing with his body weight supported on both lower limbs, the weight of his upper body is transmitted directly and equally to both femoral heads. The direction of the compression acting on the femoral heads is vertical and its magnitude equals approximately one third of the body weight per femoral head (Fig. 2.5). The remaining one third is the weight of the lower extremities.

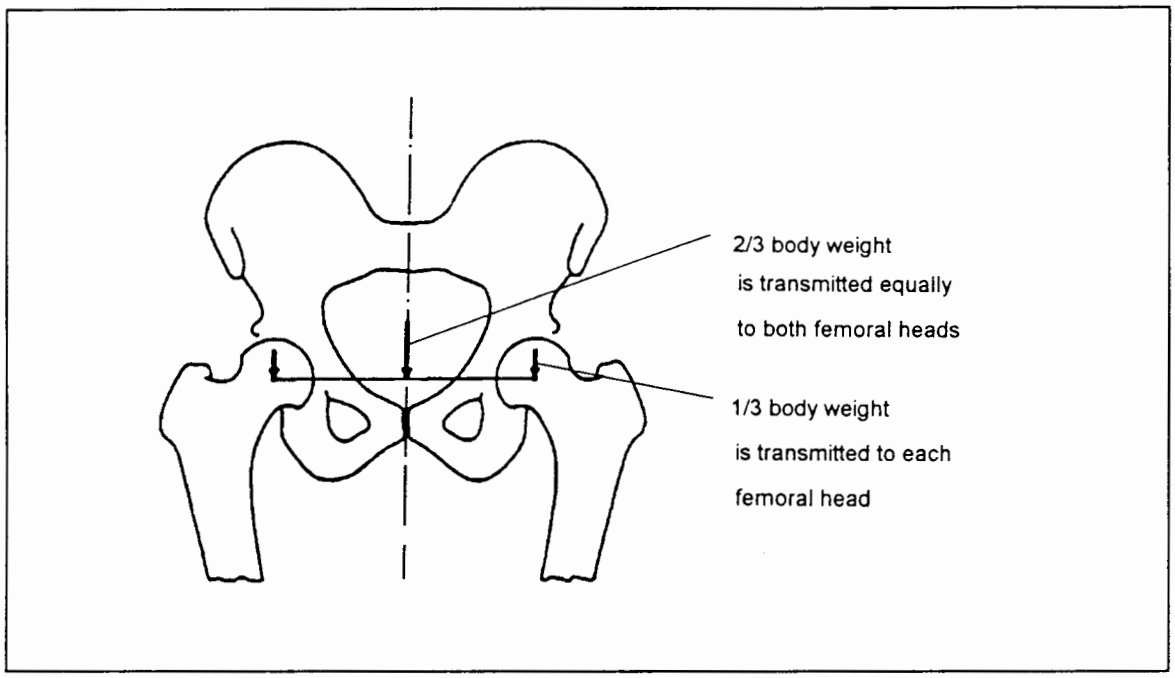

Fig. 2.5 Compressive stress on the femoral head during upright standing. (Adapted from Pauwels 1980).

However, during gait, a phase called "single-leg stance" occurs, where the body weight has to be supported on one leg alone, whilst the other leg is in the "swing phase". The pelvis needs to be kept level during this stage in order to allow the unsupported leg to clear the ground with ease. This requires contraction of the muscles surrounding the hip joint, especially the abductor muscles, including gluteus medius and minimus as well as piriformis which have their insertions on the greater trochanter (Fig.2.1). During this phase of gait the magnitude and direction of the compressive forces acting on the femoral head depend on a combination of external as well as internal / muscular forces.

The two main forces acting on the femoral head during "single leg stance" are thus:

1. **K** - the weight of the head, trunk, upper limbs and unsupported leg.
2. **M** - the tension in the abductor muscles.

From Fig. 2.6, one can see that the compressive stressing of the femoral head (at equilibrium) is determined by the following two moments:

1. On the medial side of the hip joint there is the moment produced by the body weight (**K x a**).

2. On the lateral side a moment is produced by the abductor muscle force (**M x b**).

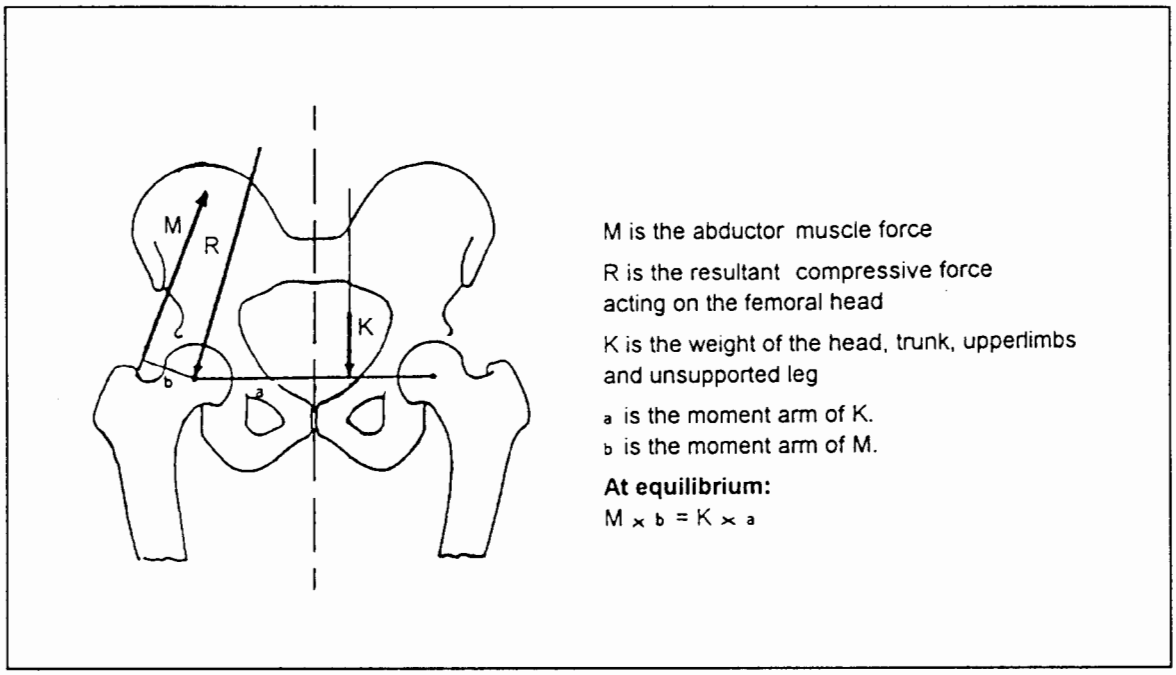

Fig. 2.6 Diagram to illustrate the forces acting at the hip joint during single leg stance. (adapted from Pauwels 1980)

At equilibrium these two moments must balance one another. The exact magnitude and direction of the resultant compressive force acting on the femoral head needs to be determined for each individual, according to his body weight and anatomy. However, generally the magnitude of the resultant force is approximately 2.7 to 3 times body weight and its direction is at angle of 16° - 21° from the vertical (Frankel and Nordin 1989, Pauwels 1980). This direction corresponds to the orientation of the principal compressive trabeculae in the proximal femur and is the direction in which the properties of the cancellous bone should be measured in this region.

During dynamic activities such as walking the Resultant Force (R.F.) on the femoral head increases to 3.5 to 5 times body weight (Crowninshield et al.1978). When lifting heavy objects, or running or jumping the R.F. may be equivalent to 10 times body

weight. Generally the forces acting on the femoral head increase as cadence increases (Rydell 1966).

2.3 RHEUMATOID AND OSTEOARTHRITIS OF THE HIP

Rheumatoid Arthritis is an auto-immune inflammatory disease which can affect all age groups, but usually manifests itself during the third to fifth decades of life. Its prevalence increases with age and **it affects twice as many females as males.** It afflicts approximately 1-2% of the adult population world wide. The disease is marked by inflammatory changes in the synovial membranes and articular structures, and by atrophy and rarefaction of the bones (Dorland's Medical Dictionary 1981).

RA is said to be associated with a generalised pattern of osteoporosis (Saville et al.1967, Kennedy et al.1975, Sambrook et al. 1987). Sambrook et al.(1990), used Dual Photon Absorptiometry (DPA) and serial computed tomography (CT) scans to measure trabecular bone loss from the distal radius, in female RA patients who had recently developed the disease. They found that bone loss occurred in the **early stages** of the disease, **2-3 cm away from the involved joints**. These findings were supported by Compston et al. (1988), but they found that the difference between normals and RA sufferers was most marked in **younger patients**, between the age 21-40 yrs.

Mellish et al. (1987) studied cancellous bone morphology in the iliac crest, and found that RA was associated with premature bone loss due to trabecular thinning. The mechanism involved in this premature bone loss which appears to occur in the early stages of the disease had to be identified. Bogoch et al. (1988) studied the changes in juxta-articular bone volume, turnover and composition; that occurred in an experimental (animal) inflammatory arthritis model. In the early stage of the "disease" they found that osteogenesis was increased fourfold, but bone resorption was increased to an even greater degree, resulting in a net negative bone balance. They

stated that the periarticular bone loss which occurs in human RA could also be associated with this increased turnover state, leading to the presence of a large proportion of less mineralised bone being present.

Since then a great deal has been learnt about the altered bone physiology that occurs in RA. This is a complex field and a more detailed account can seen in Appendix A.

Osteoarthritis is a degenerative disorder of the synovial joints, associated with progressive destruction of the articular cartilage and juxta-articular bone remodelling. It is a very common condition occurring predominantly in the older population, and it is **more common in females.** There appears to be some controversy as to the exact classification of this condition, but according to Solomon (1984), there are four main **anatomical patterns** of OA.

1. **Pauciarticular / Large Joint OA,** commonly found in the hips and knees, but rarely in the elbows and ankles.
2. **Polyarticular / Small Joint OA,** usually presenting as a nodular arthritis of the interphalangeal joints of the hands.
3. **Generalised OA,** which may be a combination of types 1 and 2.
4. **OA associated with Hyperostosis.**

Solomon (1984) also identified several **morphological** types of coxarthrosis:

1. **Hypertrophic OA,** which showed well-marked new bone formation and evidence of remodelling. Cartilage loss was usually localised to the superolateral part of the joint. Patients in this group often showed signs suggesting pre-existing acetabular or femoral dysplasia, and others showed the typical features of diffuse idiopathic skeletal hyperostosis.
2. **Atrophic OA,** which showed minimal new bone formation, more diffuse involvement of the joint and more concentric narrowing of the joint space.
3. **Rapidly Progressive OA,** this type was quite rare, but resulted in severe joint

destruction and bone loss.

Many investigators have found that subchondral bone changes accompany the cartilage degeneration in OA Hip, these bone and cartilage changes usually begin in the major load bearing areas of the joint (Byers et al.1970). It is generally believed that there is **stiffening** of the subchondral bone due to an **increase in the contiguity** of the cancellous bone. There are more laterally oriented trabeculae, which resist the bending of the walls of the porous structure, as a result the structure becomes less compliant (Pugh and Radin 1974). According to Radin et al.(1986), the stiffening of the subchondral bone leads to the degeneration of the cartilage (because the cartilage now has to act as a shock-absorber). Furthermore, the non-compliant subchondral bone leads to increased shear stresses occurring at the cartilage-bone interface. These shear stresses lead to the cartilage tearing loose from its bony bed.

It has also been found that individuals with OA affecting the hips or knees have a higher Bone Mineral Content (BMC) than age and sex matched controls (Roh et al. 1974, Cooper et al.1988). Roh et al. used a Cameron Bone Mineral Analyser (a photon absorption technique), to measure the bone mineral content of the second metacarpal and radius. Cooper et al. (1988) used Single Photon Absorptiometry (SPA) to measure the BMC at the distal forearm, and found that BMC at this site was reduced in RA, but increased in OA, **if the patients had isolated large joint disease**.

CHAPTER 3

REVIEW OF RELATED LITERATURE

3.1 BACKGROUND: CANCELLOUS BONE STRUCTURE AND PROPERTIES

The femoral head consists of a thin shell of cortical bone which encloses the all-important cancellous bone. Cancellous bone is a cellular material, and as such demonstrates mechanical behaviour typical of such materials.

Apparent density is considered to be the most important factor affecting the properties of cellular materials. Carter and Hayes (1976 & 77) established the dependence of strength and modulus of elasticity on the apparent density for cancellous bone. They proposed a power law function of the form:

$$E = a \rho^{b}$$

where: E is the Young's Modulus (MPa)

a and b are experimentally derived constants

ρ is the apparent density (g/cm^3)

There has however, been controversy over the values of a and b. This controversy is partly due to the use of cancellous bone from different species, different anatomical locations and the use of fresh hydrated and old dry bone. The results from various investigators are summarised in Table 3.1.

Table 3.1 The relationship between Young's Modulus and Apparent Density for Cancellous Bone.

Relationship	Investigators	Method
$E \approx \rho^3$	Carter & Hayes (1976)	Mechanical Testing in compression, human and bovine bone.
$E \approx \rho^2$	Rice et al (1988)	"Pooled" data, human and bovine bone.
	Gibson (1985)	"Pooled" data, human and bovine bone.
$E \approx \rho^{1.88}$	Ashman & Rho (1988)	Ultrasonic Testing, human distal femur.
$E \approx \rho^{1.4}$	Lotz et al (1990)	Mechanical Testing in compression, human proximal femur.

The strength of cancellous bone is also related to apparent density by a power law relationship:

$$\sigma_{ult} = a\ \rho^{\ b}$$

where: σ_{ult} is the ultimate stress (MPa)

a and b are experimentally determined constants

ρ is the apparent density (g/cm^3)

The findings of some investigators are shown in Table 3.2.

Table 3.2 The Relationship between Strength and Apparent Density.

Relationship	Investigators	Method
$\sigma_{ult} \approx \rho^2$	Carter & Hayes (1976)	Mechanical Testing in compression, human and bovine bone.
	Gibson (1985)	"Pooled" data, human and bovine bone.
	Rice et al (1988)	"Pooled" data, human and bovine bone.
$\sigma_{ult} \approx \rho^{1.8}$	Lotz et al (1990)	Mechanical Testing in compression, human proximal femur.

It is generally accepted that the elastic modulus is directly proportional to ultimate strength (Currey 1969, Brown and Ferguson 1980, Goldstein et al. 1987).

Galante (1970) established that the strain rate at which cancellous bone is tested has an effect on bone mechanics. Carter and Hayes (1977) found that the mechanical properties of cancellous bone were related to the strain rate raised to the power 0.06.

Linde et al.(1991) found that strength and stiffness were related to the 0.07th and the 0.05th power of the strain rate respectively. However, the effect of the strain rate on the mechanical data in the range where most experiments are performed (10^{-3} to 10^{-2} /second) is negligible when compared with other factors.

The compressive stress-strain curve for cancellous bone is also characteristic of a cellular solid (Fig.3.1).

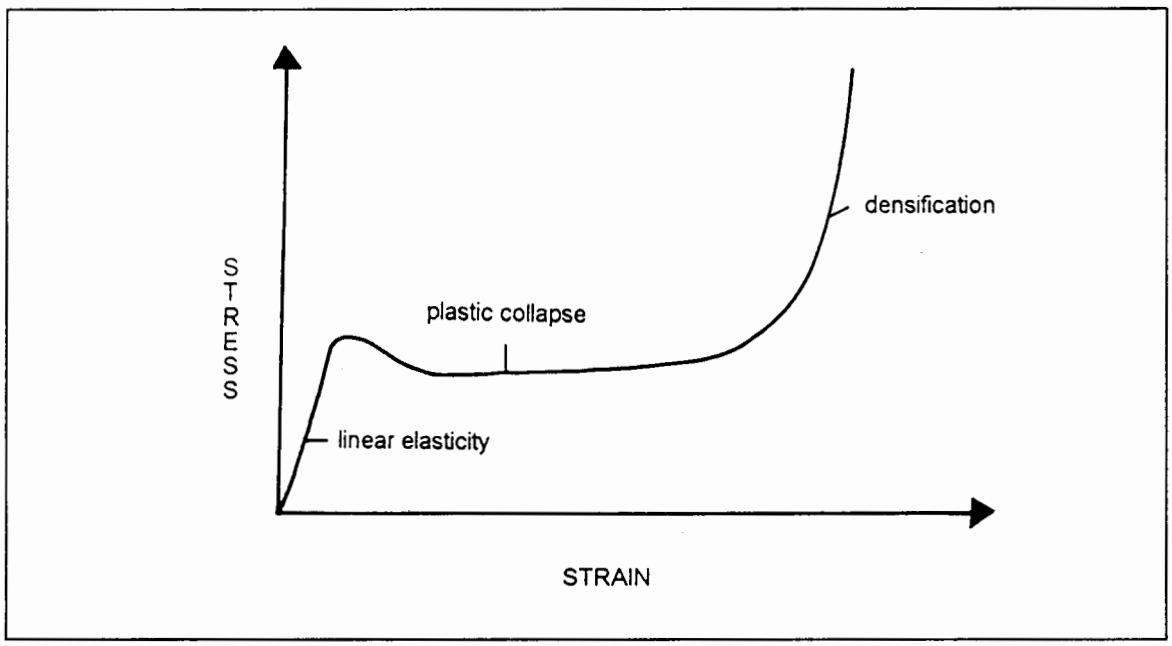

Fig. 3.1 Compressive Stress-Strain Curve for wet Cancellous bone. (Gibson 1985).

In the first portion of the stress-strain curve, cancellous bone shows linearly elastic behaviour as the cell walls bend or compress axially. In the second portion the cell walls begin to collapse by elastic buckling or plastic yielding giving a plateau of fairly constant stress. In the final stage the cell walls eventually meet and touch giving rise to the steep ascent in this part of the curve.

The structure and density of cancellous bone are known to depend on its stress environment. If the stress pattern experienced by the cancellous bone is complex, then the structure of the trabecular network is also **complex** and highly asymmetric. If the loading is mainly uniaxial, the trabeculae may develop a **columnar** structure with

cylindrical symmetry (Weaver and Chalmers, 1966; Whitehouse et al. 1971). The columnar arrangement is oriented so as to provide high stiffness and strength in the direction of principal loading, with lower stiffness and strength in the transverse directions (Gibson 1985). Whitehouse and Dyson (1974), examined the patterns of trabecular bone in the proximal femur and found structures that were isotropic or slightly anisotropic in the subchondral region, and highly anisotropic structures in the region of the compressive trabeculae. Based on the knowledge of cellular solids it would be beneficial to have a foam-like, isotropic material to act as a shock absorber in the subchondral region; and a columnar, anisotropic material in the region of the compressive trabeculae. Gibson (1985) stated that there were two basic types of cancellous bone structure: the **asymmetric type** which could be either open or closed celled, and the **columnar type** which could have plate-like cell walls, or a rod-like structure.

The structure of cancellous bone is thus not uniform for all anatomical locations, and it may even vary significantly within one anatomical region such as the femoral head (Whitehouse and Dyson 1974), or the tibial plateau (Williams and Lewis 1982). The cancellous bone in normal individuals is thus highly specialised for its functions. However, these structures may become defective in conditions such as RA or OA as we shall see in this study. The theory behind the mechanical behaviour of cellular solids is only applicable when the relative density of the material is very low. In cancellous bone in OA and RA, the relative density of the cancellous bone is usually much greater.

3.2 THE MECHANICAL TESTING OF CANCELLOUS BONE

The most widely used method for determining the mechanical properties of cancellous bone, is compression testing of uniform bone specimens between two parallel platens of a materials testing machine. This is an appropriate test on bone from the capital and subcapital regions of the proximal femur as it is the most natural mode of deformation for cancellous bone from this region. However, **the bone specimens must have been harvested in the direction of the average joint reaction force if the results are to be meaningful**. The findings of the most recent studies on cancellous bone from the femoral head are summarised in Table 3.3.

Table 3.3 Studies aimed at determining the Mechanical Properties of Cancellous Bone.

	Brown and Ferguson (1980)	Martens et al.(1983)	Lotz et al.(1990)
Investigators:			
Method:	Used human proximal femora, 5mm cube specimens. Bone was stored at -10°C until time of mechanical testing. Evaluated the elastic modulus and yield strength in three orthogonal directions for each specimen. Specimens were subjected to a series of uniaxial compression tests using an INSTRON testing machine. Their aim was to catalogue spatial and directional variations of the mechanical properties of the cancellous bone in the human proximal femur. They did not state how many proximal femora were used.	Used femoral bone specimens from 20 autopsy cases. Specimens were frozen at -20°C until use. Used cylindrical specimens (8mm diam). Specimens were taken along three orthogonal axes in three regions:femoral head, neck and inter-trochanteric region. Did bone mineral analysis using a Cameron Bone Mineral Analyser. Each specimen was only tested in one direction. Measured apparent density of specimens.	Used the proximal femora of 4 subjects (human). The bone was C.T.scanned to determine the mineral density. Specimens were frozen to -20° C until use. They used cylindrical specimens, 9mm in diameter, performed compression testing in a direction parallel to the femoral neck. Calculated Young's Modulus and strength, and determined the apparent density of the specimens. In total they tested 49 cylindrical specimens. The aim of this study was to investigate the use of QCT in the assessment of apparent density, strength and Young's Modulus of trabecular bone from the proximal femur.
Results:	Using a computer contouring program they converted their results into smoothed distribution plots of elastic moduli and yield strengths across sections of interest. They found prominent stiffness elevations in regions traversed by the primary trabeculation system. They found mechanical properties to be reduced when measured in directions other than those of habitual weight bearing. In the region of the primary trabeculation system, they found Young's Modulus to be between 4.8 and 6.9 GPa, and Strength was 310MPa, on average.	**Axis: Elastic Mod: Mean (SD) Strength: Mean (SD)** X head 900 (710)MPa 9.3 (4.5)MPa Y head 811 (604) 10.2 (3.3) Z head 403.5 (65.7) 4.9 (1.27) As can be seen, there was a difference in compressive modulus and strength in the three axes, in the head region. Compressive strength in the femoral head was greatest in the region where the compressive and tensile trabeculae intersect. They found a linear relationship between modulus, strength and bone mineral content or apparent density. They also found a strong correlation between Young's Modulus and Strength. They concluded that cancellous bone from all regions of the proximal femur was anisotropic.	They found Strength=$25\rho^{1.8}$ (R^2=0.93) Strength = $0.002(QCT)^{1.5}$ (R^2= 0.89) E= $1.310\rho^{1.4}$ (R^2= 0.91) E= $0.5(QCT)^{1.2}$ (R^2= 0.90) They found Compressive Strength to lie between 1.3 - 27.3 MPa, Mean=6.76 (S.D.=4.84) and Young's Modulus between 78 - 1530 MPa, Mean=441 (S.D.=271). They found a linear relationship between apparent density and the BMD determined by QCT.
Comments:	This study gave detailed quantitative information of the distribution of stiffness and strength in the proximal femur, showing that in healthy individuals the bone in this region is non-homogeneous and anisotropic. However they used non-destructive tests in different directions on the same specimen, to the point where yield was incipient, causing cumulative microdamage which may have influenced their results.	Because each specimen was only tested in one direction there was no cumulative microdamage.	Their sample size of only 4 proximal femora is very limited. Their testing direction deviates slightly from the material axis of the specimens. However, they found that QCT was a good predictive technique.

Table 3.3 (continued)

Investigators:	Ciarelli et al.(1991)	Deligianni et al.(1991)
Method:	Their sample included two femoral heads from one cadaver (70 yr old male), as well as many other metaphyseal regions from 4 cadavers in total. Stored the bone at -10°C. Determined the mineral density with C.T. Then cut the bone into 8mm cube specimens. Tested these mechanically in compression to pre-yield in 2 orthogonal directions and to failure in the third direction. They determined Young's Moduli and compressive strengths. Then calculated the apparent density and the ash weight.	They used femoral heads from females, in the following three groups, normal cadaveric, fractured neck of femur and osteoarthritic. Took numerous cylindrical specimens from each fem. head. A 9.5mm diameter trephine was used to harvest the bone in a direction perpendicular to the articular surface, so they only used the subarticular bone. They determined: Strength, Young's Modulus and Strain energy density, as well as apparent density.
Results:	In the prox. femur they that the modulus of elasticity was always greatest in the supero-inferior direction. They found that $E = a\rho^{2.17}$ ($R^2 = .48$) $E = a(\text{CTdensity})^{.99}$ ($R^2 = .54$), the CT mineral density was in Hounsfield Units.	In the cadaveric and the fractured neck of femur groups they found the highest correlation for Strength and Young's Modulus with app.density with the first power of the density, but for the OA group the best correlation was with the apparent density squared. The energy absorbed to ultimate stress was linearly related to the apparent density for all specimens.
Comments:	They had a very small sample. However, they found that the bone in the central part of the femoral head tended towards isotropy. They also concluded that for any given density there can be many different architectural schemes, resulting in different mechanical properties. This could account for the unexplained variance when density measures are used as predictors.	They fail to state clearly how many femoral heads were used in their study, and the exact dimensions of their specimens.

The properties of cancellous bone determined from the testing of machined specimens may be fairly precise, but not completely accurate. A number of studies have been done to see how the measurement of mechanical properties can be made more accurate and repeatable.

Studies aimed at improving the testing technique:

1. The stiffness of cancellous bone is usually determined from the stress-strain curve of one single destructive test, but the reproducibility of measurements made in this way is poor (Linde et al.1985). This group of investigators observed an increasing stiffness with **repetitive non-destructive compression** in the elastic interval. The median increase in Young's Modulus was about 45%. This was due to a build up of residual strain (Linde et al. 1987), which is most marked in the first few loading cycles. A steady-state is reached by the tenth loading cycle as can be seen in Fig.3.2.

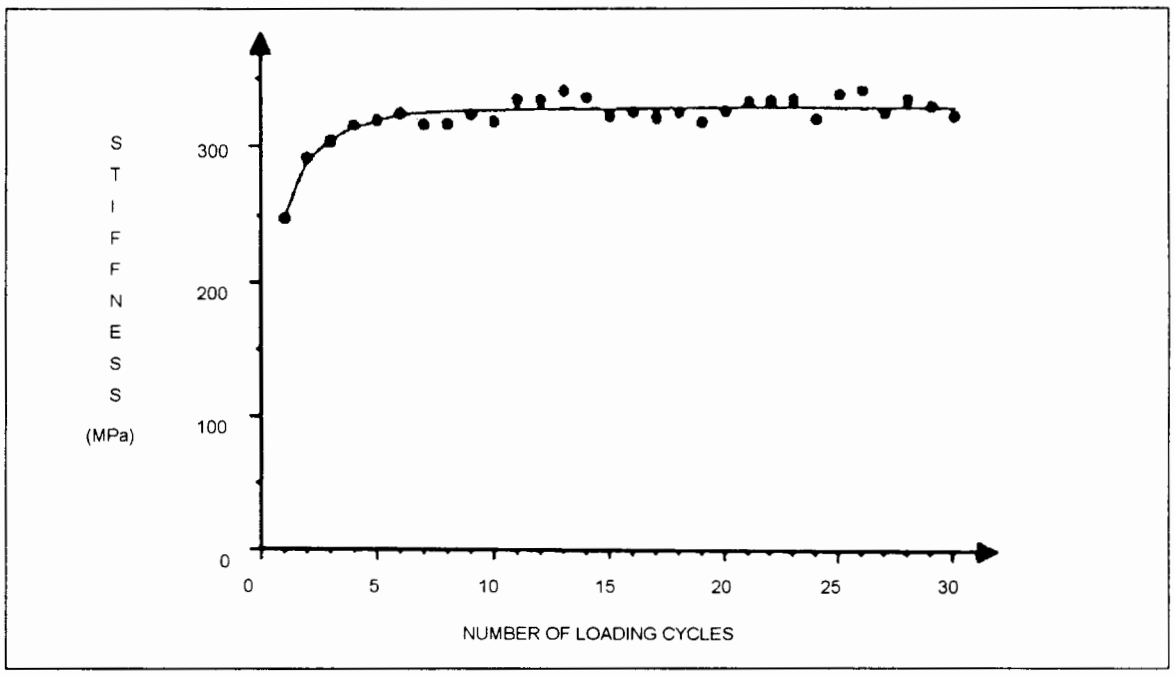

Fig.3.2 The relationship between average stiffness and the number of loading cycles. (Adapted from Linde et al.1987)

Once a steady state has been reached, the results of mechanical testing are more reproducible than results obtained from a single test on a specimen in a relaxed state.

They also found that the elastic behaviour of cancellous bone specimens in axial loading is non-linear, maximal stiffness occurred at about 49% of ultimate strength, and the interval between 40 and 65% of ultimate strength can be regarded as the linear portion of the stress-strain curve, for practical purposes. The non-linearity of the initial part of the stress-strain curve is believed to be caused by surface irregularities and "settling" of the platens (Townsend et al.1975, Carter and Hayes 1977).

2. Studies aimed at determining the mechanical properties of cancellous bone have assumed a uniform strain distribution in the direction of compression. However, the strain distribution in the specimen being tested deviates from pure uniaxial strain because of **frictional end phenomena** resulting in shearing forces at the interface between the bone and the load platens (Odgaard et al. 1989). This friction at the interface causes less expansion of the specimen near the interface than at the central part of the specimen, and axial deformation becomes non-homogeneous. This frictional end effect causes specimen stiffness to increase. They suggest that measuring strain in the central part of the specimen (where end phenomena do not affect strain measurements) would lead to more accurate results. To do this one would have to use an automated optical system, the application of which is very complex and might be impractical.

However, by cutting the cancellous bone one is disrupting its structural integrity, and removing the structural support which exists in-situ, thus causing slight underestimation of the stiffness of the specimen.

Odgaard and Linde (1991), found that friction at the specimen-platen interface results in a 3-5% overestimation of Young's Modulus (for cubic specimens), but the disruption of the structural integrity (by cutting the specimens) counteracts this. Therefore, conventional compression tests using an extensometer or similar device to measure overall strain does give an accurate value for compressive Young's Modulus.

3. It is also known that the **characteristics of the bone-platen interface** and the use of side constraint can affect the properties of cancellous bone. Linde and Hvid (1989), carried out experiments to investigate the effects of the following boundary conditions:

a) Unconstrained specimens on unpolished steel platens, which is the standard set-up, used in most experiments.

b) Bone cement at both interfaces, on unpolished steel platens, this caused a 40% increase in stiffness.

c) Unconstrained specimens on polished steel platens, resulted in a 5% decrease in stiffness when compared to standard test results.

d) Unconstrained specimens on polished steel platens with oil at the bone - platen interface, led to a 7% decrease in stiffness when compared to standard test results.

e) Side constraint with a small steel cylinder around the specimen, led to an increase in stiffness.

Their study confirmed that the mechanics of the interface between the trabecular bone and the surface of the test column are of considerable significance. They did not state which method would yield the most accurate results, but did find that the standard method, of using unpolished steel platens, and no side constraint provided the most reproducible results.

4. Specimen geometry should also affect the mechanical behaviour of the bone. Linde et al. (1992) studied the effects of specimen geometry, and found that both the length and the cross-sectional area of the specimens influenced the mechanical behaviour. For specimens that are to be used for comparative studies on trabecular bone mechanics they suggest a standard geometry:

a) a cube with 6.5mm sides or

b) a cylinder with a diameter of 7.5mm and a height of 6.5 mm.

5. The **temperature** at which the specimens are tested is also important, (Brear et al.1988). Increasing the temperature to body temperature (37°C) leads to:

a) a 7% decrease in Young's Modulus

b) a 13% decrease in compressive strength

c) a 5% decrease in strain at maximum load

d) a 22% decrease in work per unit volume.

For more accurate results one should try to test the bone at 37°C.

3.3 RADIOGRAPHIC TECHNIQUES USED TO PREDICT BONE PROPERTIES

As was stated previously, apparent density is the strongest, single variable for predicting the mechanical properties of cancellous bone. But this variable can only be measured in-vitro, and after the bone has been defatted. Fortunately, the Bone Mineral Density (BMD) is directly related to the apparent density, and so mechanical properties can be related to BMD. Radiographic techniques have been developed which can determine the BMD both in-vivo and in-vitro by measuring the X-ray attenuation of the bone. There are four major techniques available for determining BMD. **Single** and **Dual Photon Absorptiometry** were used initially to determine bone mineral densities, but they are no longer used in contemporary studies. **Quantitative Computer Tomography (QCT)** is the most up-to-date technique, which offers high sensitivity for the detection of bone mineral changes in cancellous bone. It allows one to analyse cancellous bone separately from cortical bone, which is not possible with other techniques. It can be used with great accuracy both in-vivo and in-vitro, and was used in the studies by Lotz et al. (1990), and Ciarelli et al. (1991). However, it is an expensive technique, and involves a high radiation dose for the patient. When single energy scans are performed, the presence of variable amounts of fat in the marrow can introduce errors in the determination of the bone density.

The technique which was used in this study was **Dual Energy X-Ray Absorptiometry** (DEXA), and will thus be described in more detail. DEXA is used extensively to assess the progress of osteoporosis by measuring the BMD of the lumbar vertebrae and the femoral neck. Recently software was developed to enable the measurement of BMD adjacent to joint prostheses, thus allowing investigators to monitor bone changes as a result of prosthetic implants.

The principles underlying DEXA, are that bone mineral and soft tissue can be differentiated using two different photon energies. In DEXA (Fig. 3.3), these photon energies are provided by a self-contained X-ray source, which provides alternating pulses at 70 and 140 kVp.

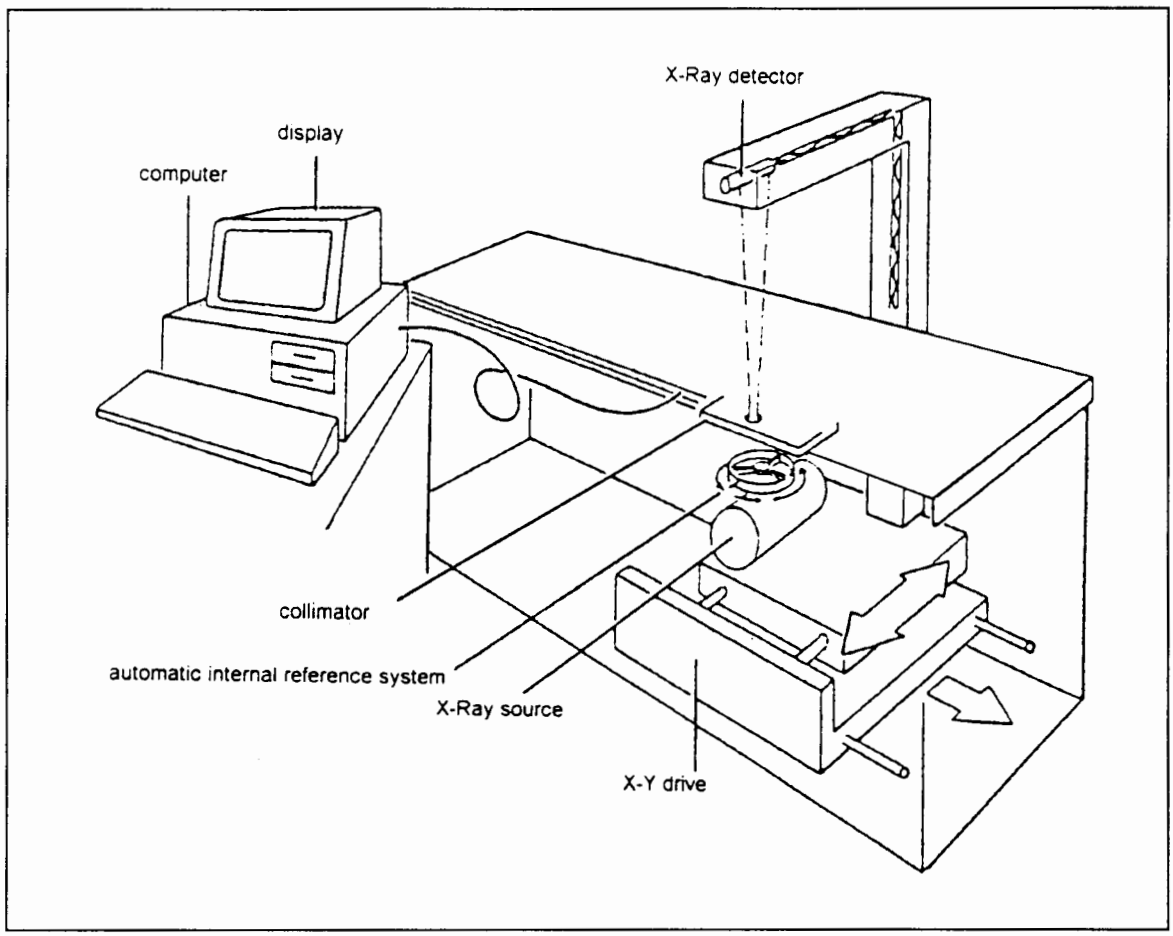

Fig. 3.3 The Hologic QDR-1000 X-Ray Bone Densitometer.

This allows the discrimination between soft tissue and bone mineral, and furthermore, because the bone mineral absorbs high energy photons, the computer system can

calculate the BMC based on the number of photons that were detected after the beam has passed through the composite object. As can be seen from Fig. 3.3, the X-ray detector is directly linked to the X-ray source, allowing them to move together across the object / patient in a serpentine pattern. The system calculates the BMC in grams, which represents the total amount of calcium hydroxyapatite present in the area scanned. From this information the system can then calculate the bone mineral density as an areal density, in g/cm^2.

However, one cannot selectively measure cancellous bone in-vivo with this technique, as the measurement includes the BMC of the surrounding cortical shell, the cortical bone makes up about 60-80% of the total measurement. For the purposes of this study the technique was however, adequate, as the BMC of the cancellous bone **cubes** was measured (in-vitro) without the surrounding cortical bone.

3.4 MORPHOMETRY OF CANCELLOUS BONE

Apparent Density and Bone Mineral Density are strong indicators of the mechanical properties of cancellous bone, but trabecular architecture is also believed to be very important in determining the behaviour of the bone. With ageing and certain pathological processes trabecular bone undergoes morphological changes in response to its metabolic and mechanical milieu. With OA these alterations include: an increase in apparent density and thickening of the trabeculae, at least in the subchondral region (Pugh et al. 1974). With RA there are believed to be reductions in density and loss of trabecular thickness and contiguity (Mellish et al. 1987). However there appears to be controversy regarding the specific architectural changes and how they affect the mechanical behaviour of the cancellous bone.

In order to determine the morphology of cancellous bone one has to make use of Quantitative Microscopy and Stereology. Quantitative Microscopy involves the measurement of parameters such as areas and perimeters in two-dimensional

images, and Stereology involves the use of mathematical methods to calculate three dimensional parameters from these fundamental measures.

The initial images may be obtained from the cut surfaces of thick bone sections, or from thin histology sections. Techniques such as scanning electron microscopy and image analysis are commonly used. When considering cancellous bone, Stereology can be used to determine:

a) the volume fraction occupied by bone, and that occupied by marrow.
b) the total surface area of the bone - marrow interface, known as the surface area density.
c) the average trabecular thickness and inter-trabecular spacing.
d) the direction of trabecular orientation and the extent to which the trabeculae are oriented in that direction.
e) the degree of anisotropy or isotropy of the material structure (Whitehouse 1974, Whitehouse and Dyson 1974).

Details on how these parameters are calculated are provided in the section on Experimental Procedures.

A number of studies, using morphometry or stereology have been done on cancellous bone from various regions in the human body, some of their findings will be discussed briefly.

It is generally accepted that there is an age related decrease in the volume fraction of cancellous bone. This was seen in the iliac crest (Merz and Schenk 1970, Aaron et al.1987) and in the vertebrae (Bergot et al. 1988). In females the loss of bone is primarily due to resorption of entire trabeculae, whereas in males there is progressive thinning of the trabeculae, but they do not necessarily disappear as in females (Aaron et al.1987, Compston et al. 1987).

The effects of RA on the micro-anatomy of cancellous bone were studied by Mellish et al.(1987). They compared morphologic parameters of **iliac crest** cancellous bone from normal individuals to those of RA sufferers who were not on steroid therapy. Their findings for both males and females can be seen in Table 3.4. They found that RA was associated with **premature bone loss**, which was most evident in the age group 34-60 years for females, and 34-50 years for males. But, total lifetime bone loss was similar to that found in the normal, ageing population.

Table 3.4 Bone Histomorphometric Data for Males and Females, Comparing RA and Normals.(Mellish et al.(1987)

FEMALES	34 - 50 yrs		50 - 60 yrs		60 - 80 yrs	
	RA	Normals	RA	Normals	RA	Normals
TBV %	19.1	26.9	18.3	22.2	17.6	14.7
MTPT(μm)	125.6	181.9	121.8	144.3	123.7	147.8
MTPS(μm)	743.1	722.3	721.2	819.2	762.6	1137.6
MTPD(/mm)	1.52	1.48	1.51	1.34	1.43	0.99

MALES	34 - 50 yrs			50 - 80 yrs	
	RA	Normals		RA	Normals
TBV %	17.8	22.4		18.7	18.3
MTPT(μm)	141.3	181.6		154	150.6
MTPS(μm)	851.1	857.2		901.7	915.3
MTPD(/mm)	1.27	1.24		1.2	1.21

TBV % = Trabecular Bone Volume Fraction

MTPT = Mean Trabecular Plate Thickness

MTPS = Mean Trabecular Plate Spacing

MTPD = Mean Trabecular Plate Density (number to be found per mm)

The following table is a summary of studies that have attempted to quantify cancellous bone structure in the proximal femur.

Table 3.5 Studies that measured cancellous bone Morphometry in the Proximal Femur.

Investigators:	Whitehouse and Dyson (1974)	Fazzalari et al.(1985)	Kawashima and Uhthoff (1991)
Method:	They used electron microscopy and stereology to study the appearances and dimensions of cancellous bone throughout the proximal femur (in the frontal plane mainly, but also in the transverse plane). They used:Left femur (female 24 yrs), Right femur (male 22 yrs). Variables measured: relative area occupied by bone, boundary perimeter length between marrow and bone, mean trabecular widths, degree of anisotropy.	The aim of their study was to determine relationships between various morphometric parameters in OA Hip and Osteoporosis. They used 75 OA Hip femoral heads and 18 osteoporotic femoral heads, as well as data from 66 normal femoral heads. They studied the cancellous bone from the region of the principal compressive trabeculae, in the frontal plane. They determined the Volume Fraction, surface density and trabecular thickness and spacing, using 10 um sections and an image analysis system.	Their aim was to study the bone loss in the proximal femur, using radiologic, densitometric and morphometric techniques. They used 141 normal proximal femurs (age ranged from 27 to 89 years). They studied the morphometry of both the compressive and tensile trabeculae of the femoral neck, in the frontal plane, directly from the specimens.
Results:	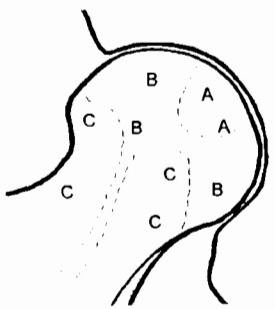 A is isotropic or slightly anisotropic. B is moderately anisotropic. C is highly anisotropic. 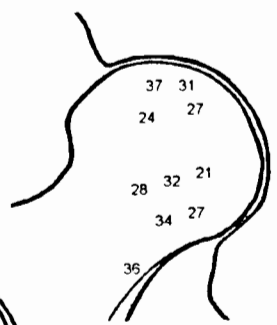 The relative area occupied by bone shown as percentages. 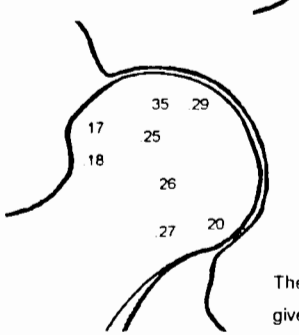 The mean widths of the trabeculae given in mm.	OA Normal Trab. Bone Vol. (%) 23.6 28.2 Trabec.Thickness (mm) .21 .15 Trabec. Spacing (mm) .71 .39 They found that OA showed a greater rate of bone loss than controls, and the Trabecular Bone Volume Fraction was less in this region than in controls. They think that the stiffened subchondral bone results in stress shielding of the underlying bone.	The width of the compressive trabeculae was .247 mm in normal adults (mean age 53 yrs) and decreased to .174 mm in the elderly (mean age 72 yrs). The spacing from the midpoint of one trabeculum to that of the next was 1.056mm in the normal adults and increased to 1.169mm in the elderly group.
Comments:	This was a good study, providing a great deal of information, and the results are easy to interpret. Unfortunately only two femoral heads were studied.	They converted the trabecular width results to trabecular thickness, which can result in errors of up to 30%, as they had to assume the material to be isotropic when converting in this manner.	This was a good study, based on a large sample. The results are meaningful and easy to interpret.

Although stereology has allowed considerable insight into the complex 3-dimensional structure of cancellous bone, it has certain shortfalls. High Resolution Computed Tomography will allow 3-dimensional information to be determined non-destructively from specimens of cancellous bone (Feldkamp et al. 1989). This technique will facilitate the study of structural anisotropy and the degree of connectivity in three dimensions. Connectivity cannot be measured accurately from 2-dimensional sections.

CHAPTER 4

THE EXPERIMENTAL PROCEDURE

4.1 OVERVIEW AND FLOW CHART OF THE EXPERIMENTAL METHODOLOGY

The experimental procedure involved numerous steps, which are summarised in the flow chart below. Femoral heads were processed two at a time, as they became available. Preparation of the sections for Image Analysis was very lengthy, and was performed in parallel with the mechanical testing, as can be seen in the following flow chart.

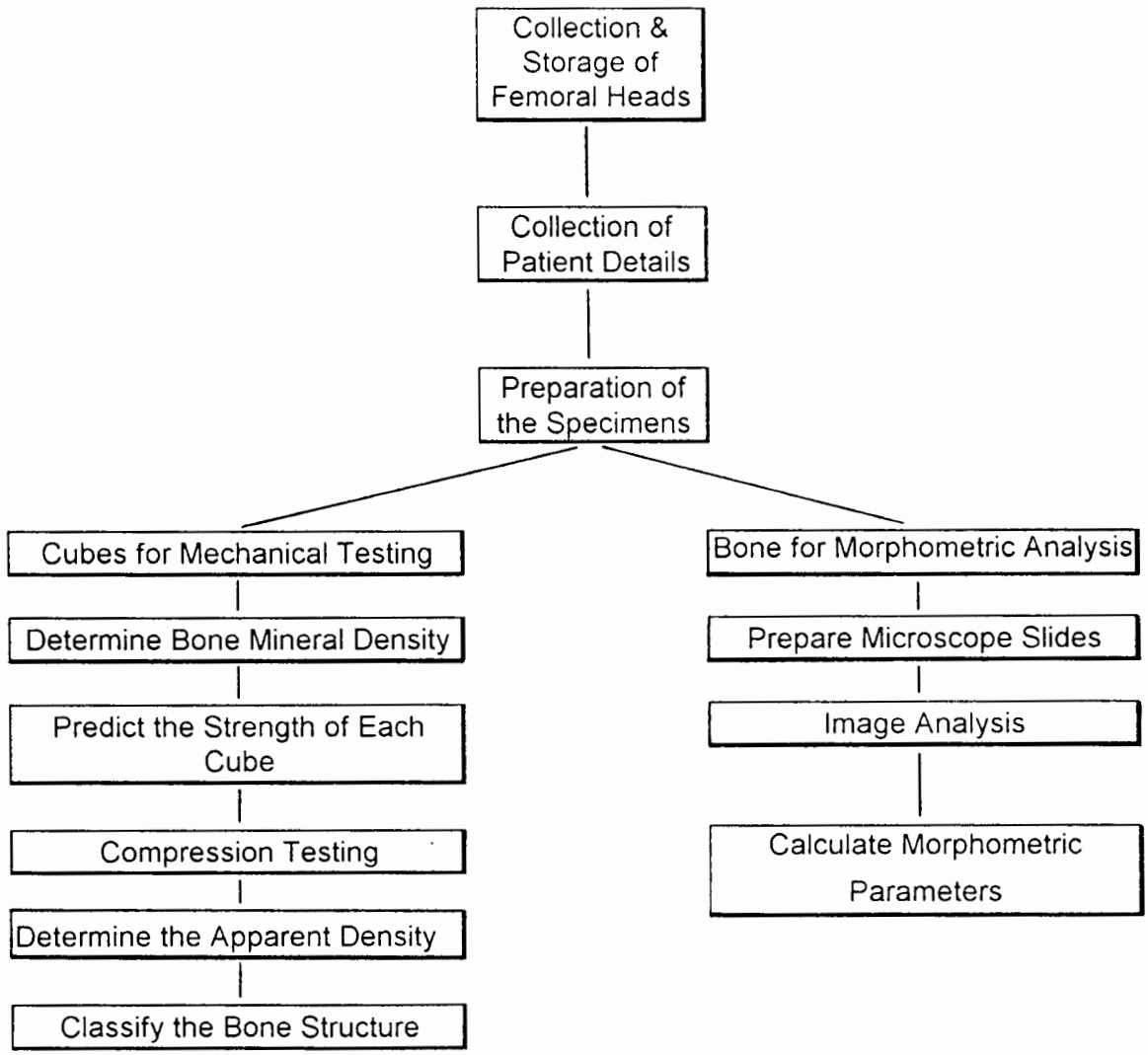

4.2 COLLECTION AND PRESERVATION OF THE FEMORAL HEADS:

The femoral heads used in this study were collected at Princess Alice Orthopaedic Hospital, where Total Hip Replacement (THR) surgery is carried out. Immediately after the femoral heads were excised they were wrapped in saline soaked gauze, sealed in a plastic bag and placed in a freezer set at -20°C. This method of preservation was described by Yamada (1970) and was also recommended by Cowin (1987). It is believed to have minimal effects on the properties of bone. The patients' details were collected on a form shown in Appendix B.

The femoral heads used in this study were collected over a twelve month period; during this period the author received: 12 female and 10 male OA femoral heads, as well as 10 RA femoral heads all of which came from females. Rheumatoid Arthritis is less common in males and very few male RA sufferers required THR during the period over which this study took place.

4.3 PREPARATION OF THE SPECIMENS:

To produce the necessary bone specimens from each femoral head, a series of four jigs had to be made (Photo 4.1). The jigs were made of high density polyethylene.
Jig 1 was used to cut the three slices of bone in the frontal plane. **Jig 2** was used to remove the central column of bone from each slice. **Jig 3** was used to cut the cubes for mechanical testing . **Jig 4** was used to finish off the cubes with glass paper. All cutting was done by hand. To allow a finer cut, the normally wavy tooth set pattern of the saw blades was ground away before the blades were used.

Each frozen femoral head was correctly oriented with the aid of a tracing of the pre-operative X-ray. The femoral head was then positioned in Jig 1, and embedded with a rigid polyurethane foam to maintain the correct position during cutting.

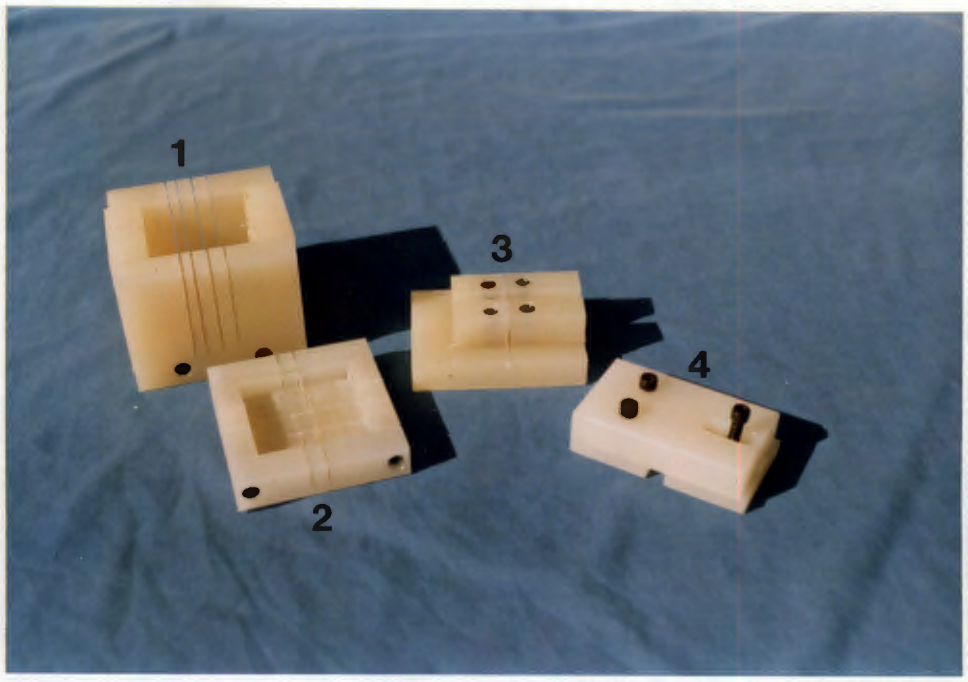

Photo 4.1 Jigs used to prepare the specimens.

The femoral head was positioned in such a way that the slices of bone were cut in the **frontal plane**. The frozen bone / polyurethane composite was then cut with a hacksaw. This step resulted in three slices of bone (Photo 4.2).

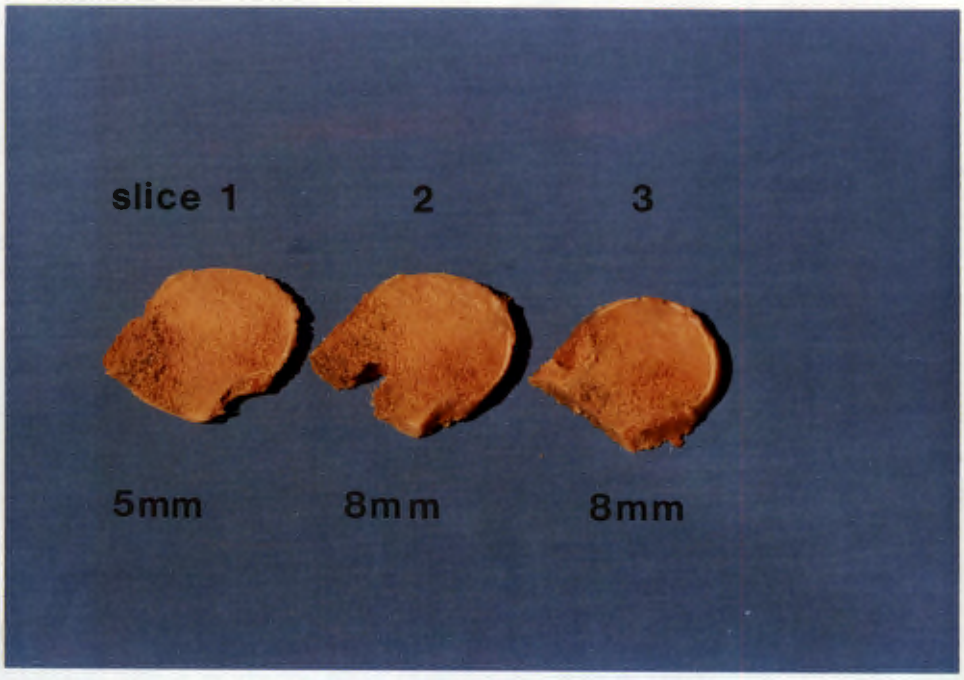

Photo 4.2 The three slices of bone taken from each femoral head.

Slice 1 was 5 mm thick and would be used for the preparation of microscope slides for morphometry. Slice 2 was perfectly aligned with the fovea capitus and the calcar femorale. Both slices 2 and 3 were each 8 mm thick, and would be used to fabricate the cubes for compression testing.

Each of these slices was then reoriented in Jig 2 so that the section containing the compressive trabeculae (corresponding to the region of principal stress) could be removed. Each bone slice was again kept in position with polyurethane foam. From Slice 1, a 15 mm wide section was removed and from slices 2 and 3 an 8mm wide section was removed (Photo 4.3). The 15mm wide section was then subdivided into 2 blocks, the first block containing bone from the proximal part of the femoral head, and the second block containing mainly compressive trabeculae (Photo 4.4).

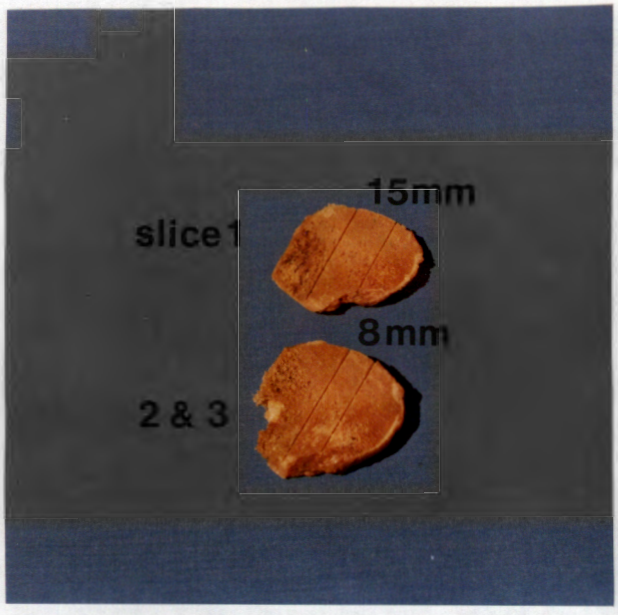

Photo 4.3 Columns of bone removed from each slice.

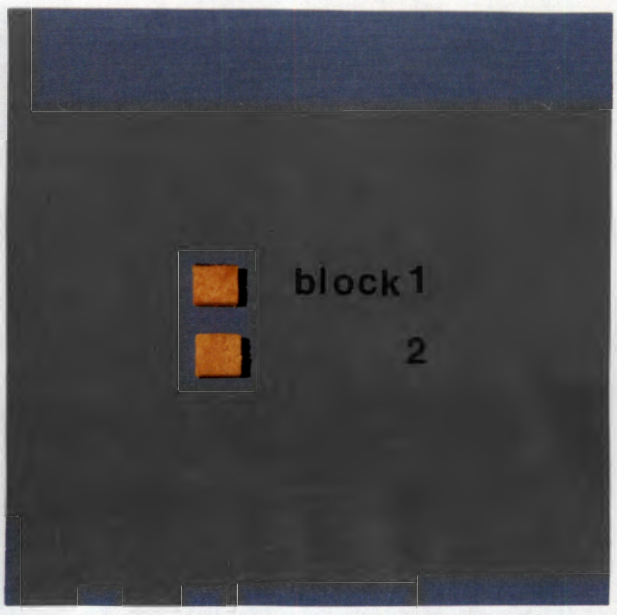

Photo 4.4 The two blocks of bone to be used for morphometry.

The 8mm wide columns of bone were then cut into 8mm cubes using Jig 3 (Photo 4.5). The cartilage (if there was any), and the subchondral plate were always removed carefully before the first cube was cut. Once all the required cubes were cut, they were finished off on fine glass paper using Jig 4 (Photo 4.6). This step ensured

that all cubes were a standard size, and that the opposite sides were parallel.

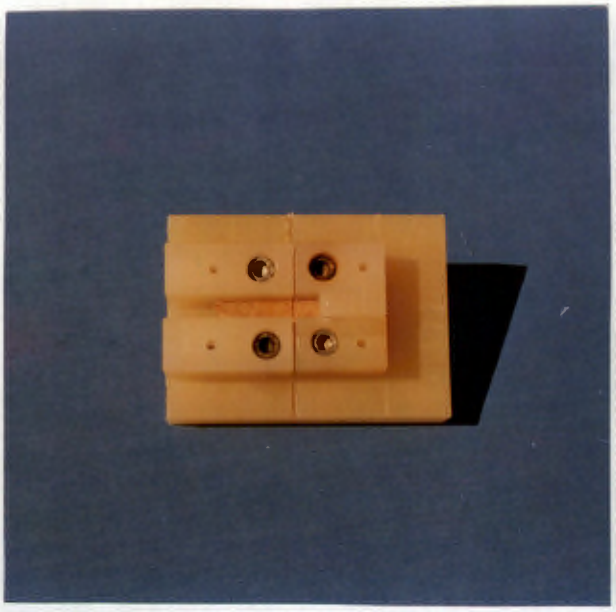

Photo 4.5 Cutting the bone cubes for Mechanical Testing.

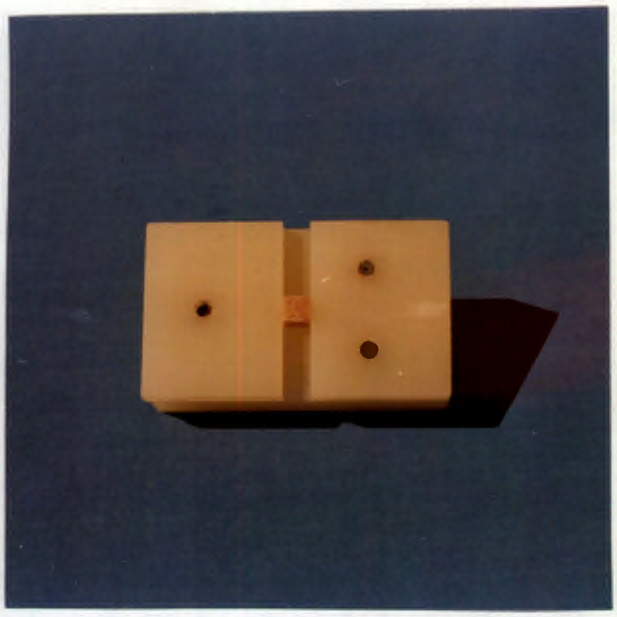

Photo 4.6 Jig 4, used to hold cube for final finishing-off.

The resulting 8 cubes were then numbered according to the layout in Fig.4.1, and the superior surface of each cube was marked.

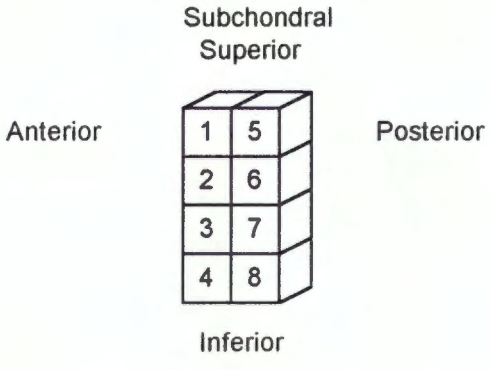

Fig.4.1 Bone cubes that would be used for Mechanical Testing.

The cubes were then washed in saline to remove any loose particles, and measured using a screw micrometer (Moore & Wright, Sheffield, England). During all the following stages the cubes for mechanical testing were stored in saline, in a refrigerator. The blocks for the preparation of microscope slides were immediately

placed in 90% alcohol and further processed according to the method described in Appendix C.

4.4 BONE MINERAL DENSITY

The bone mineral content of the bone cubes was measured using a Hologic QDR-1000 X-Ray Bone Densitometer (Hologic Inc. Waltham Masachusetts), shown in the photograph below. The system's calibration was checked before each session.

Photo 4.7 The Hologic QDR-1000 X-Ray Bone Densitometer.

This technique requires that the bone be surrounded by a soft-tissue substitute. For practical purposes, saline was used as it has X-ray attenuation properties similar to human soft tissue. A perspex box with sides 15 cm in height and width was manufactured, and an 8 mm wide strip of thin (1.5mm) perspex was mounted in this perspex tank, at a height 8 cm above the base of the box. This tank was filled with saline, and the bone cubes were mounted on the narrow perspex strip (Photo 4.8).
The bone cubes were scanned 4 at a time, at the end of each scan the computer was used to analyse the data and determine the BMC of each individual cube, the results

were printed (Fig.4.2).

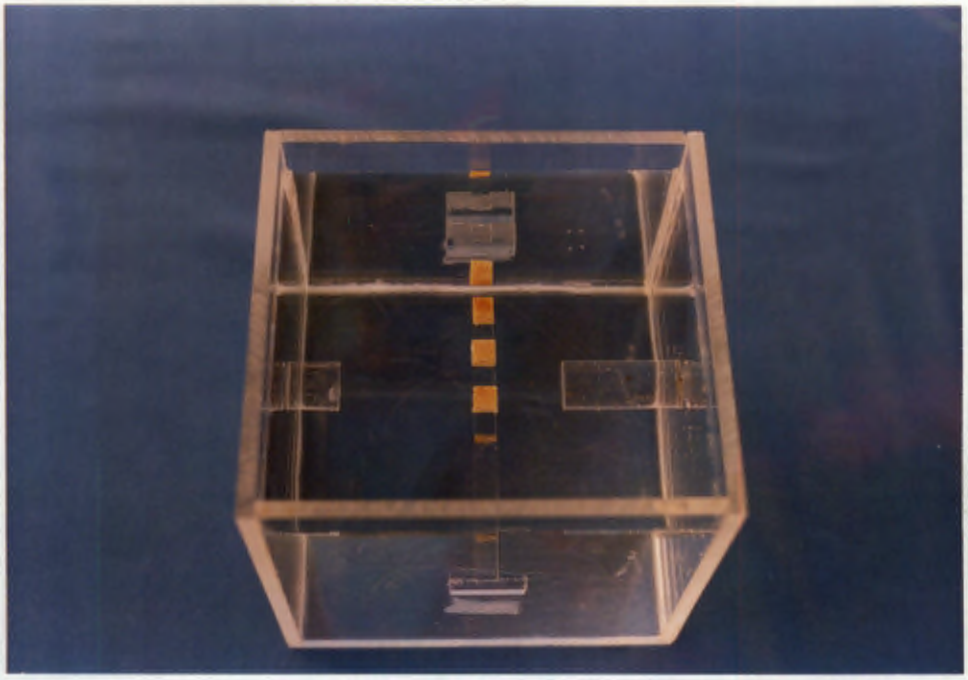

Photo 4.8 Perspex container used for Dual Energy X-Ray Absorptiometry.

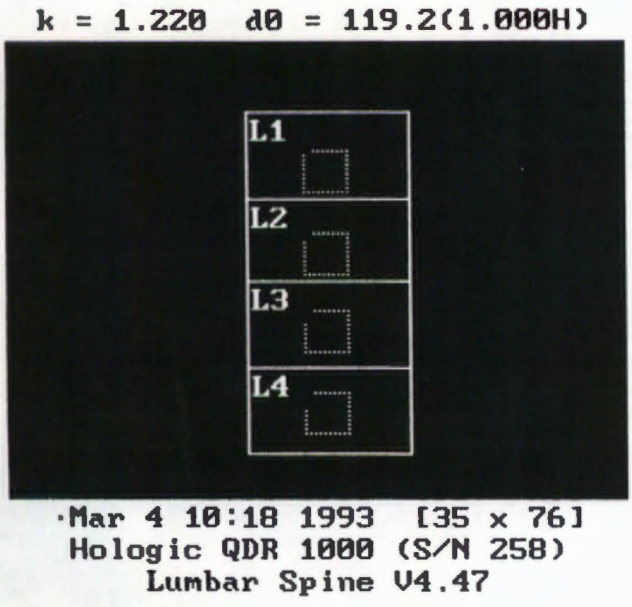

N03049302 Thu Mar 4 10:04 1993
Name: BONE SPECIMENS
Comment:
I.D.: Sex: F
S.S.#: - - Ethnic:
ZIPCode: B.M.E Height: cm
Scan Code: LB Weight: kg
BirthDate: / / Age:
Physician:

TOTAL BMD CV FOR L1 - L4 1.0%

C.F.	1.006	1.058	1.000

Region	Area (cm^2)	BMC (grams)	BMD (gms/cm^2)
L1	0.97	0.15	0.155
L2	0.97	0.12	0.120
L3	0.97	0.11	0.117
L4	0.97	0.10	0.105
TOTAL	3.90	0.48	0.124

Fig. 4.2 Printout from the QDR-1000 X-Ray Absorptiometer.

It was mentioned earlier that DEXA was developed to assess the progress of osteoporosis in patients. The software used in the analysis of bone mineral density in-vivo, is specifically designed to measure the areal density in the lumbar spine, and in regions of interest in the proximal femur. For the proximal femur analysis, the regions of interest (eg. Ward's Triangle) are positioned automatically according to the software. The lumbar spine analysis software however, permits the operator to position regions of interest interactively. Because this study involved **in-vitro** determination of BMC in bone cubes, the lumbar spine software was used so that the operator could position the areas to be analysed interactively, to correspond with the exact position of the bone cubes.

The area allocated for each bone cube was $97mm^2$, this was slightly larger than the actual cubes, but ensured that the system could find as much bone as possible and prevented under-estimation of the bone mineral content. This system uses a rectilinear scanning method and generates BMD results as g/cm^2. Because the author had determined the volume of each cube the BMC was divided by the volume of the cube in order to provide the BMD in g/cm^3, which is the way it is referred to in the literature.

4.5 PREDICTION OF ULTIMATE STRENGTH

The mechanical properties of cancellous bone should be determined on specimens that have been prestressed (Linde et al.1987). In order to prestress the bone one needs to be able to predict the Ultimate Strength of each cube. This can be achieved by determining the relationship between BMD and Ultimate Strength. For this purpose the BMD and Ultimate Strength of 50 bone cubes (from 5 femoral heads) were measured. The details of this preliminary experiment are provided in Appendix C. The statistical package used to determine this relationship was Statsgraphics version 5 (Statistical Graphics Corporation, Inc). The equation relating Ultimate Strength to BMD was found to be:

$$\text{Predicted } \sigma_{ult} = 55.149\ (BMD)^{1.467}$$

where : σ_{ult} is the predicted strength for each bone cube (MPa)

BMD is the bone mineral density for each bone cube as calculated from the bone mineral content measured using DEXA (g/cm^3).

This equation was used to predict 50% ultimate strength which is reported to be a safe stress level to use in non-destructive, repetitive loading of cancellous bone (Linde et al.1987).

4.6 COMPRESSION TESTING

The bone cubes were tested in compression in the direction of normal joint loading (supero-inferior direction). An INSTRON Universal Testing Instrument (Instron Limited, High Wycombe, England), was used (Photo 4.9). The load was measured by the calibrated load cell of the testing instrument, the load cell used in all tests allows measurement of loads to a maximum of 1000 pounds (454 kg). The system was calibrated before each testing session.

Photo 4.9 The INSTRON Universal Testing Instrument.

The cross-head travel speed was always .02 inch/min (.51 mm/min).

Specimen deformation was measured using a dial gauge attached to the load platens (Photo 4.10).

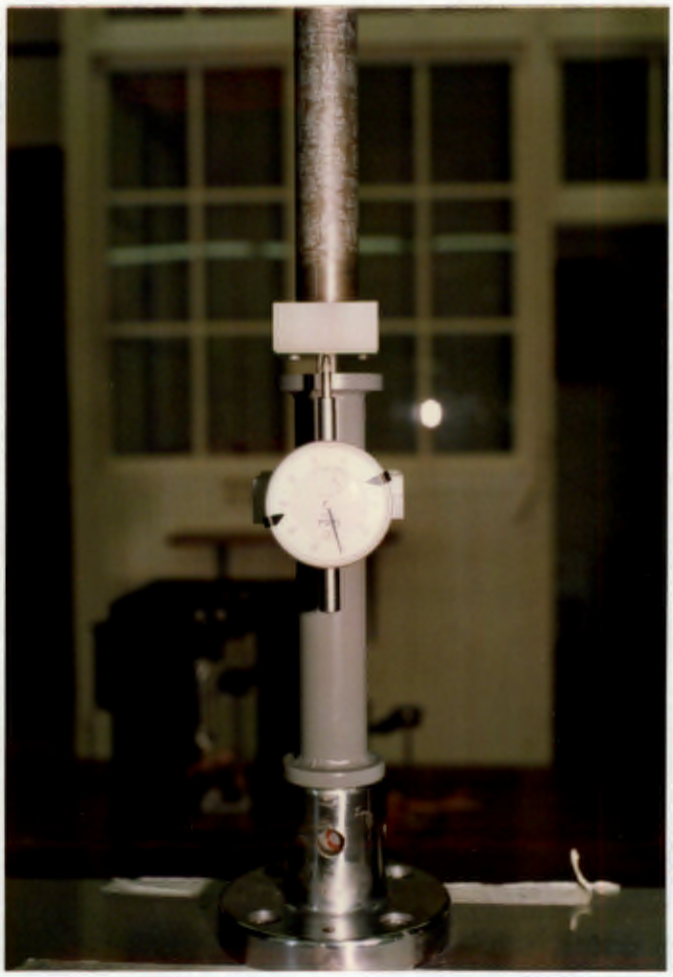

Photo 4.10 Close up view, showing the experimental set-up.

The testing procedure involved:

- 9 non-destructive load-unload cycles, compressing the bone cubes to 50% of the predicted Ultimate Strength.
- the final compression cycle was continued until the specimens were compressed to approximately 85% of their original height.

The dial gauge was used to measure the residual deformation after each compression cycle, and the deformation during the final compression cycle.

A typical recording can be seen in Fig. 4.3.

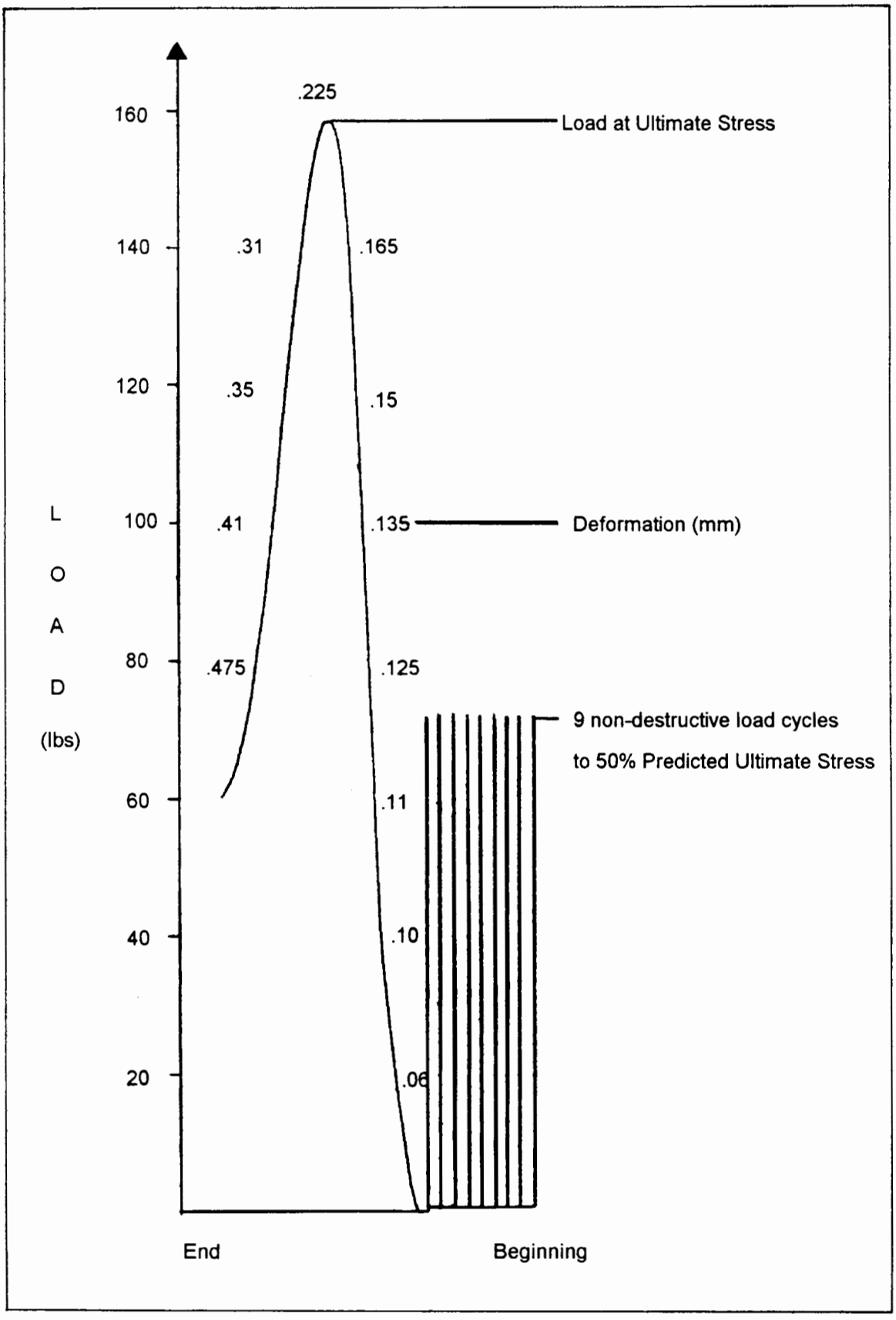

Fig. 4.3 A Typical Compression Test Recording.

The load / deformation data were entered into a personal computer and converted into stress / strain values using a spreadsheet package (Excel, Microsoft Corporation):

Stress was calculated in the standard manner:

$$\sigma = F / A$$

where: σ is stress in MPa

F is Force in Newtons

A is the area in mm^2

Strain was calculated in the following way:

$$\varepsilon = \Delta L / L$$

where: ε is strain (mm/mm)

Δ L is the deformation (mm)

L is the height of the specimen prior to the final compression cycle (mm).

A stress-strain curve for the final destructive load cycle was plotted for each cube (Fig 4.4). Zero stress was taken to equal zero strain.

Ultimate Strength was computed from the first peak of the stress-strain curve.

Young's Modulus was computed from the linear portion of the stress-strain curve, between 40 and 60% of ultimate strength, because this coincides with the steepest part of the stress-strain curves (Linde et al 1987). The Modulus was then calculated in the standard way:

$$E = \Delta\sigma / \Delta\varepsilon$$

where: E is Young's Modulus (MPa).

$\Delta\sigma$ is the change in stress (MPa)

$\Delta\varepsilon$ is the change in strain

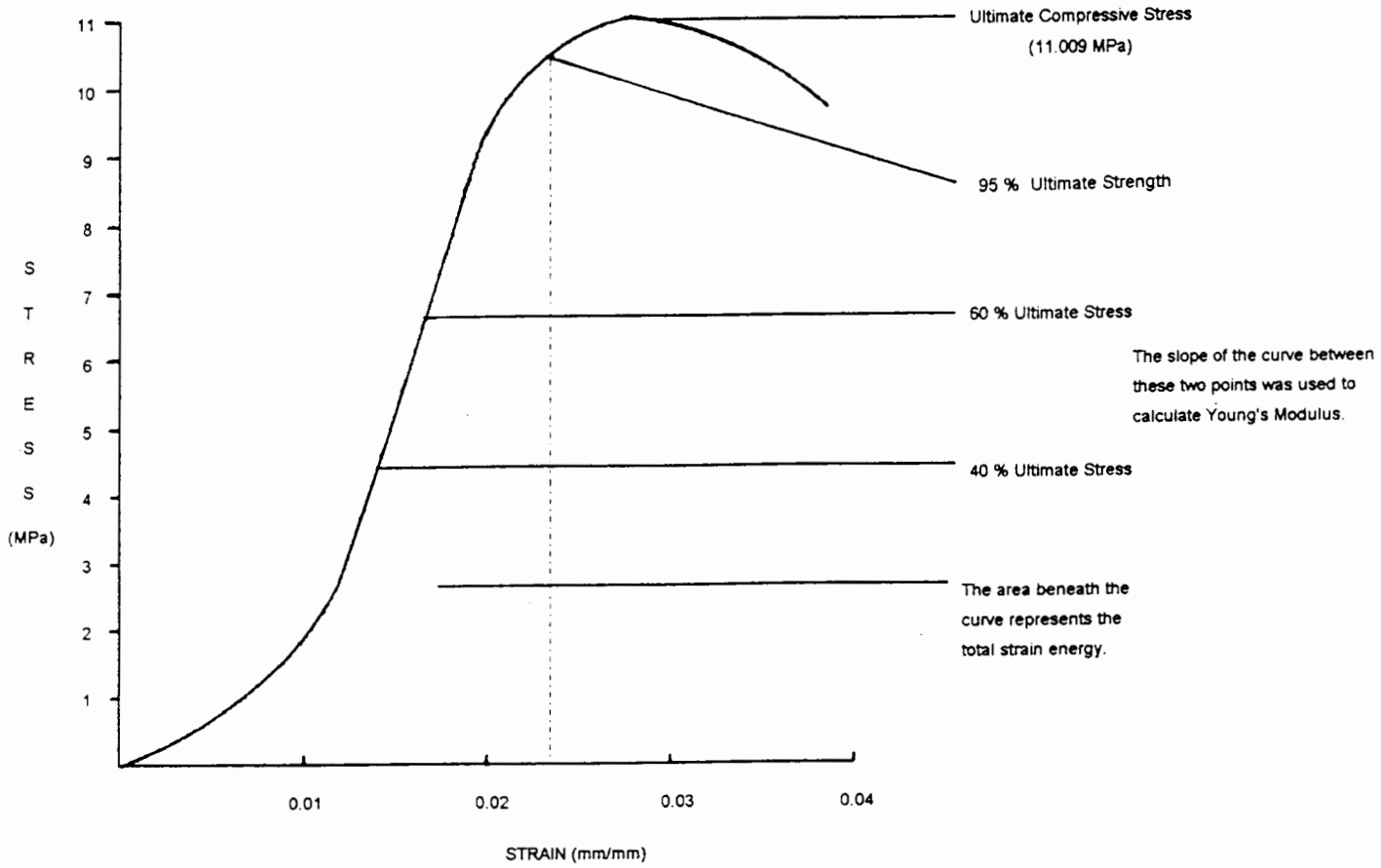

Fig. 4.4 An example of a typical Stress-Strain Curve.

Strain Energy Density was calculated by determining the area beneath each stress-strain curve. In this study, the strain energy density up to 95% of ultimate strength was measured. This point was chosen, as the peak of the curve sometimes forms a small plateau.

As an object is deformed, the kinetic energy is converted into Strain Energy. The area beneath the curve represents the total Strain Energy, which actually consists of two parts:

- the area beneath the elastic part of the curve which is largely **recoverable** (stored strain energy)
- the area beneath the plastic deformation part of the curve, which is termed **absorbed** strain energy, since this part is absorbed or dissipated in the process of producing permanent deformation.

4.7 APPARENT DENSITY

The apparent density is defined as the mass of the cancellous bone structure (free of marrow fat) divided by the bulk volume of the specimen (as measured before mechanical testing). It is important that all the fat is removed and that the actual bone structure is properly hydrated if this parameter is to be determined correctly. Sharp et al.(1990) suggested the following method:

1. After mechanical Testing the specimens are defatted in trichlorethylene in an ultrasound bath for 4 hours.
2. The specimens are washed under running water to remove any remaining chemical.
3. The specimens are rehydrated in distilled water, under vacuum for 4 hours.
4. The specimens are then centrifuged on blotting paper at 4000 r.p.m. for 15 minutes to remove any intertrabecular water.
5. The specimens are each weighed in air to determine the hydrated tissue mass.
6. The hydrated tissue mass is divided by the bulk volume of the specimen.

This method was followed exactly, except for the first step. The author did not have access to an ultrasound bath, so instead, the marrow fat was first removed with a compressed air jet, and then the specimens left in trichlorethylene heated to 65°C for one hour to remove the remaining fat. The specimens were finally weighed using an accurate balance (Zeiss Optical Instruments (Pty) Ltd, West Germany), and apparent density was then calculated in the standard way:

$$\rho = \text{hydrated tissue mass (g)} \; / \; \text{bulk volume of specimen (cm}^3\text{)}$$

where: ρ is the apparent density (g/cm^3).

4.8 CANCELLOUS BONE STRUCTURE

Following the removal of the marrow fat, it became obvious that the structure of cancellous bone varied considerably from the subchondral region down to the compressive trabeculae, especially in the osteoarthritic bone. The structural differences which had been described by Whitehouse and Dyson (1974) were clearly visible.

The structural differences could have an affect on the mechanical behaviour as was pointed out by Gibson (1985), and Gibson and Ashby (1987). This could affect the dependence of the mechanical relationships on the apparent density, and would have to be taken into consideration when analysing the results. (For this reason this section has been included in the methodology section). The section that follows contains photographs that are representative of the structural patterns that were observed.

The first structural pattern (which was called **structure 1**) resembled an equiaxed network of trabeculae (Photo 4.11). This structure only occurred in the subchondral region (in OA) and varied in density for different individuals.

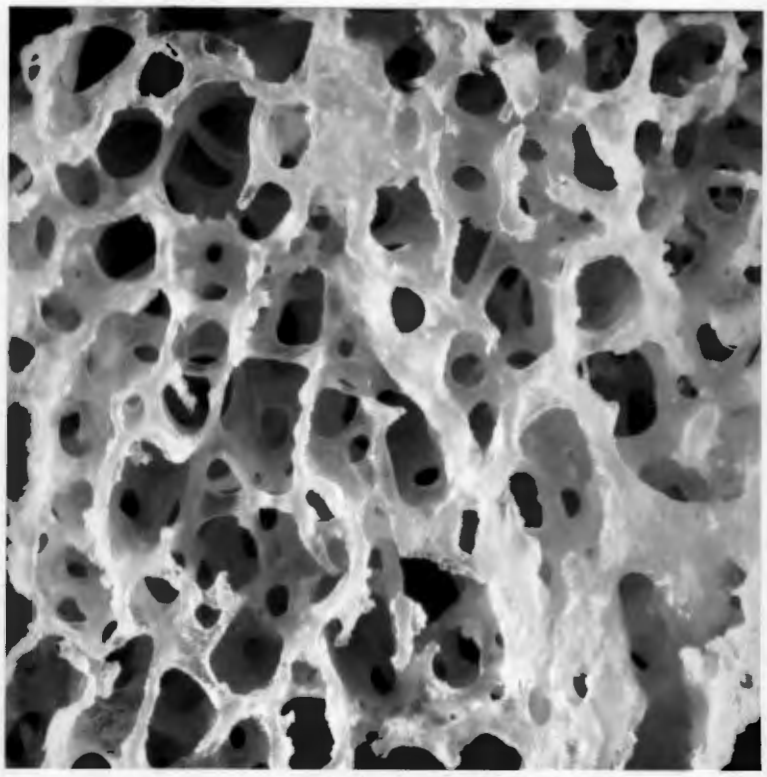

Photo 4.11 The equiaxed structure seen in the subchondral region. Original Magnification 10x. (Case 3, Female OA).

The second structural pattern (**structure 2**), had a partially oriented structure (Photo 4.12) . It was often found in the subchondral region in place of the equiaxed structure, but occurred mainly in the central region of the femoral head.

Photo 4.12 Partially oriented cancellous bone. Original magnification 10x. (Case 10, female OA)

In the region of the compressive trabeculae, the structure of the cancellous bone became highly anisotropic, this was called **structure 3**.

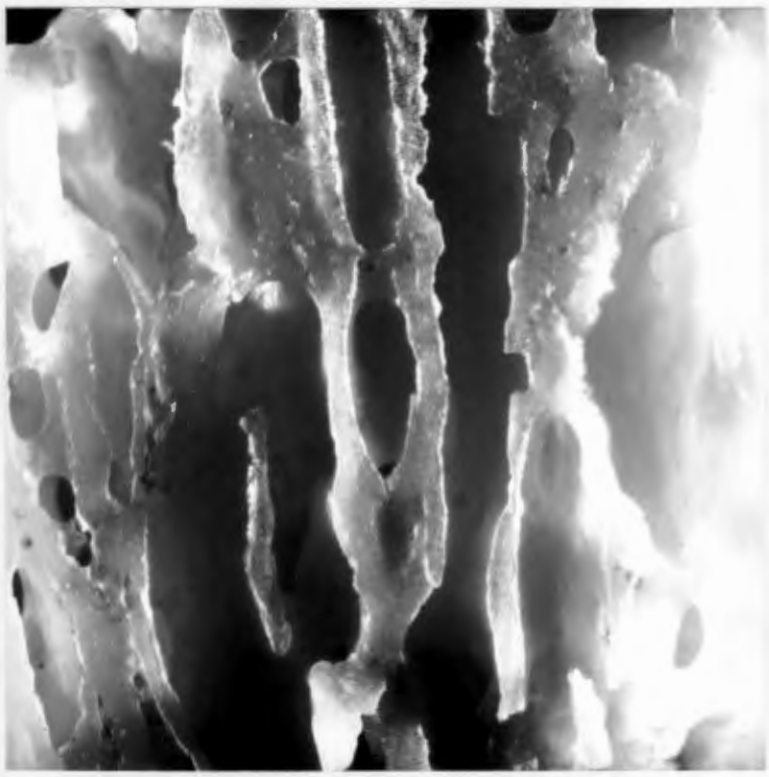

Photo 4.13 The cylindrical arrangement . Original Magnification 10x.
(Case 25, male OA)

Photo 4.14 Rods and Plates structure . Original Magnification 10x.
(Case 26, Male OA)

It consisted of a cylindrical arrangement (Photo 4.13), or a system of plates joined by transverse rods (Photo 4.14). The cylinders or the parallel plates were aligned in the direction of the compressive force acting on the femoral head, so as to transmit the stress to the calcar femorale.

The **RA bone** generally presented a very dense, partially oriented bone structure, often becoming anisotropic in the region of the compressive trabeculae. The equiaxed structure was never seen in this condition.

The cancellous bone cubes in this study were thus all carefully examined and classified into the three structural groups. This study was however, not aimed at analysing the degree of anisotropy in cancellous bone in the femoral head. To do this one would have to defat the bone to allow measurement of stereological features before compression testing. The process of determining the degree of textural symmetry is very lengthy. For these reasons the classification of the cancellous bone was done qualitatively.

4.9 CANCELLOUS BONE MORPHOLOGY

4.9.1 Preparation of the Microscope Slides

As was described in section 4.3, two blocks of bone were removed from each femoral head, to be used for making microscope slides. During the fabrication process these blocks were marked so that the slices for image analysis would be taken from the surface neighbouring cubes 1, 2, 3 and 4 used for mechanical testing. These blocks of bone were immediately placed in 90% ethanol and processed for the making of undecalcified bone sections. Details of the method are provided in Appendix D. The pieces of bone were embedded in methylmethacrylate and the bone / methylmethacrylate composite was sectioned using a Jung Polycut 5000 Microtome (Reichert-Jung, Heidelberg, Germany).

Photo 4.15 The Jung Polycut 5000 Microtome.

After "rough trimming", sections 10μm thick were cut for the manufacture of slides. A total of 200 sections were cut from each block, of these 10 slices were randomly selected (5 from each 100), and these slices were made into microscope slides and stained with Toluidine Blue.

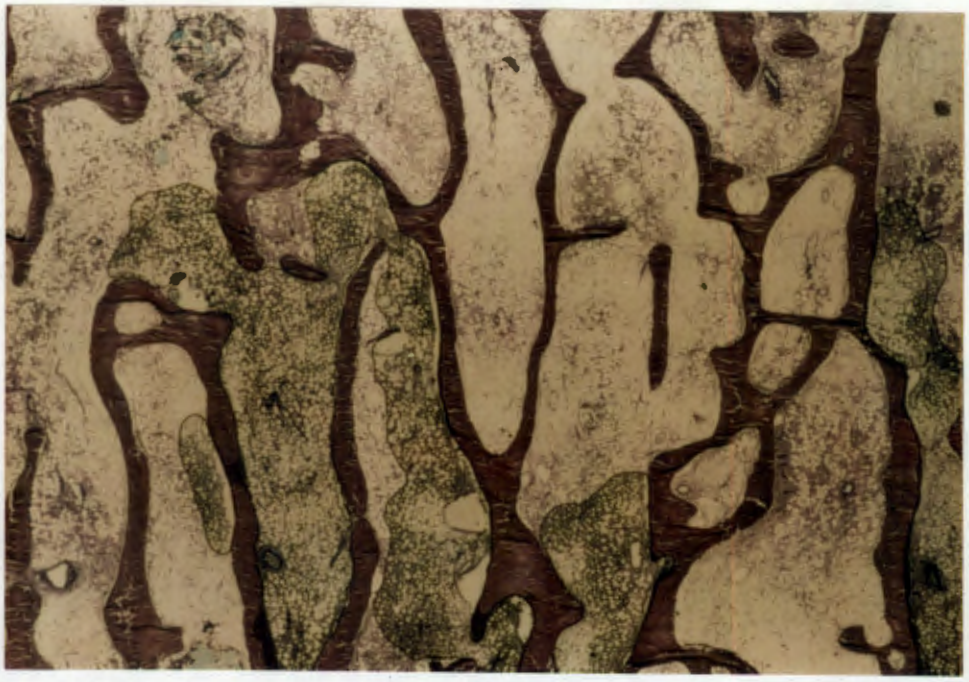

Photo 4.16 A bone section stained with Toluidine Blue.

This stains calcified bone tissue dark purple and the remaining soft tissue light blue. This stain provides adequate contrast for image analysis. The effects of this stain can be seen in Photo 4.16.

4.9.2 Image Analysis and Stereology:

The image analysis was done with a General Image Analysis System (Joyce Loebl, England). It consists of a macroviewer (light box), an IBM computer, with a TMS 320C25 DSP image analysis processor. The system's spatial resolution is 512 x 512 pixels and has 256 grey levels. The system also has a mathematics co-processor and an optical disk. There is one text screen and one image monitor (Photo 4.17). A monochrome Hitachi KP-140 solid state video camera equipped with a Macro Takumar Lens (1:4-50 ASAHI Optical Company) was used to capture the images. The system was calibrated before use, and all images were viewed at a 40x magnification. When doing image analysis of cancellous bone a low magnification is preferential (Smith and Jee 1982) as a high magnification leads to very large

perimeter measurements, as all the microscopic surface irregularities are also measured.

Photo 4.17 The Joyce Loebl Image Analysis System.

Although 10 microscope slides were made from each region for each individual, only slides that showed no obvious distortions, bone dust or perforations were used in the final analysis. For each region (in each individual) a total of 9 fields was analysed. The nine fields were usually taken from three slides. The list of steps that was executed is provided in Appendix E.

Measurements and Calculations:

There were three basic measurements that had to be made on each field, these were:

1. Size of the **reference area**, this was 21.24 mm^2 in all cases, and this measurement was named A_R.
2. Size of the **area occupied by bone**, within the reference field, this was called A_B and was given in mm^2.

3. The length of the **perimeter of the bone areas** in each field, this was named P_B in all calculations and was in mm.

From these basic measurements all the following variables could be calculated.

Area Fraction:

This represents what percentage of the reference area is occupied by bone, and is calculated in the following way:

$$A_{AB} = A_B / A_R$$

where: A_{AB} is the percentage of the area that is occupied by bone (%).

Trabecular Bone Volume Fraction (TBV%):

According to the Principle of Deless (Chayes 1965), the ratio of two areas in a cross-section of a test material, is equal to the ratio of the two volumes in that test material, therefore one may say:

$$V_V = A_{AB}$$

where: V_V is the percentage of the total volume that is occupied by bone.

Alternatively one may say:

$$TBV\ (\%) = A_B / A_R$$

where: TBV is the trabecular bone volume (%).

The TBV is a useful index which differs significantly with age, gender, and with pathologies such as osteoporosis (Parfitt et al. 1983). The method of determining the volume fraction by measuring the area fraction was verified by Chayes (1965).

Surface Area Density (S_V):

The surface area of the bone marrow interface is a three dimensional parameter and is calculated in the following way:

$$S_V = k\ (P_B / A_R)$$

where: S_V is the surface area per unit volume of tissue (mm^2/mm^3)

k is a scaling factor, if the structure is isotropic, its value is 1.273, if the structure is anisotropic, consisting mainly of plates, a value of 1.199 is used (Schwartz and Recker 1981).

Mean Trabecular Width (MTW):

This is a two dimensional parameter, used to estimate the mean width of the trabecular bands as seen in a thin section. It is important to realise that the MTW may be slightly wider than the actual trabecular thickness if the trabeculae have been cut slightly obliquely, thus the terms MTW and mean trabecular plate thickness are not synonymous. MTW can be calculated in the following manner (Parfitt 1983):

$$MTW = 2000\ (A_{AB} / (P_B / A_R))$$

where: MTW is the mean trabecular width (μm).

A_{AB} is the percentage of the area occupied by bone (%)

P_B is the perimeter of the bone areas (mm)

A_R is the reference area (mm)

Mean Trabecular Thickness:

In an **isotropic** structure, the true mean trabecular thickness would be:

$$MTT = 0.785\ MTW$$

where: MTT is the mean trabecular thickness (μm)

MTW is the mean trabecular width (μm).

Parfitt et al. (1983) provide the equations for cancellous bone that is anisotropic, consisting of parallel plates.

$$MTPT = (2000 / 1.199)(A_B / P_B)$$

where: MTPT is the mean trabecular plate thickness (μm)

Trabecular Plate Spacing:

The mean distance between trabecular plates is given by the following equation (Parfitt et al. 1983):

$$MTPS = \{(2000 / 1.199)(A_R - A_B)\} / P_B$$

where: MTPS is the mean trabecular plate spacing (μm).

This expression gives the **shortest distance between the plates**, on the assumption that they are parallel. When this result is multiplied by $\pi / 2$, it gives an estimate of the **mean marrow cavity width** (Parfitt 1983).

The basic measurements (A_R, A_B, and P_B) were made with the image analysis system, and the data was then transferred to a personal computer for further processing using a spreadsheet package (Excel, Microsoft Corporation). All the equations described above were used. The cancellous bone in the sections coming from Block 1 (subchondral to mid-head) was treated as being isotropic, whilst sections from Block 2 (the principal compressive trabeculae) were considered to be anisotropic.

CHAPTER 5

RESULTS

THE MECHANICAL PROPERTIES OF CANCELLOUS BONE

Bone from the femoral heads of 12 female Osteoarthritics, 10 Male Osteoarthritics and 10 Female Rheumatoid Arthritics was used in this study. Rheumatoid Arthritis is less common in males than it is in females, and very few males required THR in 1992, so a male Rheumatoid Arthritic group could not be included in this study. The femoral heads were removed surgically during Total Hip Replacement Arthroplasty, therefore, the **results obtained in this study represent the condition of the bone at the end stages of these diseases.** The details of each individual and the bone cubes taken from each femoral head are provided in Appendix F. Statistical Analysis of the results was performed using both BMDP routine 3V (BMDP Statistical Software, Inc), and Statsgraphics version 5 (Statistical Graphics Corporation, Inc) for the less complicated analyses. Statistical significance was set at $p < .05$ for the purposes of this study.

5.1 The Results in General:

Age and Body Mass

Age and **mass** are known to affect cancellous bone structure and its mechanical properties. It was thus necessary to compare these two variables for the three groups before performing the rest of the analyses. This was done using the t-test.

The female OA patients were between 57 - 79 years of age, the male OA group was between 52 - 83 years and the RA group between 33 - 78 years of age. The range of body mass for the female OA group was 48 - 76 kg, for the male OA group it was 65 - 113 kg, and for the female RA group 35 - 100 kg at the time of the operation. The mean values and the standard deviations are given in Table 5.1. This table shows that

the **female rheumatoid arthritics** were significantly **younger** than both the osteoarthritic females and males. The **male osteoarthritics** had a significantly **greater body mass** than both the female osteo and rheumatoid arthritic groups.

Table 5.1 Mean Ages and Masses of Subjects.

Disease Group	Age (yrs)	Mass (kg)
OA Female (A)	68.58 (7.24)	63 (10.01)
OA Male (B)	66.50 (11.24)	90.6 (15.88)
RA Female (C)	50.80 (14.44)	65.2 (17.15)
A vs B	NS	A < B p < .0005
A vs C	A > C p = .0013	NS
B vs C	B > C p = .014	B > C p = .0029

Standard Deviations in parentheses. NS = not significant

These two phenomena may have influenced the outcome of the results, but these findings are probably indicative of the trend that does exist in these disease groups.

Apparent Density, BMD, Strength, Stiffness and SED:

In the female OA group, the **apparent density** of the bone cubes examined was found to range between 0.31 - 0.88 g/cm^3. In the male OA group the range of apparent density was 0.37 - 1.016 g/cm^3, and in the RA group 0.34 - 1.281 g/cm^3. The mean values are given in Table 5.2. As can be seen in this table, the mean value for OA females was significantly lower than that found in the male group and in the RA group.

Table 5.2 Mean values for the Apparent and Bone Mineral Densities and Mechanical Properties.

Disease Group	Apparent Density (g/cm^3)	BMD (g/cm^3)	Strength (MPa)	Young's Modulus (MPa)	Strain Energy Density(kJ/m^3)
OA Female (A)	0.57	0.29	11.601	666	162
OA Male (B)	0.68	0.37	16.180	1088	193
RA Female (C)	0.77	0.38	16.702	1055	224
A vs B	A < B p = .011	A < B p = .001	A < B p = .001	A < B p < .0005	A < B p = .06
A vs C	A < C p < .0005	A < C p = .002	A < C p = .001	A < C p = .002	A < C p = .007
B vs C	NS	NS	NS	NS	NS

NS = not significant

In the OA female group **Bone Mineral Density** was found to range between 0.12 - 0.47 g/cm^3. In the male OA group it ranged between 0.18 - 0.58 g/cm^3, and in the female RA group between 0.18 and 0.68 g/cm^3. Again the mean value for the female OA group was significantly lower than in either the OA male or the RA female groups.

The **strength** found in the OA female group ranged between 4.515 - 24.759 MPa, for males the range extended from 5.958 - 27.347 MPa, and for the female RA group from 4.368 - 30.788 MPa. The mean value for the female OA group was again the lowest, and significantly so.

Young's Modulus followed much the same trend with the mean value for the female OA group being significantly less than for the other two groups. The range of values found in the OA female group was between 148 - 1849 MPa, for the male group the range was much higher, 238 - 2503 MPa. The female RA group also ranged between 218 - 2123 MPa.

Finally, **Strain Energy Density** in the female OA group was found to lie between 51 - 354 kJ/m^3, for males the range was between 68 - 516 kJ/m^3 and RA females 74 - 585 kJ/m^3. Thus, the male OA and female RA groups had significantly higher mean values than the female OA group.

It must be pointed out that the data for these last three variables was **not normally distributed** about the mean, therefore, in order to ensure approximate normality these three variables had to be **log transformed** before hypothesis testing could be carried out. The standard deviations have been omitted from the table because they are not very meaningful if the variance is not normally distributed about the mean.

The **distribution of the bone properties** through the eight blocks measured in the femoral heads is shown in the bar charts that follow (Fig. 5.1 a-d). These represent the properties for OA bone, including both males and females.

Fig. 5.1 The mean values found for Blocks 1-8 in OA (males and females).

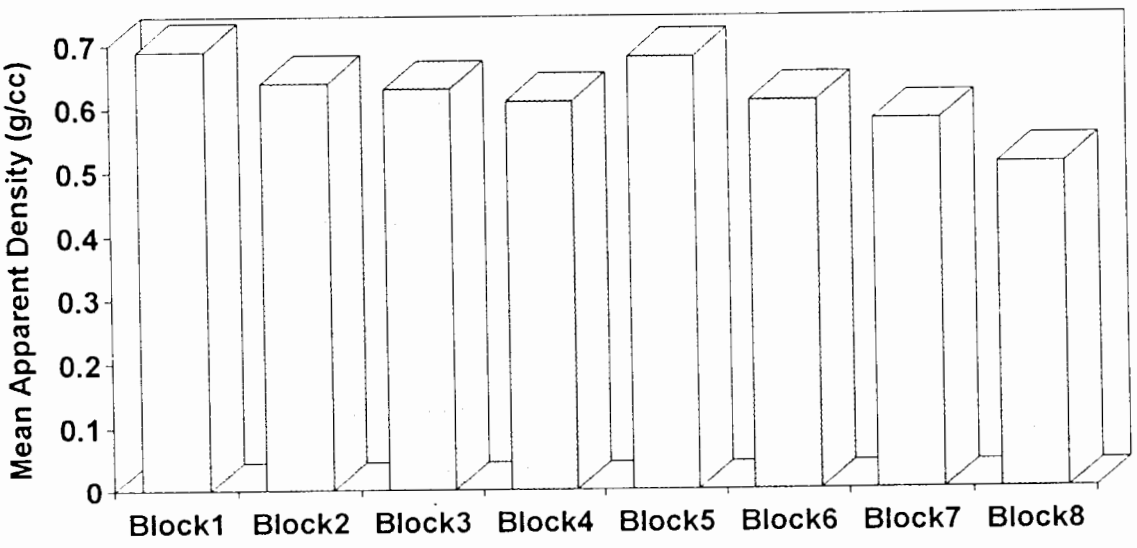

a. Mean Apparent density.

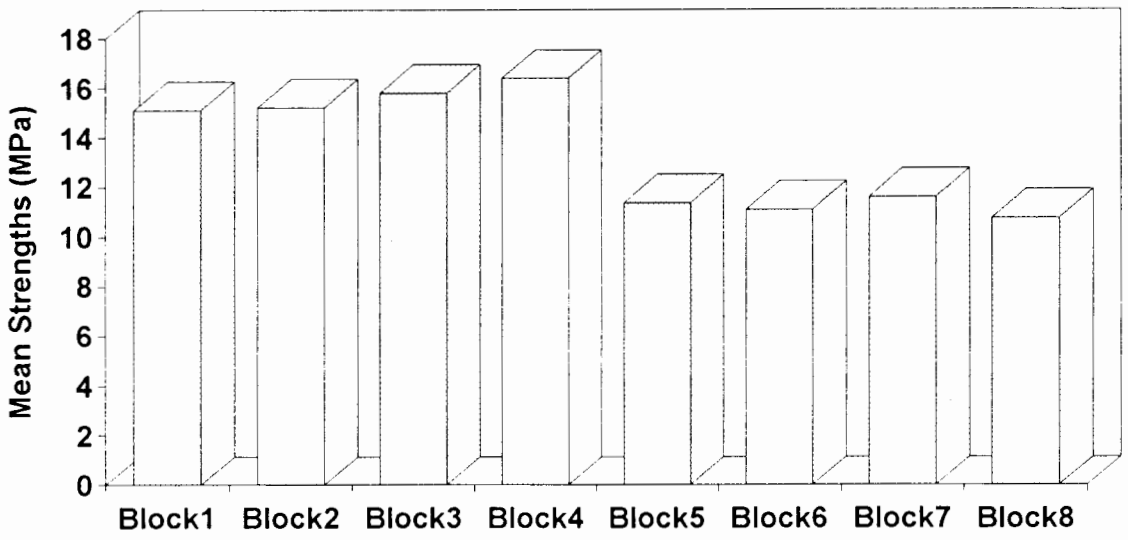

b. Mean Strength

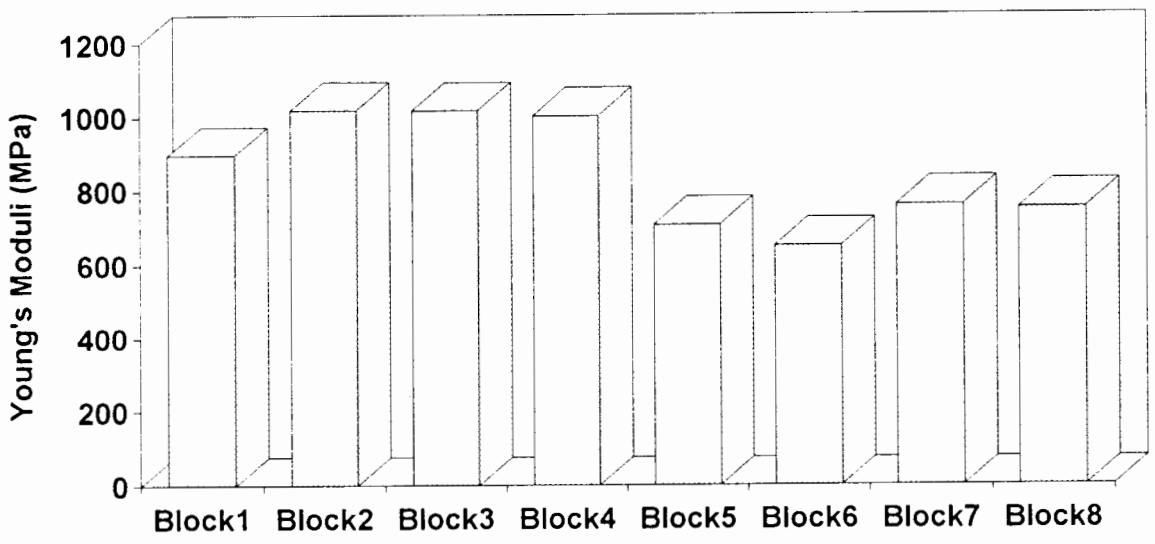

c. Mean Young's Modulus

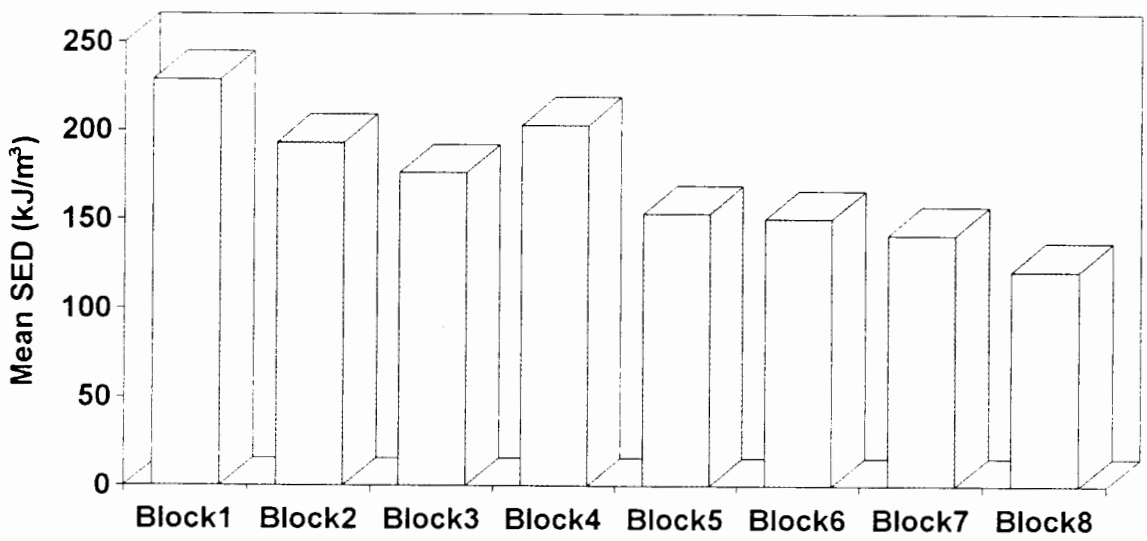

d. Mean Strain Energy Density

The results for the female RA bone can be seen below (Fig. 5.2 a-d). Results for cubes 4, 5 and 8 were not included in these barcharts because they could only be obtained in very few femoral heads (there were three Block 4's, two Block 5's and no Block 8's). The femoral heads are much smaller in RA than in OA, due to the destructive nature of the disease.

Fig. 5.2 The mean values found for Blocks 1-8 in RA .

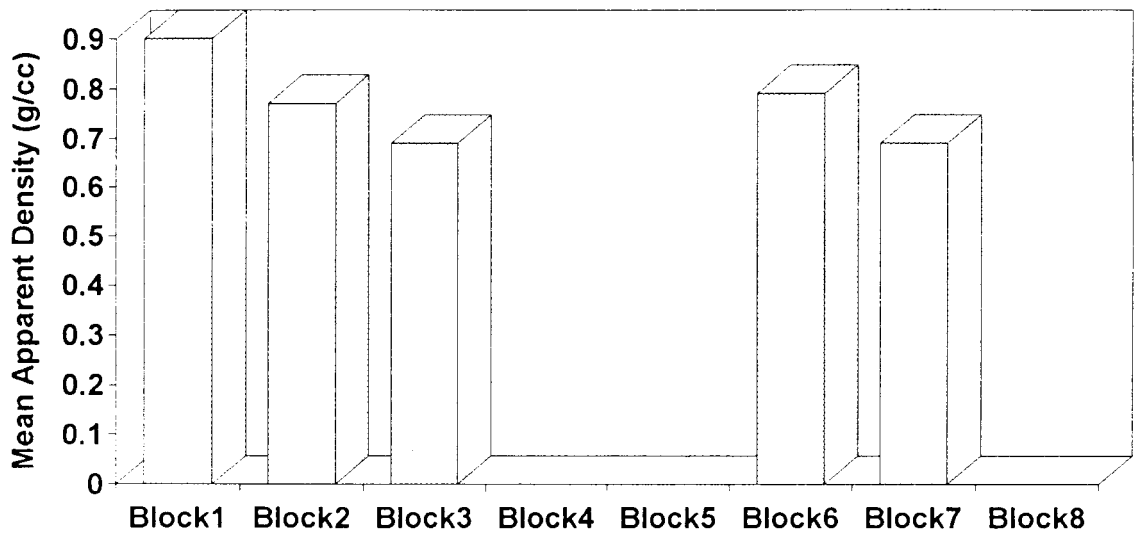

a. Mean Apparent Density.

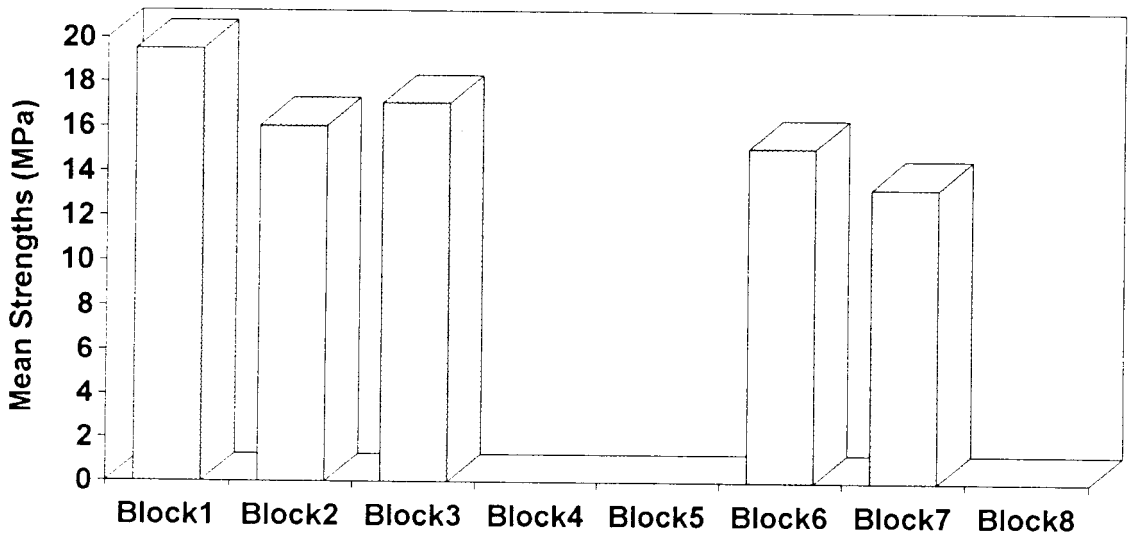

b. Mean Strength.

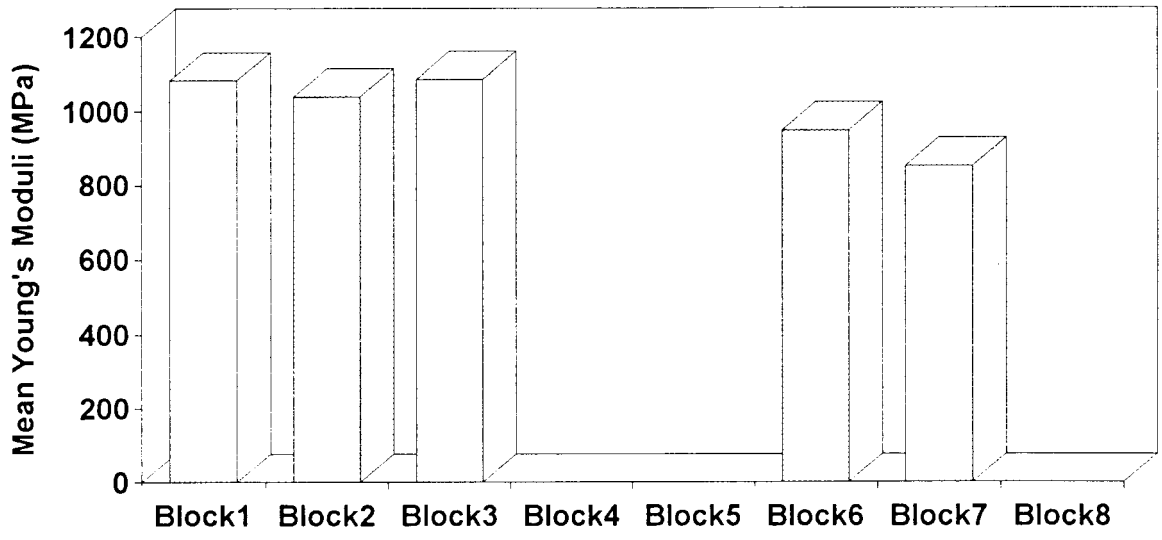

c. Mean Young's Modulus

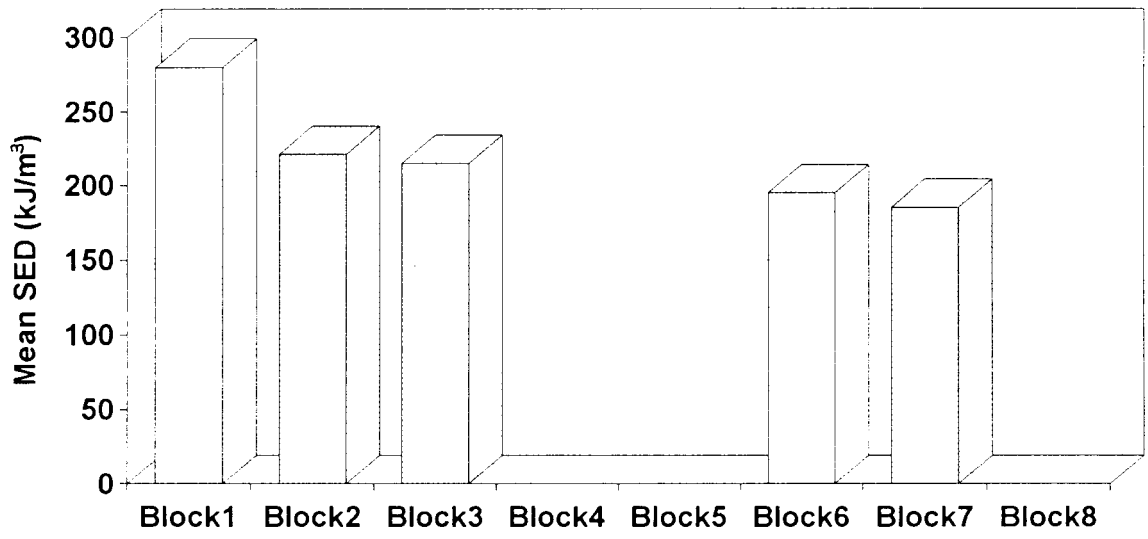

d. Mean Strain Energy Density.

5.2 Relationships between Apparent Density, BMD and Mechanical Properties.

The next step involved determining the nature of the relationships that exist between these variables, specifically for diseased bone. These analyses were carried out in collaboration with the Statistics Department (UCT), using the BMDP routine 3V (BMDP Statistical Software, Inc). The following bivariate relationships were considered:

1. the relationship between Apparent Density and Bone Mineral Density as measured using Dual Energy X-Ray Absorptiometry (in-vitro).
2. the relationships between Strength, Young's Modulus , Strain Energy Density and Apparent Density.
3. the relationships between Strength, Young's Modulus and Bone Mineral Density.
4. the relationship between Young's Modulus and Strength.
5. the relationship between Strain Energy Density and Strength.

In fitting regression models to these data, we allowed for adjustments for the possible effects of gender, and the structural arrangement of the cancellous bone (whether it was equiaxed, partially oriented or highly anisotropic). Allowance was also made for the correlation of observations within individuals.

Firstly the data from the Osteoarthritics was analysed using the following regression model:

$$Y_{ijkl} = \mu + \alpha_i + \beta_j + (\alpha\beta)_{ij} + c_{ik} + d_{ijk} + \gamma_{ij} X_{ijkl} + e_{ijkl}$$

where: Y_{ijkl} is the dependent variable (eg. Strength)

X_{ijkl} is the independent variable (eg. Apparent Density)

{i = 1, 2 (gender);

j = 1, 2, 3 (structure);

k = 1, 2,...n_i (n_i is the number of subjects in the group);

l = 1, 2, ...m_k (m_k is the number of observations per individual)}

μ is the intercept

α_i is the gender adjustment to the intercept (i = 1 females,

2 males)

β_j is the structure adjustment to the intercept (j = 1 equiaxed, 2 partially oriented , 3 highly anisotropic)

$(\alpha\beta)_{ij}$ is the gender - structure interaction to the intercept

γ_{ij} is the slope adjustment for gender and structure

c_{ik} is the between structure variability

d_{ijk} is the within structure variability

e_{ijkl} is the residual

It is assumed that :

$c_{ik} \sim N(0, \sigma_c^2)$

$d_{ijk} \sim N(0, \sigma_d^2)$

$e_{ijkl} \sim N(0, \sigma_e^2)$

and that they are independent. It is the inclusion of the variance components: σ_c^2 and σ_d^2 which allow for correlation of repeated measures on the same individual both between and within structures.

The normality of the residuals was assessed after the model fitting.

Following the analysis of all the OA bone results, it was found that gender had no effect on the relationships. So, when analysing the results of the Rheumatoid Arthritic, female group, their results were compared to the female Osteoarthtritic Group, by simply replacing the gender adjustments (in the model above) with a disease adjustment, either OA or RA. There were fewer cubes of Rheumatoid Arthritic bone, mainly because the femoral heads are very small in this condition possibly due to the collapse of the trabecular bone (Sambrook et al.1990). Almost all the cubes had the same type of asymmetric bone structure , so the structure adjustment which was used in the first regression model was not required in the second model. A simpler regression model could thus be used :

$$Y_{ijk} = \mu + \alpha_i + b_{ij} + \gamma_i X_{ijk} + e_{ijk}$$

where : Y_{ijk} is the dependent variable

X_{ijk} is the independent variable

μ is the intercept

α_i is the disease adjustment to the intercept (i = 1 osteoarthritis,

2 rheumatoid arthritis)

b_{ij} is the within patient variability, where it is assumed that $b_{ij} \sim N(0,\sigma_b^2)$

e_{ijk} is the residual, where it is assumed that $e_{ijk} \sim N(0,\sigma_e^2)$

γ_i is the slope adjustment for disease

For both the OA and the RA groups only the relationship between apparent density and bone mineral density could be analysed by applying these models directly to the variables. In the rest of the analyses the variables first had to be logged before a model of the above form could be fitted to the transformed data. This then corresponds to the form $Y = a X^b$. Logarithms to the base 10 were used throughout. It is obvious that this model would pass through zero, which would not happen in reality (Rice et al 1988), so these relationships are only valid over the observed ranges of X, and care must be taken when extrapolating beyond the observed ranges.

In the following analyses, results for which the associated p - values were less than 0.05 are referred to as "significant".

The results found for Osteoarthritic and Rheumatoid Arthritic bone will be discussed together, under the sub - heading for each relationship that was assessed. Certain scatterplots of the raw data have been included in this section, but it was disruptive to include them all. Those that do not appear in the following section can be seen in Appendix H.

5.2.1 Apparent Density vs Bone Mineral Density

A linear relationship was found to exist between these two variables. For OA bone the general relationship was found to be :

$$\rho = 0.123 + 1.526\ BMD \qquad p < .0005$$

However, the structure of the OA bone was found to have a significant effect on the slope of this relationship (Fig. 5.3a).

$$\rho = 0.14 + \hat{\beta}\ BMD$$

where : β is the slope.

For structure 1 $\hat{\beta} = 1.579$ $p < .0005$

For structure 2 $\hat{\beta} = 1.452$ $p = .007$ (cf. structure 1)

For structure 3 $\hat{\beta} = 1.371$ $p < .0005$ (cf. structure 1)

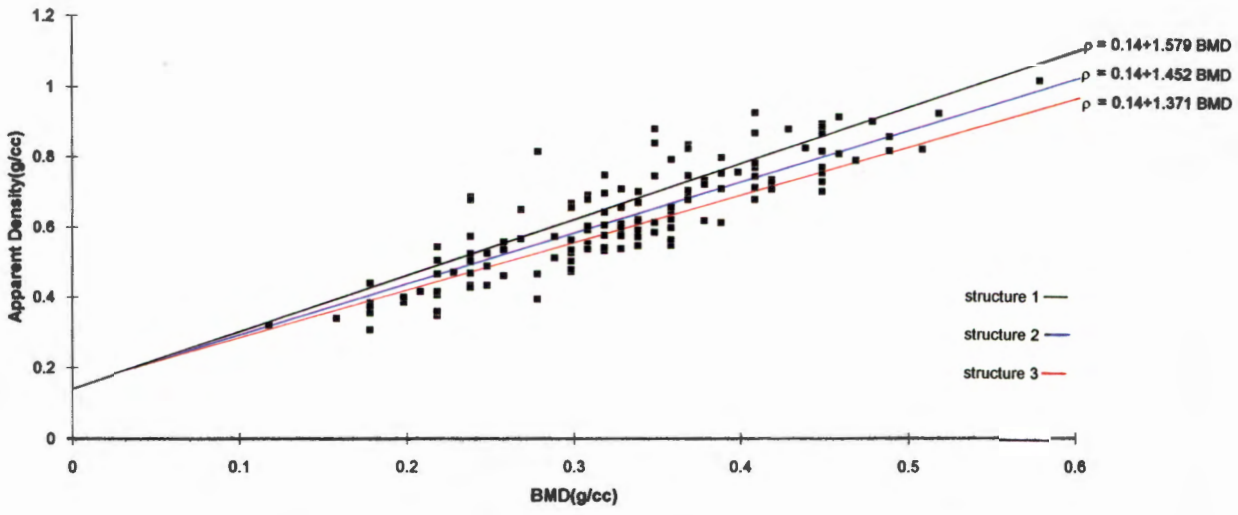

Fig. 5.3a Apparent density vs BMD in OA bone.

For RA bone the relationship between apparent density and bone mineral density was found to be :

$$\rho = 0.112 + 1.764\ BMD$$

This relationship can be seen in Fig. 5.3b. There was a significant difference between the slope of this relationship, and that for the OA female group (p=.003). So disease (RA vs OA) was found to affect this relationship.

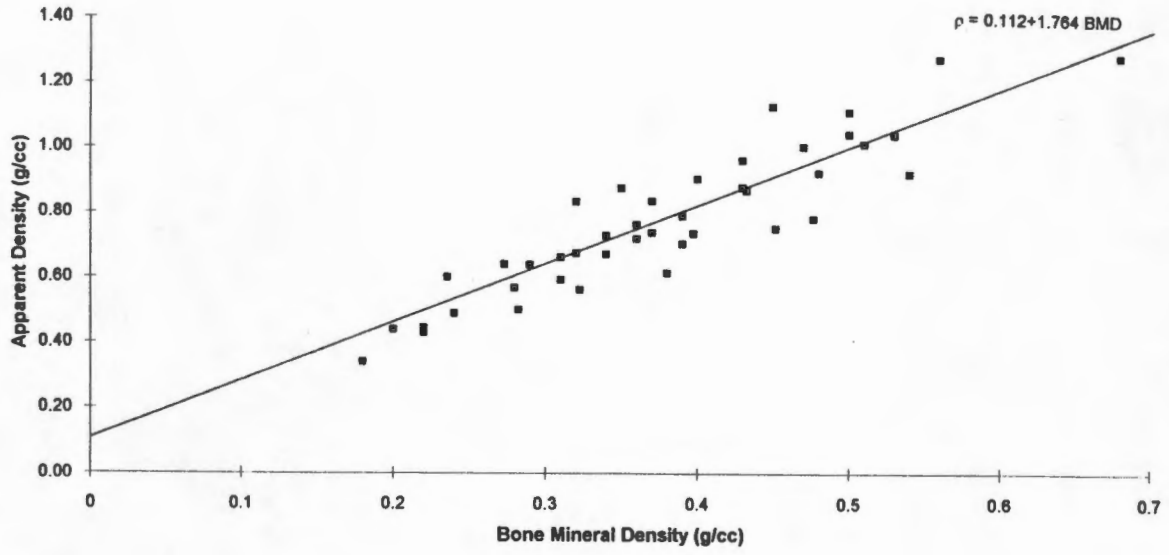

Fig. 5.3b Apparent density vs BMD in RA bone.

5.2.2 Apparent Density and the Mechanical Properties

Compressive Strength vs Apparent Density:

Scatterplots of the raw data for **OA** and **RA** bone can be seen below (Fig. 5.4a & b).

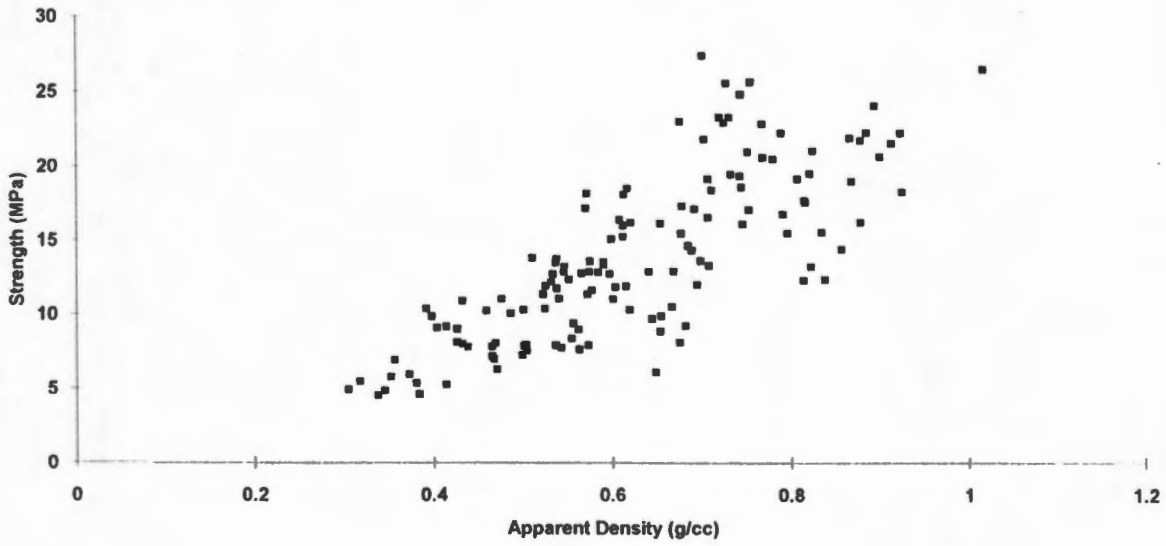

Fig. 5.4a Scatterplot of Strength vs Apparent Density in OA bone.

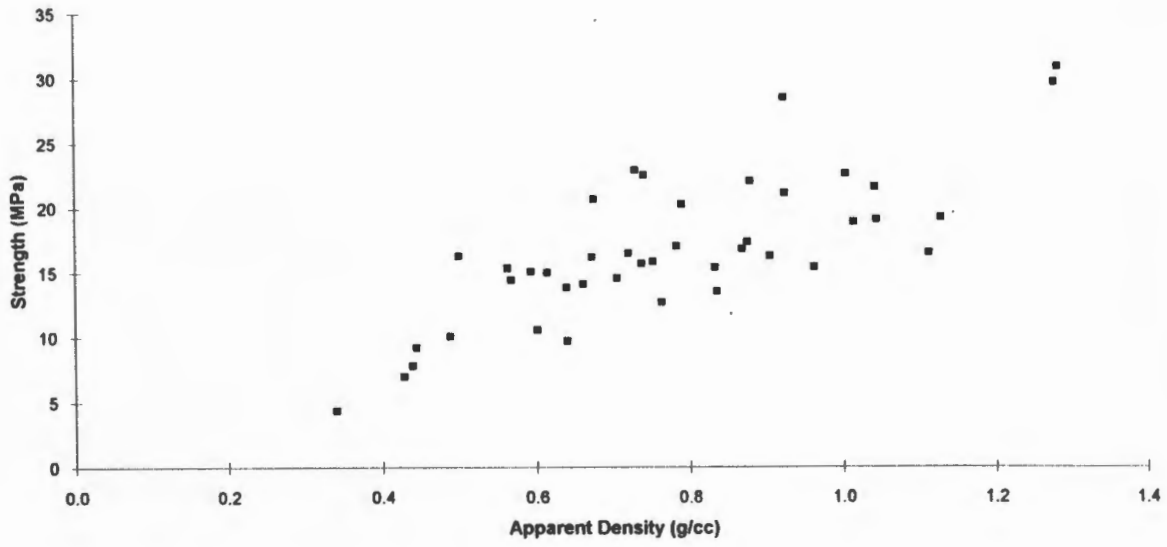

Fig. 5.4b Scatterplot of Strength vs Apparent Density in RA bone.

From these scatterplots it can be seen that the variance in strength increases with an increase in the value of the apparent density. This creates a problem because linear regression requires normality, and homogeneity of variance. In order to achieve this, a log transform has to be applied to the data before a model of the above form can be fitted to the transformed data. The result of this transformation can be seen in the graphs which follow. This transformation had to be applied in all the analyses which follow. A relationship of the following form was then found:

$$\sigma_{ult} = a\,\rho^{b}$$

The **general equation for OA bone** was found to be :

$$\sigma_{ult} = 24.660\,\rho^{1.322} \qquad p < .0005$$

However, in **OA** the bone structure, or degree of bone orientation was found to have a significant effect on the constant multiplier and the exponent of this relationship.

For structure 1 $\sigma_{ult} = 19.95\,\rho^{0.991}$

For structure 2 $\sigma_{ult} = 23.88\,\rho^{1.319}$

For structure 3 $\sigma_{ult} = 35.89\,\rho^{1.8}$

Both the constant multiplier and the exponent increase as the bone becomes more highly anisotropic. However, the difference between structure 1 and 2 was not statistically significant, so the model could treat the results for these two groups together giving the final relationships as:

For structures 1 and 2 $\sigma_{ult} = 23.01\ \rho^{1.261}$ $p < .0005$

For structure 3 $\sigma_{ult} = 35.48\ \rho^{1.782}$ $p = .001$ (cf. structure 1,2)

The difference between these two relationships can be seen in Fig. 5.4c.

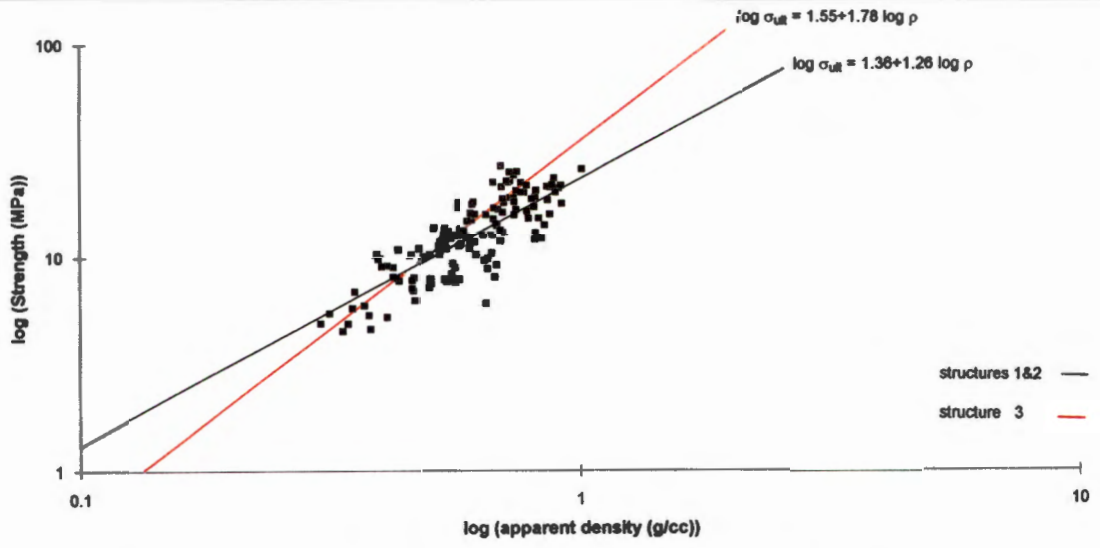

Fig. 5.4c Strength vs Apparent Density after log transformation, for OA bone.

For the RA group the relationship was found to be:

$$\sigma_{ult} = 21.928\ \rho^{1.213} \qquad p < 0.0005$$

which did not differ significantly from that of the female OA group when structural differences were ignored. Therefore, disease (OA vs RA) had no significant effect on this relationship. The relationship for RA bone is plotted in the following graph.

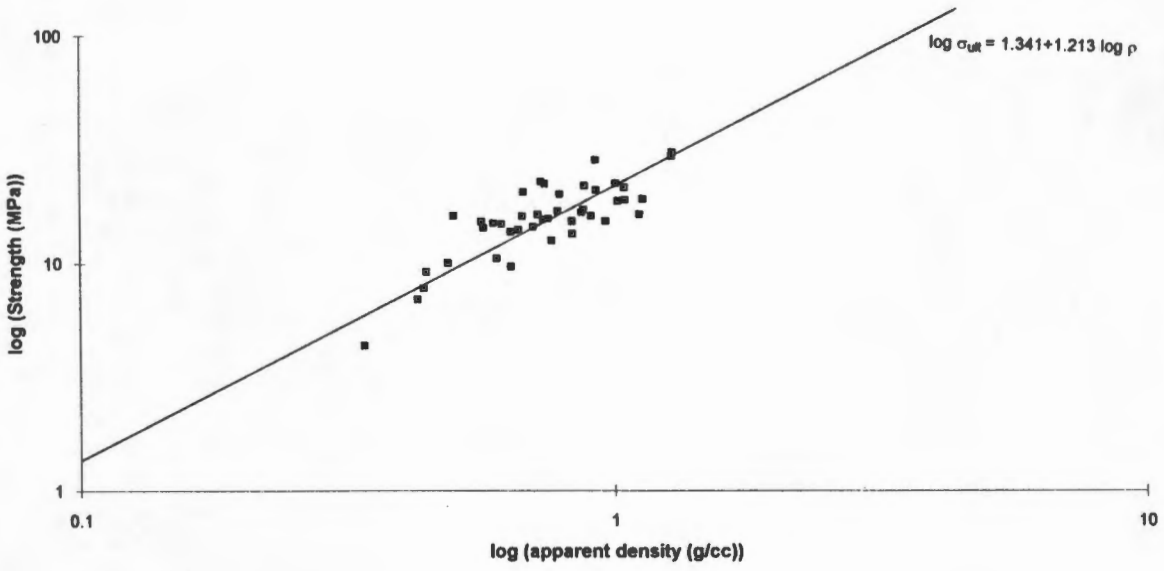

Fig. 5.4d Strength vs Apparent Density after log transformation, in RA bone.

Young's Modulus vs Apparent Density:

Scatterplots of the original data can be seen in Appendix H. As was mentioned previously, a log transform had to be applied to the data giving a relationship of the form:

$$E = a\,\rho^{b}$$

For the **OA bone,** the general relationship was found to be :

$$E = 1741.807\,\rho^{1.706} \qquad p < .0005$$

However, structure was again found to have a significant effect on this relationship, causing both the constant multipliers and the exponents to increase as the structure becomes more highly anisotropic:

For structure 1	$E = 1035.14\,\rho^{0.712}$	$p = .046$
For structure 2	$E = 1737.80\,\rho^{1.780}$	$p = .005$ (cf. structure 1)
For structure 3	$E = 2917.43\,\rho^{2.375}$	$p < .0005$ (cf. structure 1)

These relationships can be seen in (Fig. 5.5a)

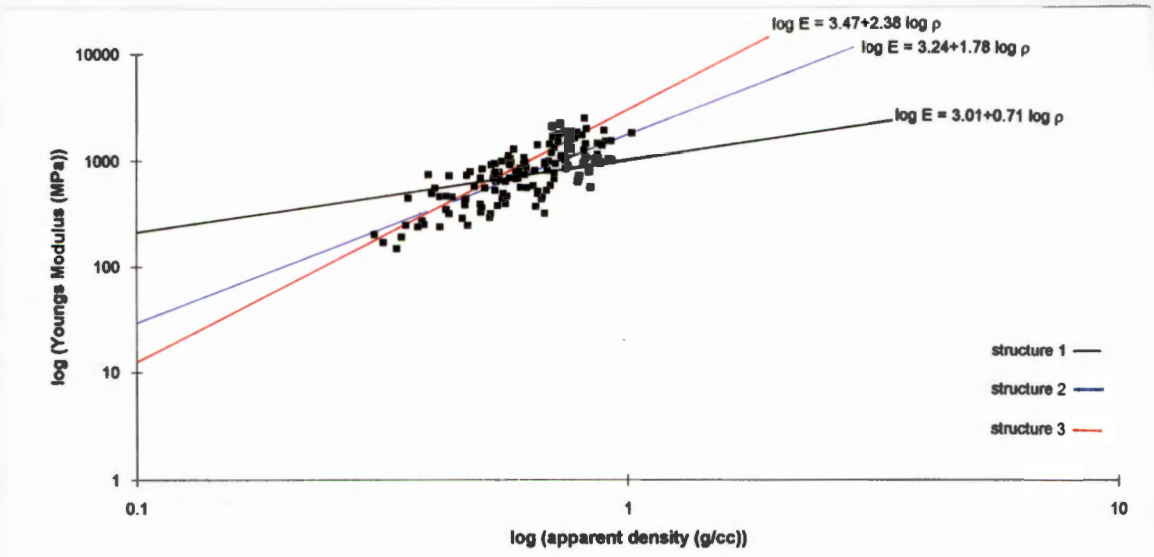

Fig. 5.5a Young's Modulus vs Apparent Density, in OA bone.

In the **RA bone** the relationship between these two variables was found to be:

$$E = 1445.440\ \rho^{1.557} \qquad (p< 0.0005)$$

which was also not significantly different from the relationship found in the female OA group when structural effects are ignored. The relationship for the rheumatoid arthritic bone is plotted in Fig 5.5b.

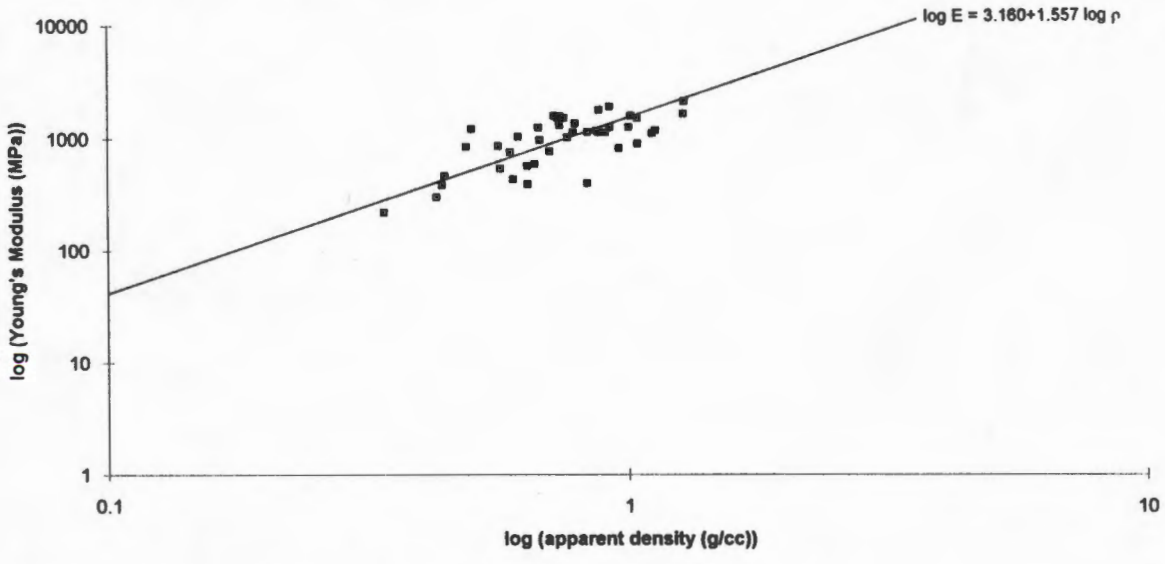

Fig. 5.5b Young's Modulus vs Apparent Density, in RA bone.

Strain Energy Density vs Apparent Density:

Once the data had been transformed, the following relationship was found for **OA bone** irrespective of structure or gender (Fig. 5.6a):

$$SED = 294.44\ \rho^{1.201} \qquad (p < .0005)$$

For **RA bone** the relationship between these two variables was found to be (Fig. 5.6b):

$$SED = 276.694\ \rho^{1.086} \qquad (p < 0.0005)$$

which is not significantly different from the relationship found for the osteoarthritic females. It must be noted that Strain Energy Density in this study was only measured up to 95% Ultimate Stress.

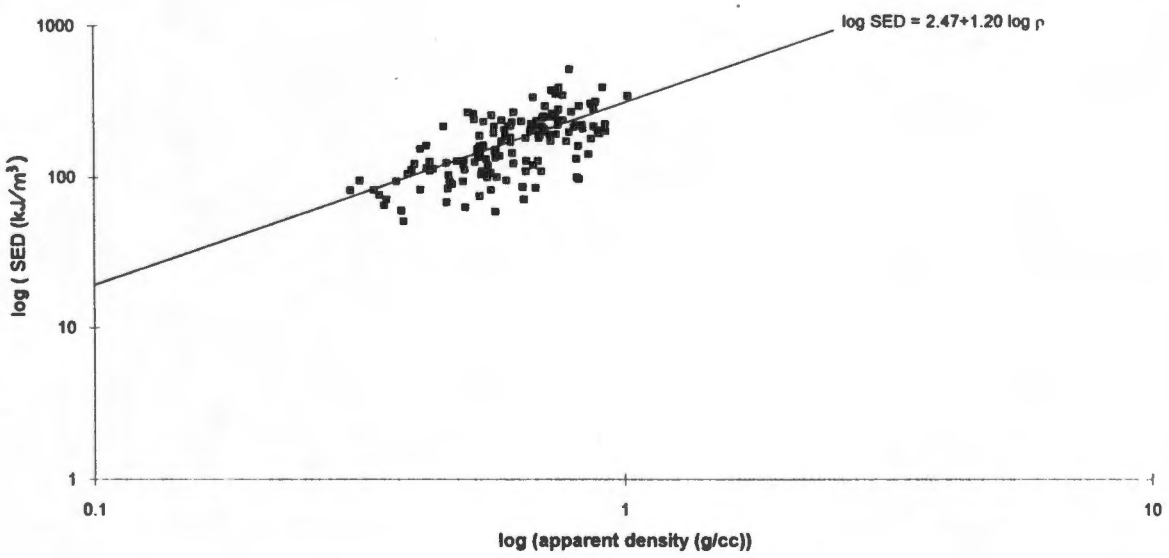

Fig. 5.6a Strain Energy Density vs Apparent Density, in OA bone.

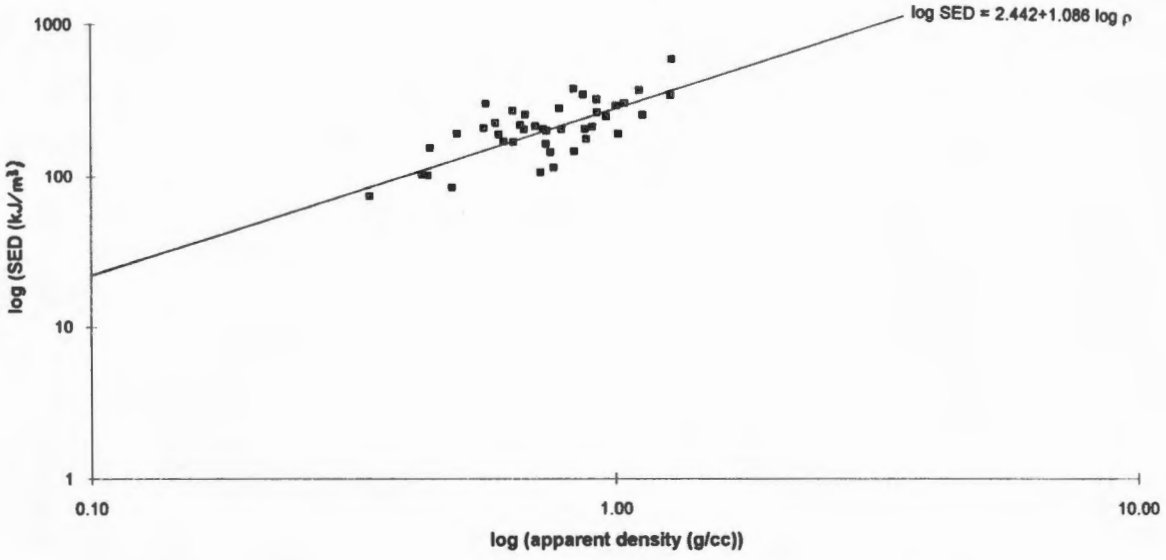

Fig. 5.6b Strain Energy Density vs Apparent Density, in RA bone.

5.2.3 BMD and Mechanical Properties

Compressive Strength vs Bone Mineral Density:

The relationship between compressive strength and bone mineral density as calculated from the DEXA measurements can be seen in the scatterplots below for both OA and RA bone (Fig. 5.7 a & b). Once again, the variance in strength increased with an increase in the value of the independent variable, making it necessary to transform the data.

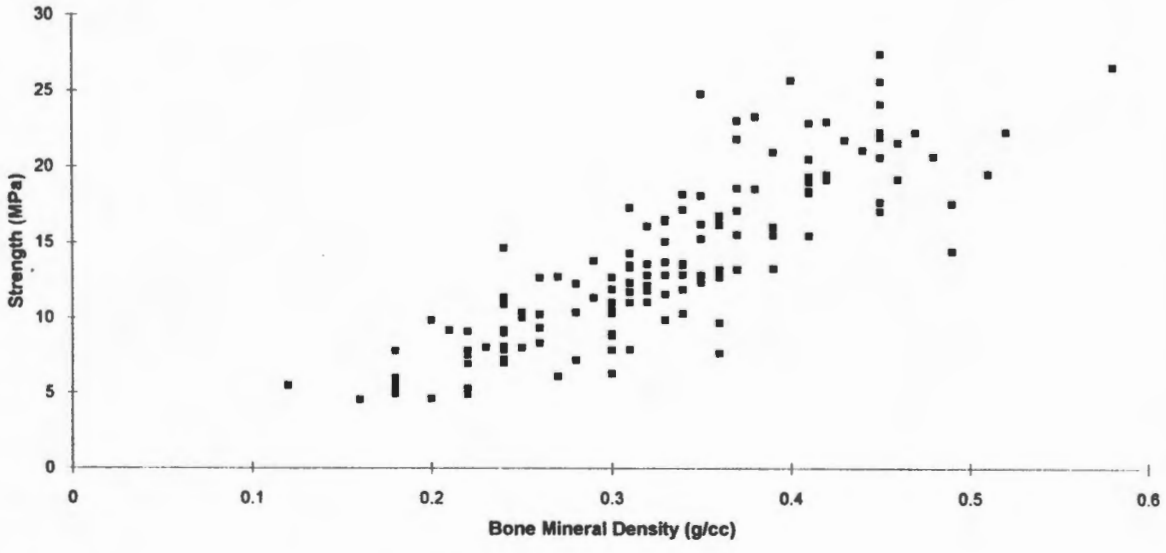

Fig. 5.7a Scatterplot of Strength vs BMD, in OA bone.

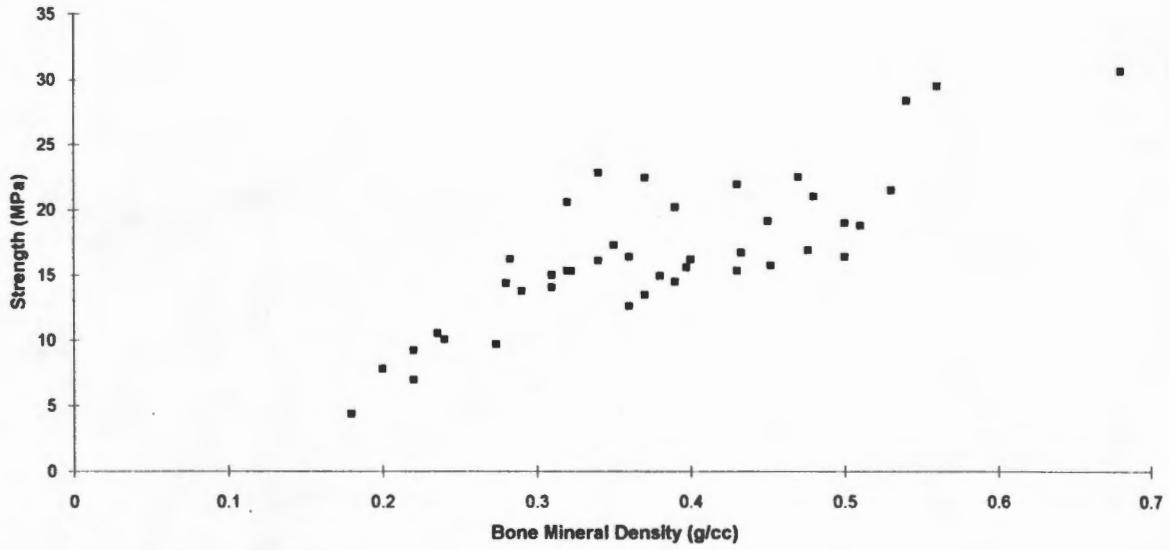

Fig. 6.7b Scatterplot of Strength vs BMD, in RA bone.

In **OA bone** neither structure nor gender had any effect on this relationship, which was found to be (Fig. 5.7c):

$$\sigma_{ult} = 59.16\ BMD^{1.339} \qquad (p < .0005)$$

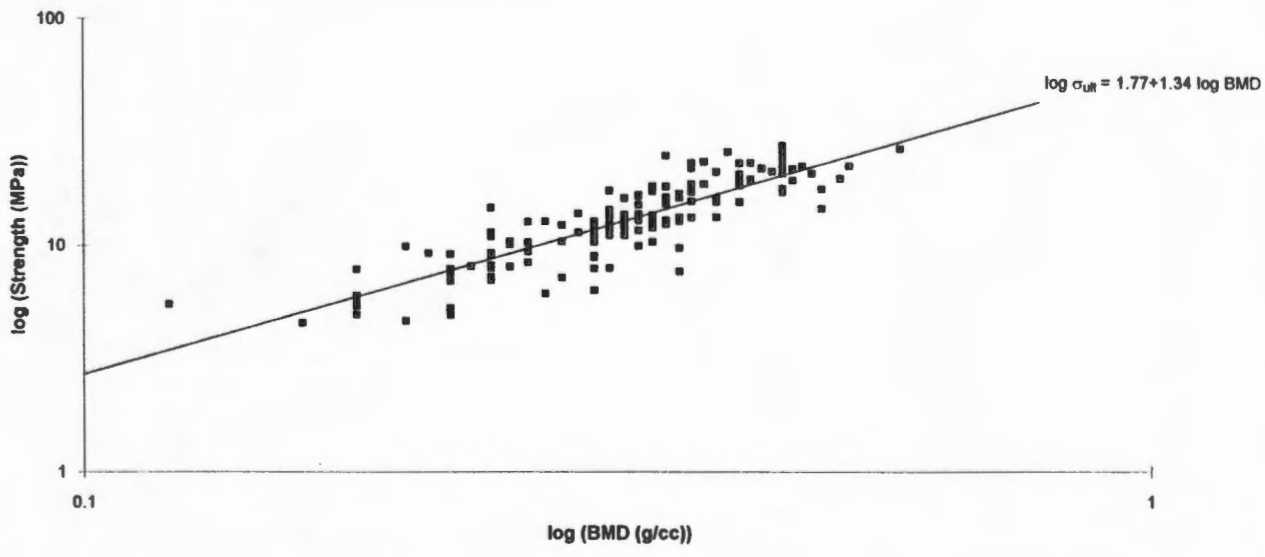

Fig. 5.7c Strength vs BMD after log transformation, in OA bone.

The following relationship was found for **RA bone**:

$$\sigma_{ult} = 52.723\ BMD^{1.248} \qquad (p < 0.0005)$$

Neither the intercept nor the slope was significantly different from that found for the female Osteoarthritic group. The relationship is plotted in the graph below.

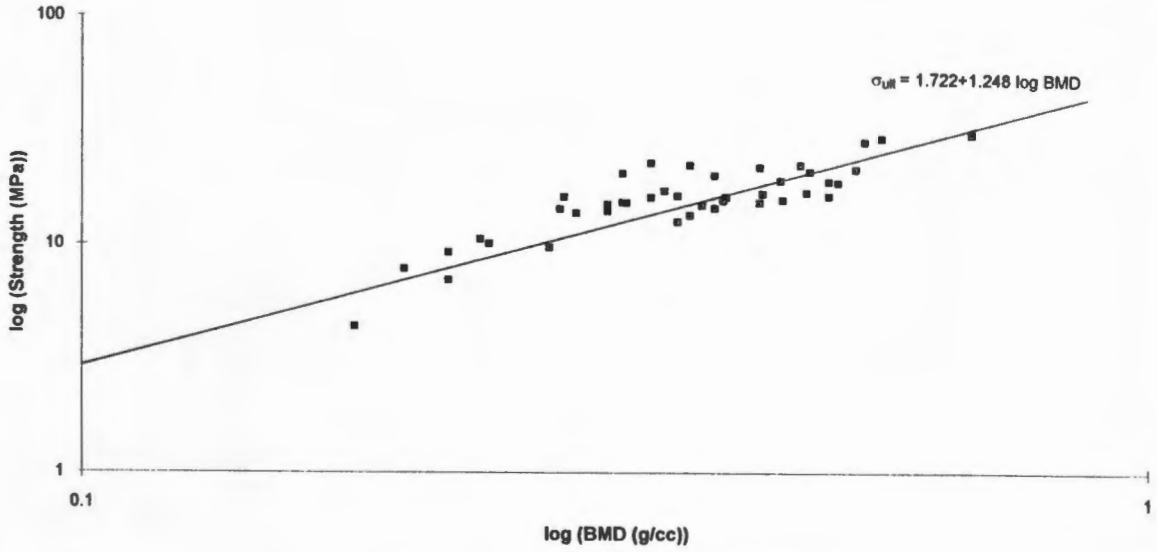

Fig. 5.7d Strength vs BMD after log transformation, for RA bone.

Young's Modulus vs Bone Mineral Density

For **OA bone** the relationship between Young's Modulus and bone mineral density was again influenced by the degree of structural orientation of the cancellous bone. The general relationship was:

$$E = 5714.786\ (BMD)^{1.781} \quad p < .0005$$

but then for the various structures the intercepts and slopes differed.

For structure 1 $E = 3169.57\ (BMD)^{1.280}$

For structure 2 $E = 5152.29\ (BMD)^{1.721}$

For structure 3 $E = 9036.49\ (BMD)^{2.096}$

However, the difference between structures 1 and 2 was not statistically significant, so they could be combined, making the final relationships:

For structures 1 and 2 $E = 4830.59\ (BMD)^{1.661}$ $p<.0005$

For structure 3 $E = 8953.65\ (BMD)^{2.087}$ $p = .05$ (cf. structures 1, 2)

These final relationships can be seen on the graph below.

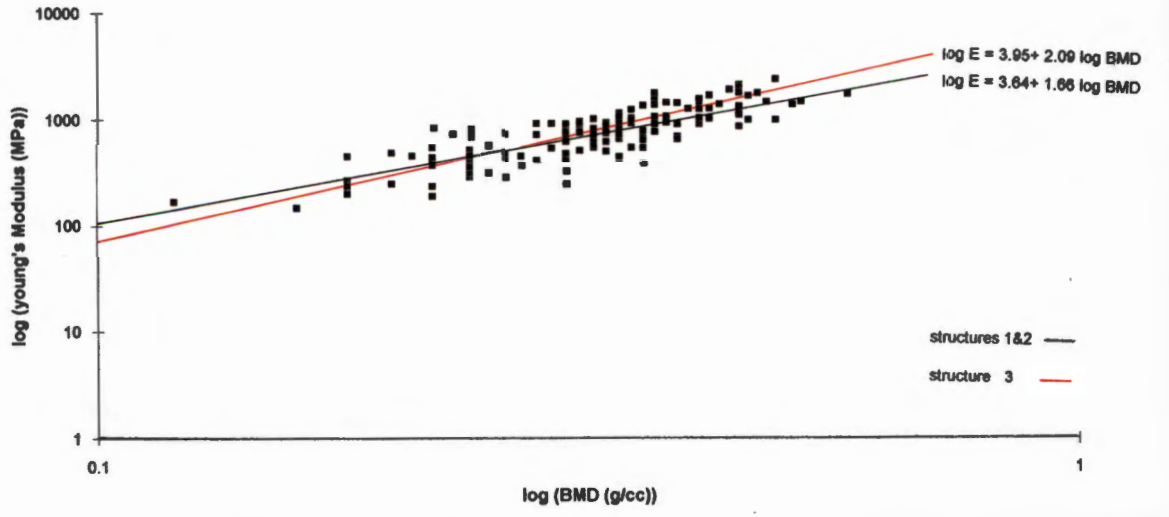

Fig. 5.8a Young's Modulus vs BMD, in OA bone.

For **RA bone** the following relationship was found after the data had been transformed:

$$E = 4720.630\ BMD^{1.648} \qquad (p < 0.0005)$$

Neither the slope nor the intercept differed significantly from that of the relationship found for the female osteoarthritic group. The graph relating these two variables is seen below.

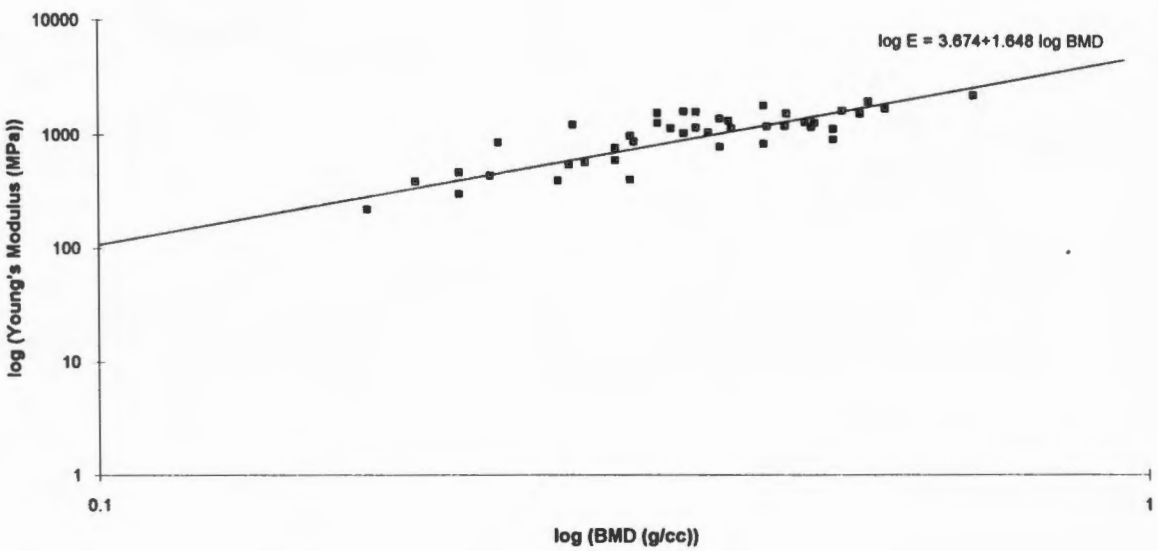

Fig. 5.8b Young's Modulus vs BMD, in RA bone.

5.2.4 Relationships between the Mechanical Properties

For completeness the following relationships were also assessed, since they are commonly described in the literature. The variables again had to be transformed in all cases. In the following relationships there was never a significant difference between the relationships for the female RA and OA groups.

Young's Modulus vs Strength

In the previous sections it could be seen that both strength and stiffness are strongly dependent on the apparent density or the bone mineral density of the material, for this reason it should follow that strength and stiffness are strongly related. This was indeed found to be the case. In the **OA group**, Young's Modulus was found to be related to strength by the following relationship:

$$E = 34.51\ \sigma_{ult}^{1.206} \qquad p < .0005$$

which can be seen in the graph below.

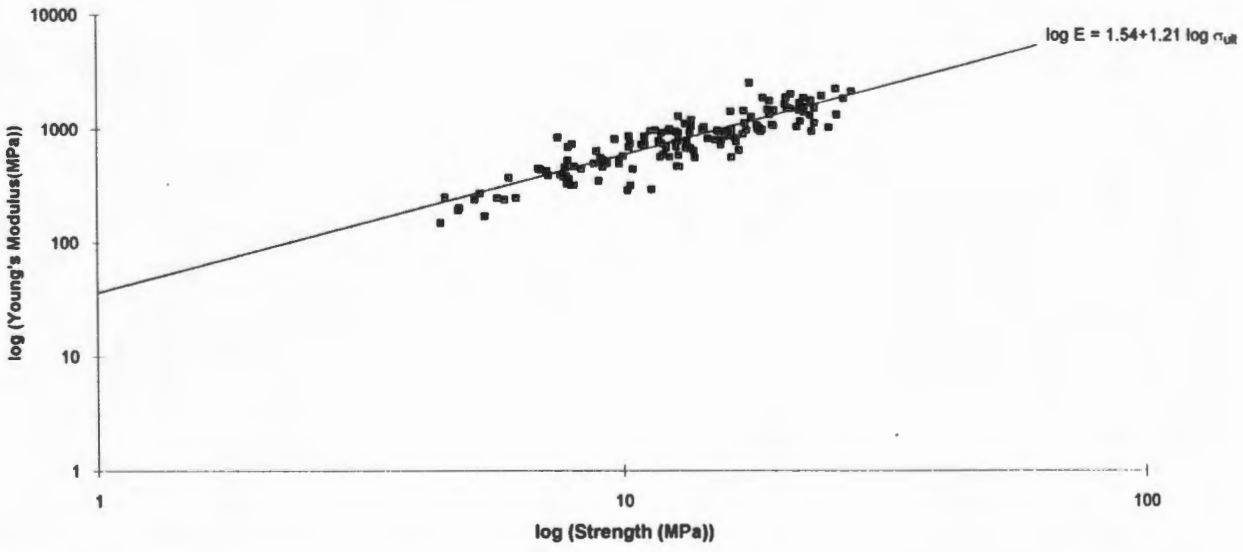

Fig. 5.9a Young's Modulus vs Strength, in OA bone.

For the **RA group** a very similar relationship was found:

$$E = 33.343\ \sigma_{ult}^{1.207} \qquad p < .0005$$

It has been plotted on the transformed data below.

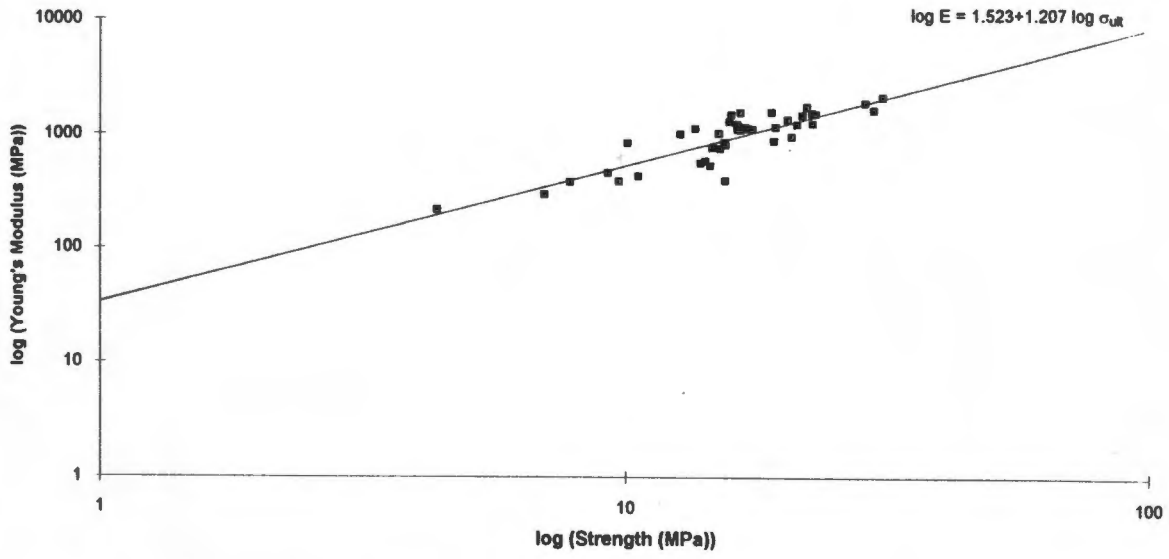

Fig. 5.9b Young's Modulus vs Strength, in RA bone.

Strain Energy Density vs Strength

For both OA, and RA bone, strain energy density and strength were directly related. But again the data had to be transformed, and the final relationships were found to be:

Male and Female OA bone $SED = 15.67\ \sigma_{ult}^{0.916}$ $(p < 0.0005)$

Female RA bone $SED = 16.48\ \sigma_{ult}^{0.918}$ $(p < 0.0005)$

These relationships are plotted on the graphs below (Fig. 5.10 a & b).

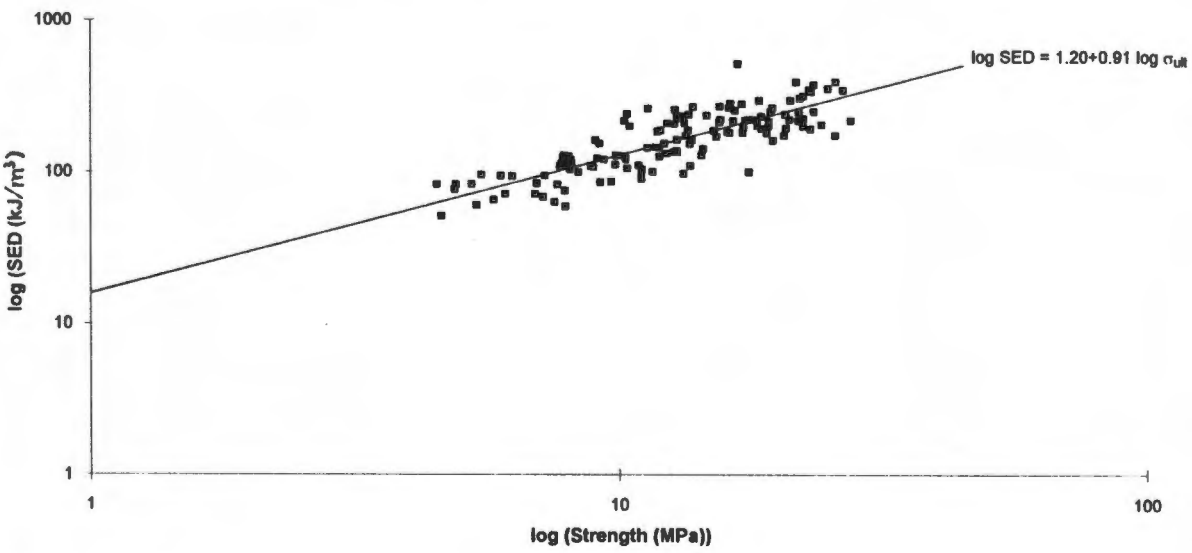

Fig. 5.10a Strain Energy Density vs Strength, in OA bone.

Table 5.3 Summary of the relationships for OA and RA bone.

Relationship	OA	RA
App. Dens. vs BMD	$\rho = 0.123 + 1.526$ BMD	$\rho = 0.112 + 1.764$ BMD
structure 1	$\rho = 0.14 + 1.58$ BMD	
structure 2	$\rho = 0.14 + 1.45$ BMD	
structure 3	$\rho = 0.14 + 1.37$ BMD	
Strength vs App.Dens.	$\sigma_{ult} = 24.66\ \rho^{1.322}$	$\sigma_{ult} = 21.93\ \rho^{1.213}$
structures 1&2	$\sigma_{ult} = 23.01\ \rho^{1.261}$	
structure 3	$\sigma_{ult} = 35.48\ \rho^{1.782}$	
Young's Mod. vs App. Dens.	$E = 1741.81\ \rho^{1.706}$	$E = 1445.44\ \rho^{1.557}$
structure1	$E = 1035.14\ \rho^{0.712}$	
structure2	$E = 1737.80\ \rho^{1.780}$	
structure 3	$E = 2917.43\ \rho^{2.375}$	
SED vs Apparent Density	$SED = 294.44\ \rho^{1.201}$	$SED = 276.69\ \rho^{1.086}$
Strength vs BMD	$\sigma_{ult} = 59.16\ (BMD)^{1.339}$	$\sigma_{ult} = 52.72\ (BMD)^{1.248}$
Young's Mod. vs BMD	$E = 5714.79\ (BMD)^{1.781}$	$E = 4720.63\ (BMD)^{1.648}$
structures 1 & 2	$E = 4830.59\ (BMD)^{1.661}$	
structure 3	$E = 8953.65\ (BMD)^{2.087}$	
Young's Mod vs Strength	$E = 34.51\ \sigma_{ult}^{1.206}$	$E = 33.34\ \sigma_{ult}^{1.207}$
SED vs Strength	$SED = 15.67\ \sigma_{ult}^{0.916}$	$SED = 16.48\ \sigma_{ult}^{0.918}$

(ρ = apparent density (g/cm^3), BMD = bone mineral density (g/cm^3),
σ_{ult} = strength (MPa), E = Young's Modulus (MPa), SED = strain energy density(kJ/m^3)
structure 1 = equiaxed, structure 2 = partially oriented, structure 3 = highly anisotropic)

Table 5.4 The ranges and mean values found for the variables.

	OA Male & Female		RA Female	
	Range	Mean	Range	Mean
Apparent Density (g/cm^3)	0.31 - 1.016	0.62	0.34 - 1.28	0.77
Bone Mineral Density (g/cm^3)	0.12 - 0.58	0.33	0.18 - 0.68	0.38
Strength (MPa)	4.515 - 27.347	13.791	4.368 - 30.788	16.702
Young's Modulus (MPa)	148 - 2503	868	218 - 2123	1055
Strain Energy Density (kJ/m^3)	51 - 516	177	74 - 585	224

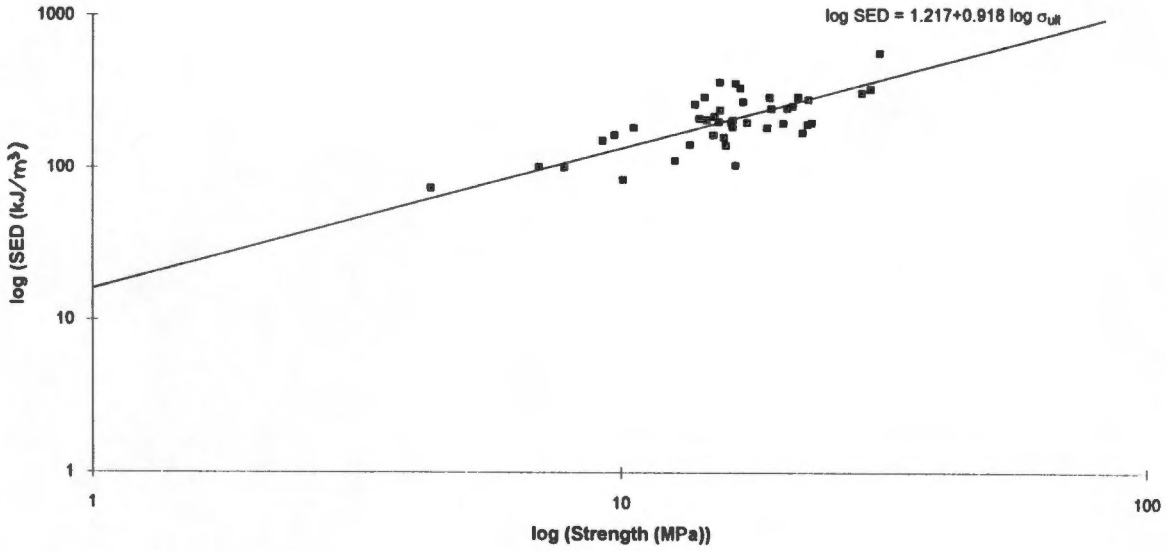

Fig. 5.10b Strain energy density vs Strength, in RA bone.

5.3 Summary

A summary of the relationships that were determined in this experiment are provided in Table 5.3. The ranges and mean values for each of the variables are summarised in Table 5.4, the relationships are only valid over the observed ranges of the independent variables.

CHAPTER 6

RESULTS

CANCELLOUS BONE MORPHOLOGY

The detailed results for the morphometric analysis of the cancellous bone are provided in Appendix G. Statistical analysis of these results was done using Statsgraphics version 5 (Statistical Graphics Corporation, Inc). Statistical significance was set at $p < .05$.

6.1 Subchondral Bone

A summary of the results found in the region immediately below the subchondral plate is provided in the Table 6.1.

Table 6.1 Cancellous bone morphology in the Subchondral Region

Disease Group	TBV %	Sv (mm^2/mm^3)	MTW (μm)	MTT (μm)
OA Female (A)	28.33 (6.02)	3.65 (0.73)	198 (30)	156 (23)
OA Male (B)	35.63 (10.39)	3.93 (0.5)	238 (73)	187 (57)
RA Female (C)	40.71 (8.29)	4.33 (0.77)	246 (66)	193 (52)
A vs B	A < B p = .06	NS	NS	NS
A vs C	A < C p = .002	NS	NS	A < C p = .052
B vs C	NS	NS	NS	NS

Standard Deviations in parentheses. NS = not significant. TBV = Trabecular Bone Volume Fraction, S_V = Surface Area Density, MTW = Mean Trabecular Width, MTT = Mean Trabecular Thickness.

In the **female OA group** the TBV% in this proximal part of the femoral head was between 16 - 38 %, the surface area density was between 2.58 - 5.1 mm^2/ mm^3. The trabecular width was found to be between 158 - 249 μm, giving a trabecular thickness range of 124 - 195 μm.

In the **male OA group** the TBV % was between 22 - 54%, which is much greater than the female group. The surface area density was however only between

2.84 - 4.44 mm^2/ mm^3. The trabecular width was between 128 - 332 μm, and trabecular thickness was calculated to be 101 - 261 μm.

In the **female RA group TBV %** ranged between 30 - 53%, however it must be pointed out that only 7 of the 10 cases in this group actually had sufficient bone for this analysis, often the RA bone contains large cysts and a specimen cannot be taken, or the femoral head is just too small. Surface Area Density was between 3.49 - 5.78 (mm^2 /mm^3), trabecular width was between 185 - 350 μm, and trabecular thickness ranged from 145 - 274 μm.

It can be seen that the Trabecular Bone Volume is much lower in the female OA group than their male counterparts (p = .06). This group's Trabecular Bone Volume was also found to be significantly lower than that of the RA female group (p = .002). The Mean Trabecular Thickness of the RA females was also significantly greater than that of the OA females. One can understand these findings more easily when one looks at the bone morphology qualitatively, as will be done in the following sections.

6.2 Compressive Trabeculae

In the region of the Principal Compressive Trabeculae, the following variables were determined: Trabecular Bone Volume, Surface Area Density, Trabecular Width or Thickness and the Mean Width of the Marrow Spaces. Although there were slight differences between means of the three groups (Table 6.2), they were never statistically significant.

Table 6.2 Cancellous bone morphology in the Compressive Trabeculae

Disease Group	TBV %	Sv (mm^2/mm^3)	MTW (μm)	MTPT (μm)	Marrow Space Width (μm)
OA female (A)	25.86 (6.2)	2.81 (.35)	222 (52)	185 (43)	865 (162)
OA male (B)	25.38 (4.79)	2.99 (.49)	204 (20)	170 (17)	833 (179)
RA female (C)	30.32 (9.30)	3.30 (.79)	233 (65)	194 (55)	725 (279)

Standard Deviations in parentheses. TBV = Trabecular Bone Volume Fraction, S_V = Surface Area Density, MTW = Mean Trabecular Width, MTPT = Mean Trabecular Plate Thickness.

The range of each of these variables was particularly large in the RA female group, where TBV ranged between 18.77 - 48.25%, Surface Area Density ranged between 1.87 - 4.18 mm^2/ mm^3, Mean Trabecular Thickness ranged from 108 -279 μm, and Marrow Space Width ranged between 393 - 1300 μm. This indicates that certain RA patients were definitely osteoporotic, whilst others had a good bone structure in the region of the compressive trabeculae.

6.3 Relationships between the Morphological Parameters.

Generally one would expect an increase in trabecular bone volume to be associated with an increase in surface area density, as the structure becomes more interconnected. One would also expect the trabecular thickness to increase with an increase in TBV, and marrow space width to be inversely related to TBV. In diseased bone these relationships were found to exist.

Surface Area Density vs Trabecular Bone Volume

There was a general increase in Sv as TBV increased, indicating that the cancellous bone structure does become more interconnected as the amount of bone present increases. This was true in both the subchondral region (Fig. 6.1) and the region of the principal compressive trabeculae (Fig 6.2).

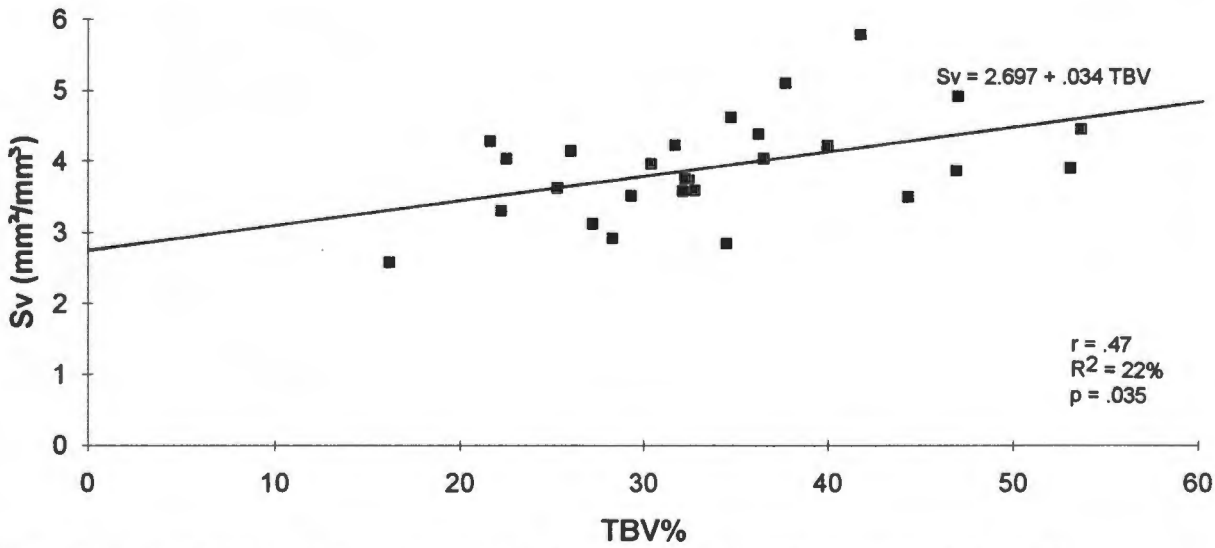

Fig. 6.1 Surface Area Density vs Trabecular Bone Volume in the subchondral region. (OA and RA combined)

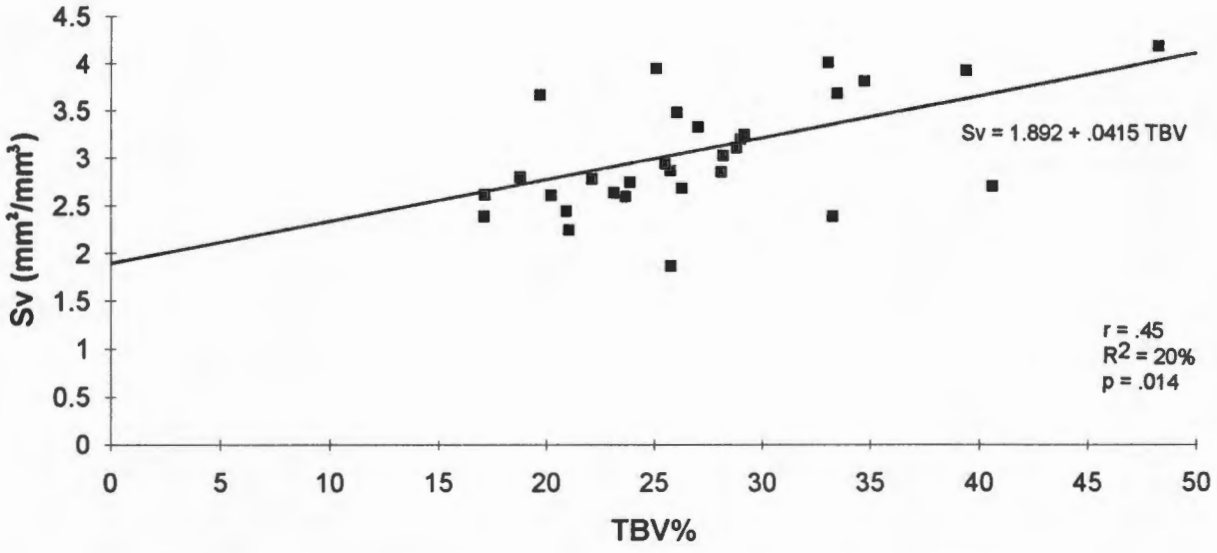

Fig. 6.2 Surface Area Density vs Trabecular Bone Volume in the region of the principal compressive trabeculae. (OA and RA combined)

Theoretically this relationship will pass through zero again as the TBV approaches 100%, and the cell walls become so thick that the marrow spaces become filled-in and the structure becomes totally solid.

Mean Trabecular Thickness vs Trabecular Bone Volume.

In both the subchondral region and the region of the compressive trabeculae, the trabecular thickness was directly related to the trabecular bone volume fraction (Fig. 6.3 & 4).

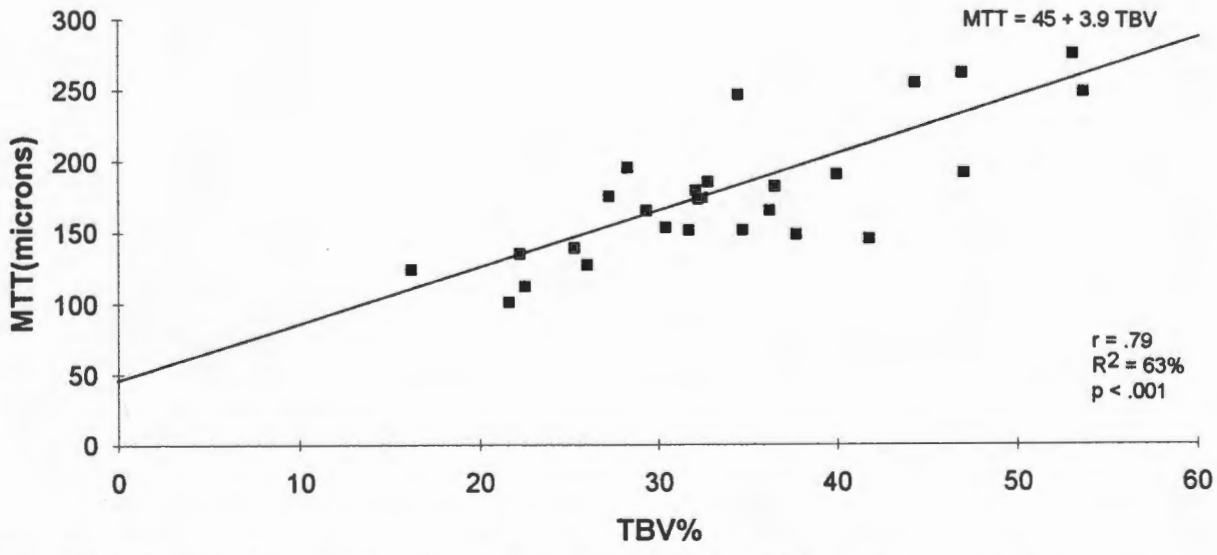

Fig. 6.3 Mean Trabecular Thickness vs Trabecular Bone Volume in the subchondral region. (OA and RA combined)

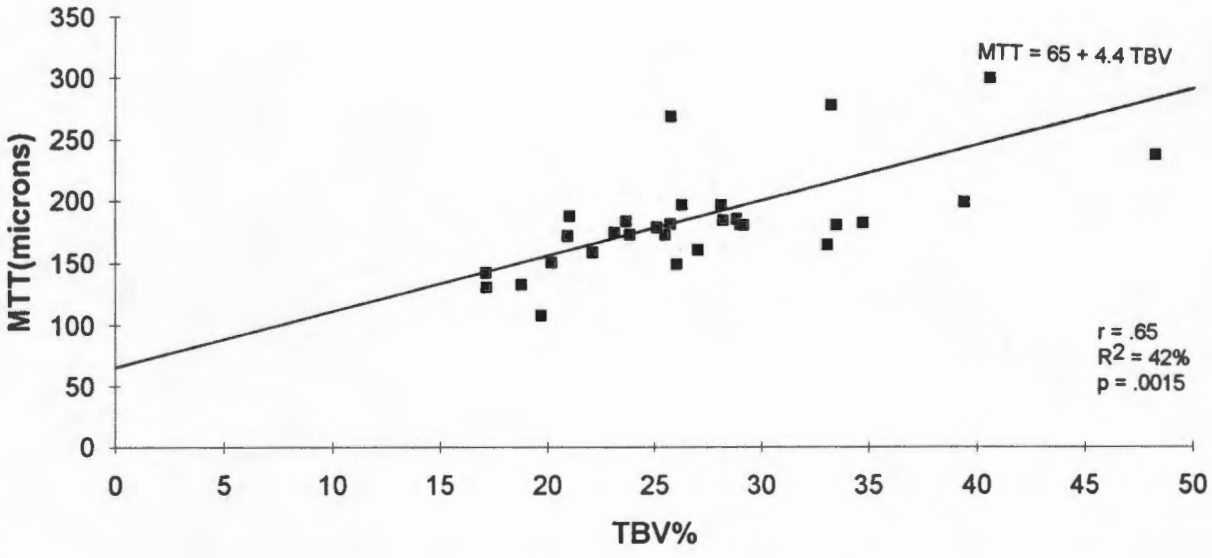

Fig. 6.4 Mean Trabecular Thickness vs Trabecular Bone Volume in the region of the principal compressive trabeculae. (OA and RA combined)

Marrow Space Width vs Trabecular Bone Volume.

In the region of the compressive trabeculae the marrow space width was inversely related with the TBV (Fig. 6.5), the width of the marrow spaces increasing as the TBV decreased.

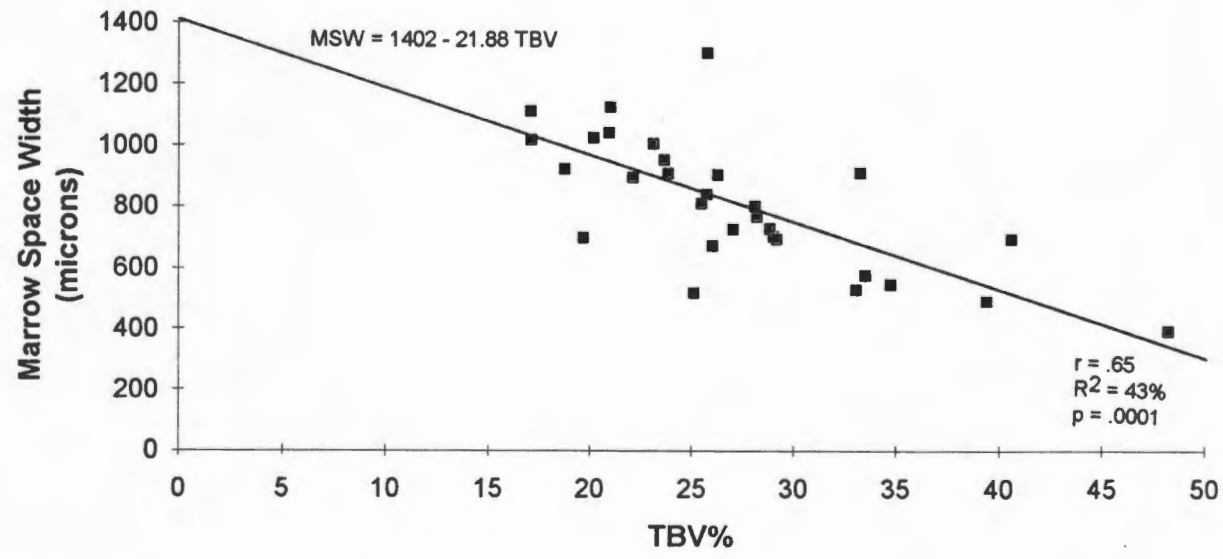

Fig. 6.5 Marrow Space Width vs Trabecular Bone Volume in the region of the principal compressive trabeculae.

Since significant relationships were found between the morphological parameters it was hoped that these variables would improve the strength of the relationships between the mechanical properties and a simple scalar quantity such as apparent or bone mineral density. Multiple regression analysis was carried out, using the mechanical properties as the dependent variable, and apparent density plus the morphological parameters as the independent variables. The morphological parameters did contribute very slightly to the strength of the relationships, but never enough to be statistically significant.

6.4 Qualitative Assessment of Cancellous Bone

In Section 6.1 it became apparent that the changes found in the subchondral cancellous bone varied greatly within the OA group. For example, the TBV in the subchondral region ranged from 16 - 38% in the female group, and from 22 - 54% in the male group. This suggests that OA is not necessarily associated with very dense subchondral bone in all individuals.

Very dense subchondral bone was found in a small group of OA sufferers. In this study these patients were all males, (this need not be the case if a larger group of patients were included). The dense subchondral bone can be seen in the photo below.

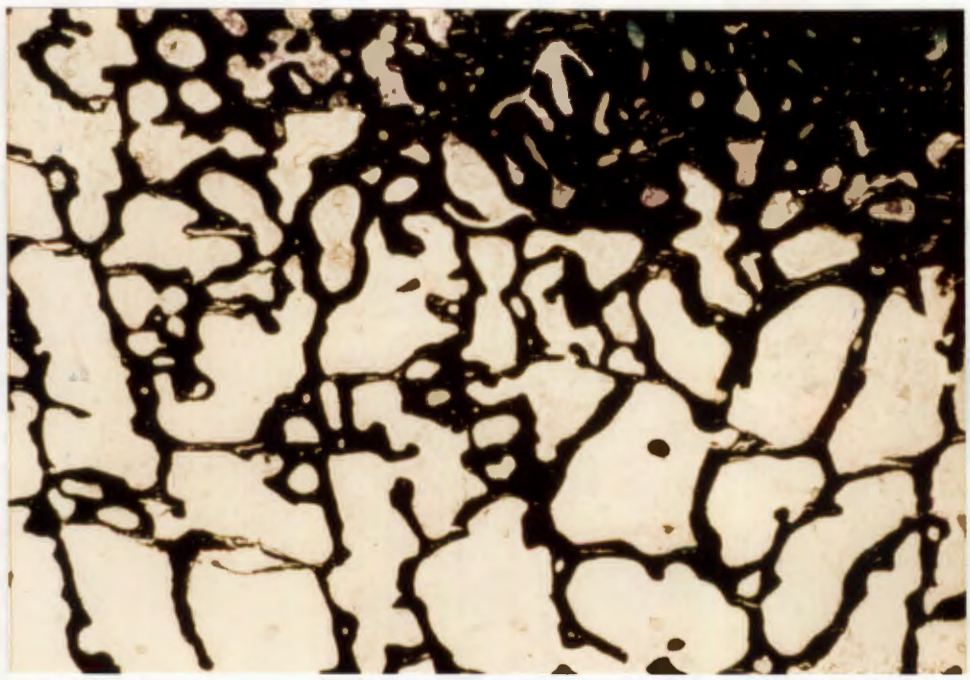

Photo 6.1 Subchondral cancellous bone showing very dense area.
Original Magnification 8x, von Kossa Stain. (Case 19, Male OA)

The preoperative X-rays of all subjects included in this study were assessed by the Head of the Department of Orthopaedic Surgery, and were classified according to the subgroups of coxarthrosis described by Solomon (1984). Cases with dense subchondral bone were found to have Hypertrophic OA (based on X-ray assessment). Their X-rays revealed osteophytes on the acetabulum as well as the perimeter of the

femoral head, and cartilage loss was limited to the superolateral part of the joint (Photo 6.2).

Photo 6.2 X-ray showing features typical of Hypertrophic OA. (Case 18, OA Male)

There were also a number of cases, mainly females as well as two males, who showed very **low density cancellous bone** in the subchondral region, with very thin trabeculae that were poorly connected (Photo 6.3). Their X-rays showed features typical of **Atrophic OA** as described by Solomon (1984), with minimal new bone formation, a more diffuse involvement of the joint, and more concentric narrowing of the joint space (Photo 6.4).

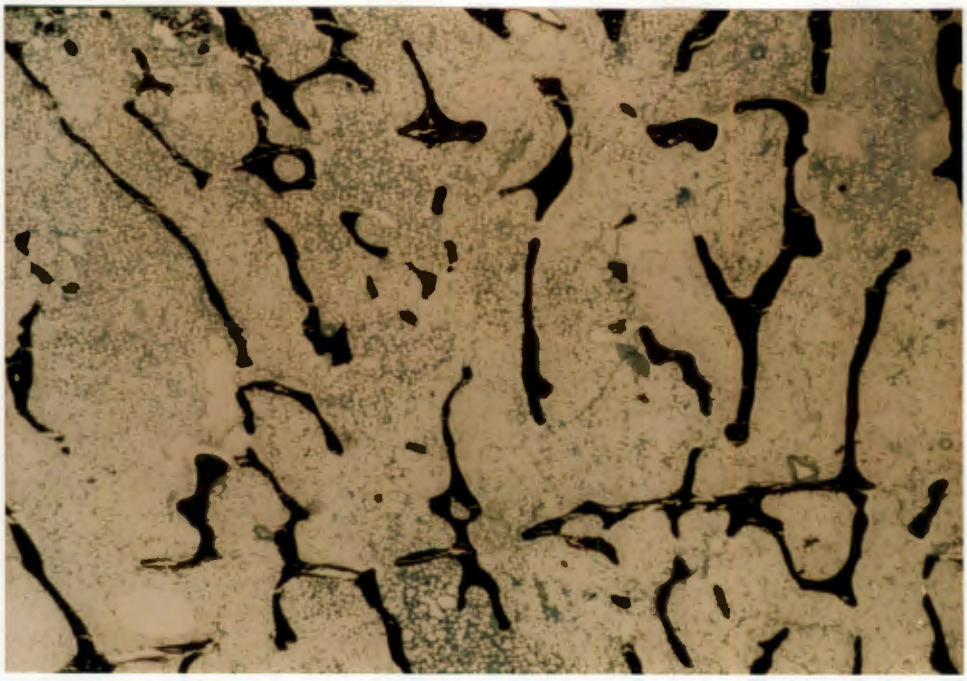

Photo 6.3 Subchondral Cancellous bone showing low density bone with thin trabeculae, that are poorly connected. Original Magnification 9x (Case 22, Male OA)

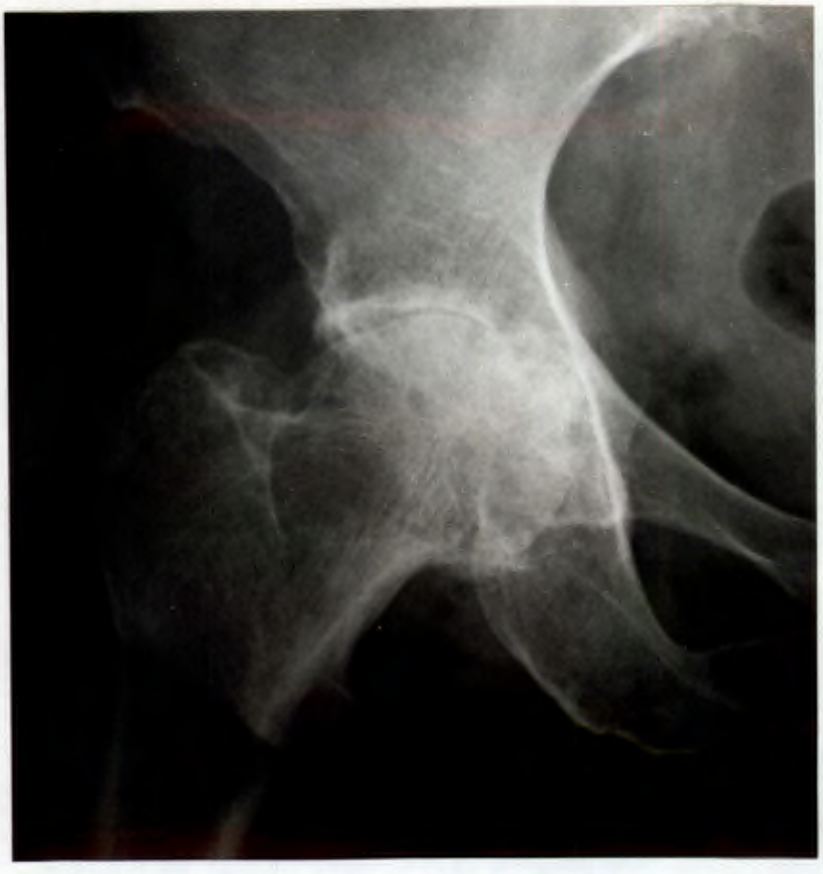

Photo 6.4 X-ray showing signs typical of Atrophic OA. (Case 3, Female OA)

Then there was a third group of patients, who presented differently. This group consisted of males and females, and was named "Normotrophic".

Photo 6.5 Subchondral cancellous bone from Case 11, Female OA. Original Magnification 8x.

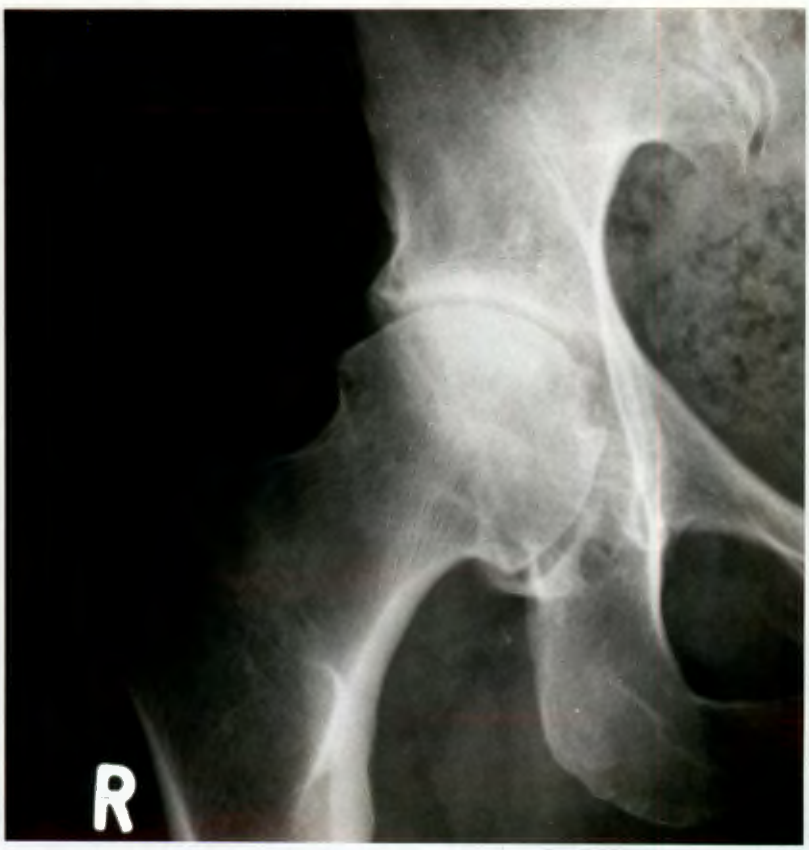

Photo 6.6 X-ray of a Normotrophic Hip. (Case 11, OA female)

The subchondral bone in this group was of **medium density** (Photo 6.5), showed a well connected structure but with no very dense patches as seen in the Hypertrophic group. The X-rays of such cases showed few signs of OA, with minimal new bone formation, and little loss of joint space as can be seen in Photo 6.6.

OA Hip does not appear to be a uniform disorder, but can present in a number of different ways. In order to state conclusively that these three sub-groups exist one requires a larger number of cases. This aspect deserves further investigation.

The results found in the Rheumatoid Arthritics (in sections 5 and 6.1 & 2) were at first surprising, because it was not expected that these patients would have such high density bone in the subchondral region. If one looks at the (RA) cancellous bone from the subchondral region qualitatively, one can see that the system is very asymmetric and may be quite dense (Photo 6.7). The cancellous bone in this disease may very well have undergone some collapse and remodelling.

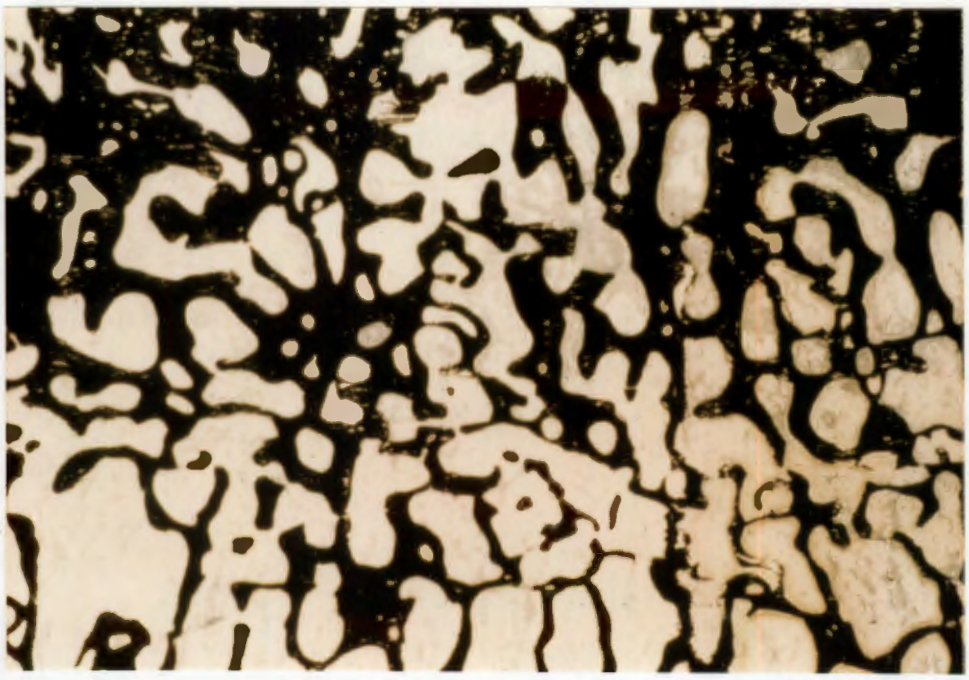

Photo 6.7 RA subchondral bone. Original Magnification 9x (Case 26, Female RA)

RA is associated with severe joint destruction, and there is often thinning of the medial acetabular wall (Photo 6.8), and subsequent protrusion of the femoral head into the pelvis.

Photo 6.8 X-ray showing a hip joint with RA. (Case 26, female RA).

CHAPTER 7

DISCUSSION

In this study the morphological and mechanical properties and relationships of cancellous bone were investigated in RA and OA Hip. Insight into the quality of the periarticular cancellous bone was gained, and the distribution of the bone changes from the subchondral region to the region of the compressive trabeculae was determined.

The present study differs from similar studies reported in the literature for a number of reasons. Firstly, our cancellous bone was cut and tested in alignment with the principal compressive trabeculae, any cubes which were not well aligned with the trabecular structure were not included. Any cubes containing bone cysts were also excluded from the sample. Secondly, because a number of bone cubes were taken from each femoral head our statistical analyses always allowed for "repeated measures". Usually studies done on cancellous bone from normal individuals include bone specimens cut in alignment with the axis of the femoral neck (e.g. Lotz et al. 1990). This means that the mechanical properties are tested slightly off the actual material axis which may lead to a slight underestimation of the results. In such studies many more bone specimens (10 - 20) are taken from each femoral head (e.g. Martens et al. 1983, Lotz et al. 1990 and Deligianni et al. 1991), therefore the mean values are calculated over a much wider range of cancellous bone, which may contribute to lower mean values being reported. Furthermore, the researchers do not always state clearly how they dealt with "repeated measures" in their statistical analyses.

There is a further reason why the mean values for the mechanical properties of OA and RA bone found in this study cannot be compared directly with mean values given

for normal cancellous bone in the literature. The reason is that in order to test the difference between two means the data must be normally distributed; in the present study we found that the raw data for the mechanical properties was not normally distributed. The same phenomenon may / may not have been found in similar studies. However, to test the difference between the mean values reported for normal bone and those found for diseased bone one needs to log transform the data to ensure approximate normality. The log transform would have to be applied to the raw data of the study one wishes to compare the data with, which is not possible.

In this study the following mean values for **compressive strength** were found: in **OA females 11.601 MPa**, **OA males 16.180 MPa** and in **RA females 16.702 MPa**. Lotz et al. (1990), found values for normal bone (mean age 64 years) to range between 1.3 - 27.3 MPa, with a mean value of 6.76 (SD 4.84) MPa. The mean compressive strength value reported by Evans and King (1961) for bone from the proximal femur (7.6 (SD 2.2) MPa), was also lower than the values found in this study . Martens et al. (1983) found a mean value of 9.3 (SD 4.5) MPa in the direction of the femoral neck, and 10.2 (SD 3.3) MPa in the direction perpendicular to this. The mean age of the donors in their group was 45 years. Their results are only slightly lower than those found for the female OA group in this experiment. Deligianni et al. (1991) found the strength of subchondral bone (in eburnated areas of the femoral head) in individuals with Hypertrophic OA to have a mean value of approximately 14 MPa, which is in good agreement with our results for OA, where the mean value for both genders combined is 13.791 MPa.

The mean values found for the **elastic modulus** were : **OA females 666 MPa**, **OA males 1088 MPa**, and **RA females 1055 MPa**. Lotz et al. (1990), found values for normal bone to range between 78 - 1530 MPa with a mean value of 441 (SD 271) MPa. This value is slightly lower than that found in the OA female group in the present study. Martens et al. (1983) found Young's Modulus to be 900 (SD 710)

MPa in the direction of the femoral neck, but 811 (SD 604) MPa in a direction perpendicular to this. This is in agreement with the overall mean value (868 MPa) found for OA bone in the current study, but the OA males (considered separately) and RA females had higher values.

Brown and Ferguson (1980), found extremely high values for both Young's Modulus (4800 - 6900 MPa) and Compressive Strength (up to 310 MPa), in the region of the "primary trabeculation family". Their results, which are much higher than ours, may be due to the microdamage caused by testing each specimen in three different directions, to pre-yield stress.

The results found for **RA** bone in this study represent the properties of the remaining, viable bone from the femoral heads. In general, the femoral heads in this condition are diminutive and deformed, with bone cysts. The high values of strength and stiffness which were found in the RA bone were at first unexpected, because it was originally believed that this group would present a very osteoporotic picture. Sambrook et al. (1990) state that in a joint with active disease there is increased bone turnover and marked trabecular bone loss, which may be followed by local collapse of the bone. It is the author's opinion that the collapse results in densification of the bone, which is probably followed by remodelling. Furthermore, once the cartilage has been destroyed by the disease process the joint no longer has a low friction gliding interface, so the bone now has to deal with stresses it would not normally be exposed to. The densification of the bone in hypertrophic OA is part of the actual condition, but it is not known whether these changes precede the cartilage degeneration or whether they happen as a result of the cartilage degeneration.

In most studies of cancellous bone no **gender** distinction is made. However, Weaver and Chalmers (1966), found that the compressive strength of cancellous bone was lower in females than in males, (over the age of 50) in the vertebrae and

calcanea. In the OA group in this study the values of the mechanical properties of cancellous bone were always significantly lower than those of their male counterparts. The mean body mass of the female OA patients was however significantly less than in the male group, which may well have contributed to this trend. The post menopausal status of the female group may also influence this result. The Trabecular Bone Volume Fraction (TBV%) found in the subchondral bone of the female OA patients was also less than in the male group (28.33% vs 35.63%), possibly for the same reasons. However, in the region of the compressive trabeculae gender was found to have no effect on TBV% (25.86% in females vs 25.38% in males). A possible explanation for this is that in hypertrophic OA, which occurred predominantly in males, the dense subchondral bone shields the deeper compressive trabeculae.

The **relationships between apparent density and the mechanical properties** were summarised in Table 5.3. Previous studies have demonstrated that compressive strength and Elastic Modulus of cancellous bone can be expressed as power functions of density (Gibson 1985, Currey 1986, Gibson and Ashby 1988, Rice et al. 1988, Hayes 1991). In this study power law functions were also found to describe these relationships well.

For **RA bone** the relationship for strength was found to be : $\sigma_{ult} = 21.98\ \rho^{1.213}$ and Young's Modulus was related to apparent density by the following relationship $E = 1445.44\ \rho^{1.557}$. Strain Energy Density was related to apparent density $SED = 276.694\ \rho^{1.086}$. Rice et al. (1988) and Gibson (1985) concluded that both strength and modulus should be related to the apparent density squared. Results of a two-tailed t-test revealed a statistically significant difference between the exponents (1.213 vs 2 for strength) and (1.557 vs 2 for Young's Modulus), the respective p-values were $p < .0001$, and $p = .0002$.

Lotz et al. (1990), found the following relationships in their study $\sigma_{ult} = 25\ \rho^{1.8}$ and $E = 1310\ \rho^{1.4}$ for bone from normal individuals, which was tested at a slight angle to the principal architectural axis. When comparing their relationship found for **strength**

with that found for RA bone, there was a significant difference between the constant multipliers 21.98 and 25 (p=.0044), and the exponents 1.213 and 1.8 ($p < .0001$). But for the relationships between **Young's Modulus** and apparent density there was no significant difference between the relationship found by Lotz et al. and that found in the present study for RA cancellous bone.

Thus it would appear that the exponents suggested by Rice et al. (1988), and Gibson (1985) do not apply to RA cancellous bone. The relationships found in this study may provide more accurate results for cancellous bone within the apparent density range (.34 - 1.28 g/cm^3), which was found in this study.

Deligianni et al. (1991) state that Strain Energy Density (SED) should be directly proportional to apparent density, our results are in agreement with this, the exponent 1.086 found for RA bone was not significantly different from 1.

Young's Modulus and Strength are said to be linearly related (Rice et al. 1988), however this was not found to be the case for RA bone. The relationship was found to be $E = 33.343\ \sigma_{ult}^{1.207}$, the exponent 1.207 is significantly different from 1 ($p = .0012$). So these two variables are not linearly related in RA.

The relationship between SED and strength is also said to be a direct linear relationship (Linde et al. 1989). The relationship found for RA bone is in good agreement with this, $SED = 16.482\ \sigma_{ult}^{.918}$, the exponent 0.918 is not significantly different from 1.

For **OA bone** the following **general relationships** between the mechanical properties and apparent density were found: $\mathbf{\sigma_{ult} = 24.66\ \rho^{1.322}}$, $\mathbf{E = 1741.81\ \rho^{1.706}}$ and $\mathbf{SED = 294.44\ \rho^{1.201}}$. When compared to the relationships suggested by Rice et al. (1988) and Gibson (1985), there were again significant differences. Results of a

two- tailed t-test revealed a statistically significant difference between the exponents (1.322 vs 2 for strength) and (1.706 vs 2 for Young's Modulus), the respective p - values were $p < .0001$, and $p = .03$.

Lotz et al. (1990), found the following relationships in their study $\sigma_{ult} = 25\ \rho^{1.8}$ and $E = 1310\ \rho^{1.4}$ for bone from normal individuals. When comparing their relationship found for **strength** with that found for OA bone there was no difference between the constant multipliers 24.66 and 25, but there was a significant difference between the exponents 1.322 and 1.8 ($p < .0001$). For the relationships between Young's Modulus and apparent density there was a significant difference between the relationship found by Lotz et al. and that found in the present study for OA cancellous bone. The constant multipliers (1741.81 vs 1310) differed, $p < .0001$, and the exponents (1.706 vs 1.4) differed significantly, $p = .03$.

Thus it would appear that the exponents suggested by Rice et al. (1988), and Gibson (1985) do not apply to OA cancellous bone, **in general**. The relationships found in this study may provide more accurate results for cancellous bone within the apparent density range (.31 - 1.016 g/cm^3), which was found in this condition.

However, in **OA** the **cancellous bone structure**, which is not uniform throughout the femoral head was found to have a significant effect on the above mentioned relationships. An **increase in the degree of orientation of the bone structure** led to an increase in the values of the **constant multipliers** and the **exponents** when strength and Young's Modulus were related to apparent density. For a highly anisotropic cancellous bone structure the exponents increased to 1.782 for the relationship between strength and apparent density. The exponent increased to 2.375, for the relationship between Young's modulus and apparent density. So the exponents suggested by Rice et al. (1988), and Gibson (1987), are closer to those found for cancellous bone that is **anisotropic** with a columnar structure, or a

structure with parallel plates connected by thin rods. (The relevant equations are provided in table 5.3.)

As was mentioned earlier, SED was found to be linearly related to apparent density by Deligianni et al. (1991). For OA bone SED was also found to correlate with apparent density by the following relationship, SED = 294.44 $\rho^{1.201}$, the exponent 1.201 is not significantly different from 1.

Rice et al. (1988) proposed that Young's Modulus and strength would be directly, linearly related; however, this was again not found to be the case in OA. The relationship was found to be E = 34.514 $\sigma_{ult}^{1.206}$, and the exponent 1.206 differs significantly from 1 ($p = .0006$).

In the relationship between SED and strength, SED = 15.67 $\sigma_{ult}^{0.916}$, the exponent 0.916 was not different from 1, supporting the finding by Linde et al. (1989), that these variables are linearly related in cancellous bone.

Bone Mineral Density proved to be a good predictor of the **apparent density.** However, it is of interest to note that the slopes of the relationships found for OA and RA female bone differed significantly ($p = .003$). This may indicate that RA cancellous bone contains less bone mineral than OA bone (in females), which may be due to the increased bone turnover rate which is believed to occur in RA. Mineralization of newly formed osteoid takes time, therefore, if the bone turnover rate is increased as was found by Bogoch et al. (1988), who studied the effects of inflammatory arthritis in an animal model, then there will be a large proportion of newly formed, less well mineralised bone. This aspect deserves further investigation using a more sensitive method of measuring bone mineral density, and comparing it to a group of normal individuals as well.

The **bone mineral density** calculated for each bone cube individually from the DEXA measurements also correlated very well with strength and Young's Modulus. For **RA,** the relationships were:

$\sigma_{ult} = 57.723\ BMD^{1.248}$, and $E = 4720.63\ BMD^{1.648}$.

For **OA** bone the general relationships were found to be:

$\sigma_{ult} = 59.16\ BMD^{1.339}$, and $E = 5714.79\ BMD^{1.781}$. However, structure was again found to have a significant effect on the relationships for Young's Modulus, resulting in an increase in the constant multipliers and the exponents as the structure became more highly anisotropic. For the equiaxed and asymmetric structures the exponent was 1.661, but it increased to 2.087 for the highly anisotropic cancellous bone (detailed equations are provided in table 5.3). DEXA worked well in the determination of BMD but it would not be well suited to in-vivo studies in the femoral head as the acetabulum covers part of the femoral head, and also DEXA gives an integral measure of cortical and cancellous bone. Other techniques such as Quantitative Computed Tomography which can measure the bone mineral density of purely cancellous bone will be very useful in in-vivo studies.

Disease (RA vs OA), was not found to have any significant effect on the **relationships** between the mechanical properties and the density measurements when these were compared for the two female groups.

The results for the **morphometric analysis** of the cancellous bone also helped to provide more insight into the bone changes associated with these two conditions.

The Trabecular Bone Volume Fractions (TBV%) found for the **subchondral bone** in these two disease conditions were:

OA female TBV = 28.33% (SD 6.02)

OA male TBV = 35.63% (SD 10.39)

RA female TBV = 40.71% (SD 8.29)

TBV% for this region is not usually provided in morphometric studies, but Whitehouse and Dyson (1974) gave an overall mean of approximately 30% for this region based on the study of two femoral heads from young individuals. This is in agreement with values found for the OA female bone, but the means for the OA male and RA female subchondral bone are definitely much greater. The OA male subchondral bone TBV% covered a wide range, from 22 % in some individuals to 53 % in other cases. This indicates that OA Hip is not necessarily associated with dense subchondral bone in all individuals. OA is a protean condition and the classification into morphological subgroups can be justified. The hypertrophic cases were mainly males and the atrophic cases were mainly females in this study. This aspect may warrant further research, because, if OA hip is due to a mechanical overuse (due to activity or increased body weight), or a mechanical abnormality, then one would expect the cancellous bone in the subchondral region to be very dense and very strong in all cases of OA, but this is not so. One also needs to determine how the density of the subchondral bone compares with **age-matched**, non-osteoarthritic individuals.

The findings of the increased TBV% in the subchondral region for the RA group may be due to the collapse of the cancellous bone.

In the region of the **compressive trabeculae** we found the following results:
TBV% was 25.86 % and 25.38 % for females and males respectively, these results are in good agreement with those found by Fazzalari et al. (1985) who found mean values of 24.5% and 23.3% in OA, in this region. In the present study Mean Trabecular Widths were found to be:

OA female MTW = 222 μm (SD 52)

OA male MTW = 204 μm (SD 20)

RA female MTW = 233 μm (SD 65)

and the Mean Widths of the Marrow Spaces were:

OA female MSW = 866 μm (SD 162)

OA male MSW = 833 μm (SD 179)

RA female MSW = 726 μm (SD 279)

Our results are in agreement with those found by Fazzalari et al. (1985) who found MTW to be 210 μm, and MSW to be approximately 710 μm for OA patients. Kawashima et al. (1991) found very similar results for normals, at a mean age of 63 they found MTW to be 213 μm and the width of the marrow spaces was 875 μm , at a mean age of 53 the trabeculae were found to be wider (247 μm) and the width of the marrow spaces was narrower, 809μm.

Thus, the morphological and qualitative abnormalities appear to occur mainly in the subchondral regions of OA and RA. However, some individuals with RA may have a very poor bone structure in the region of the principal compressive trabeculae, indicating osteoporotic changes. This is demonstrated by the large ranges associated with their results: TBV% (18.77 - 48.25%), S_V (1.87 - 4.18 mm^2/mm^3), MTW (130 - 335 μm), Marrow Space Width (393 - 1301 μm).

When multiple regression analysis was carried out using the mechanical properties as the dependent variable and apparent density plus the morphological parameters as independent variables, the morphological parameters only contributed very slightly to the strength of the relationships. Their contribution was never sufficient to be of statistical significance. This might have occurred because:

- The morphology was measured from bone immediately next to the specimens used for mechanical testing, not from the exact same cubes that were compressed.
- Stereology is subject to certain limitations (Feldkamp et al. 1989). As bone loss occurs (due to aging or disease), the plate model becomes inapplicable because the remaining bone may consist entirely of rods. This trend was seen in the current study and has also been noted in vertebral cancellous bone (Amstutz &

Sissons 1967). Even when plates are the predominant structures they are not perfectly parallel, as it is assumed in all calculations. Furthermore, evidence of plate perforation cannot be obtained from 2-D sections and would have to be determined from 3-D reconstructions.

CHAPTER 8

CONCLUSIONS AND RECOMMENDATIONS

Conclusions:

1. The **densities** (Bone Mineral and Apparent Density), and **mechanical properties** (Strength, Young's Modulus and Strain Energy Density) of cancellous bone from the principal weight bearing region of the femoral head were successfully determined for RA and OA, using the described methodology.
   - **Gender** had a significant effect on the mechanical properties and densities within the OA group. The values obtained for all the variables were always higher in males than in the females.
   - **Disease** (RA vs OA) was also found to have a significant effect on the mean values of all the variables. The values for density and the mechanical properties were always greater for the RA group than for the OA females.
2. The **relationships** between the mechanical properties and the apparent and bone mineral density were determined.
   - For the relationships between strength, Young's Modulus and apparent density, power relationships were found, but the exponents for diseased bone differed significantly from 2, the value suggested in the literature. This was only found to be the case if all the cubes were included **irrespective of their bone structure**.
   - The **structure** of the cancellous bone (which is not uniform throughout the femoral head), was found to have a **signicant effect** on the relationships between apparent density , Young's Modulus and strength. The values of the constant multipliers and the exponents of these relationships tended to increase as the structure became more anisotropic. For highly anisotropic cancellous bone,

in the region of the principal compressive trabeculae, the exponents for the relationships increased to 1.782 (for strength vs apparent density), and 2.375 (for Young's Modulus vs apparent density).

- Strain Energy Density was found to be directly related to apparent density.
- Young's Modulus and strength were always strongly related, but the relationship was not directly linear, as has been suggested in the literature.
- Neither gender, nor disease (OA vs RA) were found to affect these relationships.

3. **Bone Mineral Density** correlated very well with apparent density, and was found to be a good predictor of the mechanical properties.
   - **Disease** (OA vs RA) was found to have a significant effect on the relationship between apparent density and BMD.
4. **Morphometry** of the cancellous bone in the femoral head provided important information.
   - In **RA**, the remaining, viable bone is very dense in the subchondral region, possibly due to previous collapse and remodelling of the trabeculae.
   - In the region of the compressive trabeculae (in RA), the structure ranged from good to poor, with few, poorly connected trabeculae suggesting evidence of osteoporosis in some individuals.
   - The morphological features of the subchondral bone in **OA** varied from very dense, with well connected trabeculae, to low density bone with poorly connected trabeculae. These features were found to coincide with the sub-groups of OA Hip as determined radiographically, based on the features noted by Solomon (1984), ie. Hypertrophic and Atrophic OA Hip.
   - There was also a third group of individuals who had bone of intermediate density, with well connected trabeculae in the subchondral region, but this group did not fit into either of the sub-categories described by Solomon.
   - In the region of the compressive trabeculae the morphometry in OA was found to be in agreement with the values given in the literature.

5. It is hoped that the information obtained in this study, regarding disease specific bone properties and morphology will be of benefit to clinicians and bioengineers involved in bone research and endoprosthesis design. Qualitative interpretation of the results may be useful for clinicians, while bioengineers may be interested in the quantitative aspects of our findings.

Recommendations:

- A study using the methodology and statistical analyses applied in this work should be applied to bone from normal, age-matched individuals so that one can determine how the values found in RA and OA differ from normals. This can be done by using fresh cadaveric specimens (as long as the cadavers have been screened to exclude any bone pathology).

- The fact that RA cancellous bone may be less well mineralised than bone in OA individuals is important. It may well be that the degree of mineralization in both these conditions differs from normals. This aspect deserves further investigation using a more sensitive technique to measure the bone mineral content of actual bone tissue.

- To gain insight into the course of events that occur in RA, as well as the course of events that occur in the later stages of OA it would be necessary to do a longitudinal study using a non-invasive technique such as Quantitative Computed Tomography. Such a study would also show whether the subgroups found in OA Hip are actual morphological subgroups, or whether they are different steps in a a long process of joint degeneration.

- The possible existence of different morphological groups of coxarthrosis requires further investigation. There are a number of factors which can

contribute to the development of these different groups. The results of a thorough investigation would also clarify aetiological factors.

- If morphometric studies are to be carried out it is recommended that this be done on the actual bone specimens that are tested for mechanical properties. A non-destructive technique such as High Resolution Computed Tomography would be of great benefit. This technique allows the determination of three dimensional information such as the degree of anisotropy and connectivity, as well as trabecular thickness and spacing. However, if thin histological sections are to be used for image analysis, then the von Kossa Stain is highly recommended. Although this staining technique is very tedious, it is well worth the extra effort.

APPENDIX A

BONE REMODELLING PHYSIOLOGY AND THE EFFECTS OF RA

The human skeleton serves as a structural framework as well as a reservoir for the body's calcium, magnesium and phosphorus. In fulfilling its metabolic and structural roles the skeleton depends on the osteoclastic and osteoblastic cell lineages, certain endocrine hormones as well as local mediators known as cytokines. It is believed that bone remodelling responds to some "time averaged value of typical repeated peak strains", that enter or exceed the "Minimum Effective Strain" range (Frost 1990). Most pathological changes of bone are related to an imbalance between the processes of bone resorption and bone formation. Since both Osteoarthritis of the hip and Rheumatoid Arthritis involve bone changes, it is important to gain an understanding of the physiological factors involved and the effects they have on the two cell lineages responsible for bone remodelling.

Osteoclastic Cells:

These cells are most likely derived from migrating monocytes of the macrophage type. They are responsible for the resorption of bone during remodelling. Osteoclasts are large multinucleated cells formed by the fusion of a number of mononuclear cells (Raisz and Rodan 1990). Osteoclasts appear to be 20-40 times more efficient (per nucleus) at removing bone than osteoblasts are at forming bone. Osteoclasts can only resorb mineralized bone, not demineralized bone. They have a large amount of ruffled plasma membrane, surrounded by a clear zone, which attaches to the resorption surface and may act as a very large, confined extracellular lysosomal space. Bone resorption is associated with inflammation in R.A.

Osteoblastic Cells:

These are most likely derived from osteoprogenitor cells, which are present in a quiescent state and become activated when they are required for bone remodelling. When they become activated they become preosteoblasts, which proliferate and differentiate to become osteoblasts (Raisz and Rodan 1990). Osteoblasts actively synthesize and secrete the bone matrix. They are cuboidal cells organized in a layer over the matrix they have secreted. Ultrastructural examination of these cells has revealed cytoplasmic microtubules, tight cell junctions and numerous radially directed cell processes containing microfilaments. It is thus believed that cell-to-cell communication is possible. Some of the osteoblasts become embedded in the matrix they produce, they become trapped in lacunae and are known as osteocytes. Quiescent osteoblasts (which have completed matrix production), may also be present in the form of bone lining cells.

Bone Remodelling:

In cancellous bone the following process occurs:

Osteoclasts erode the surface to form scalloped irregular bays known as Howships Lacunae. The filling of which is initiated by the formation of a cement line, which is a layer of collagen free connective tissue. New bone is secreted by osteoblasts as osteoid, which mineralizes after a lag time of about 10 days. The calcification rate is about 0.7 μm/day. The term osteon thus refers to the unit of bone formed by this local remodelling process (Kragstrup 1985).

Biochemical Mechanisms involved in Bone Physiology:

The main endocrine hormones which need to be considered in bone physiology are Parathyroid Hormone, Calcitriol and Calcitonin.

1. Parathyroid Hormone (PTH):

PTH levels increase in response to a calcium deficit, acting to maintain serum and tissue Ca levels. PTH causes an increase in the number and activity of osteoclasts, probably by acting on osteoclast precursor cells because mature osteoclasts do not have PTH receptors on their cell membranes. The end result is an increase in bone resorption and a decrease in bone formation (Raisz and Rodan 1990).

2. Calcitriol:

This is a potent stimulator of bone resorption, the levels of this hormone also increase in response to calcium or phosphate deficits. Again, no receptors for this hormone have been found on the osteoclastic cell membrane, the end result is however that it increases bone resorption and inhibits bone formation.

3. Calcitonin:

This hormone causes the osteoclasts to lose their ruffled border, and move away from the resorption surface, resulting in a rapid decrease in bone resorption, but this inhibitory action does not persist for very long (Raisz and Rodan 1990).

Although these hormones control the metabolic processes of bone, the actual coupling of bone formation and resorption is believed to be mediated locally, by growth factors and cytokines.

Cytokines:

The term cytokine identifies soluble cell products that can modulate or influence the activity of other cells. They are peptides, secreted from a variety of activated inflammatory cells. In pathologic conditions it is believed that the production of inappropriate cytokines or alterations in the amounts or temporal sequencing of their release, may result in abnormalities of connective tissue remodelling or disregulation of cell proliferation. There is probably a degree of redundancy in the mechanisms by which cytokines act; a specific cellular response probably requires the integration of a number of signalling pathways. These are a few examples of cytokines:

Interleukin-1: This is a product of the immune cells, it stimulates Prostaglandin E2

synthesis in bone cells, and generally results in bone resorption. (It is believed that it may / may not lead to increased bone formation.)

Tumour Necrosis Factor: This also stimulates Prostaglandin E2 production and inhibits collagen synthesis.

Insulin-like Growth Factor II: Can increase osteoblast proliferation and differentiation and stimulate collagen synthesis.

The list of known cytokines is growing rapidly. In Rheumatoid Arthritis the inflammatory activity results in the production of a variety of cytokines, these can be seen in the table below:

Table A: Cytokines found in Rheumatoid Arthritis (from Cush and Lipsky 1991)

Cytokine	Possible cellular source	Sites of detection	Cellular Targets
IL-1	Mo, MP, FB, EC	Plasma, Syn Fluid, Syn Tissue	Fibroblasts, chondrocytes, osteoclasts, T & B cells, endothelial cells.
IL-2	TL	Syn Fluid, Syn Tissue	Macrophages, T & B cells
IL-6	TL,MP, FB, BL	Serum, Syn Fluid, Syn Tissue	Fibroblasts, T & B cells
IL-8	MP, EC, FB	Syn Fluid, Syn Tissue	T cells
TNF	TL, Mo, MP	Serum, Syn Fluid, Syn Tissue	Chondrocytes, Fibroblasts, T & B cells, osteoclasts, endothelial cells
IFN	TL	Serum, Syn Fluid, Syn Tissue	Fibrobasts, endothelial cells, macrophages, T & B cells
GM-CSF	FB, EC, TL	Syn Fluid, Syn Tissue	Macrophages, edothelial cells
Macrophage Colony Stimulating Factor	FB, EC, Mo, MP	Syn Fluid	Macrophages
Epidermal Growth Factor	MP, SV	Syn Fluid	Fibroblasts, osteoclasts, endothelial cells
FGF	Plt, MP, EC	Syn Tissue	Fibroblasts, endothelial cells
Insulin-like Growth Factor	MP	Syn Fluid	Fibroblasts

Mo = monocyte, MP = macrophage, FB = fibroblast, EC = endothelial cell, TL = T Lymphocyte, BL = B Lymphocyte, SV = synoviocyte, Plt = platelets, Syn = synovial.

It is also known that with the onset of RA the patient's PTH levels increase, this hormone is known to amplify the bone resorptive actions of Interleukin-1 and Prostaglandin E2. Interleukin -1 and Prostaglandin E2 are also known to be produced in excess in RA Another factor is, that macrophages in the involved joints synthesize calcitriol. Thus the interaction of PTH, Calcitriol and cytokines can very quickly lead to a picture of periarticular osteoporosis. To make matters worse, calcitonin levels are lower in both males and females suffering from RA (Weisman 1986).

APPENDIX B

PATIENT HISTORY PROFORMA

NAME: _____

HOSPITAL NUMBER: _____

CONDITION:	RA	OA HIP
SEX:	MALE	FEMALE
SIDE:	LEFT	RIGHT

AGE: _____

RACE: _____

BODY MASS: _____ kg

OCCUPATION: _____

ACTIVITY LEVEL: _____

MEDICAL DETAILS:

Relevant Medical History: _____

_____

Relevant Surgical History: _____

_____

Medication: _____

_____

APPENDIX C

PRELIMINARY EXPERIMENT TO DETERMINE THE RELATIONSHIP BETWEEN BONE MINERAL DENSITY AND ULTIMATE STRENGTH

It has been suggested that, if a relationship exists between the BMD and ultimate stress of the bone cubes, then this relationship can be used to predict the strength of the cube prior to testing. In this way one can predict 50% of ultimate stress, which is a safe stress level to use in non-destructive, repetitive loading of cancellous bone. According to Linde et al.(1985), steady state is reached by compression to 50% of expected ultimate strength after five compression cycles with intervals not exceeding 2 minutes. This **improves the accuracy of stiffness measurements** in cancellous bone.

Materials and Methods:

Because the cancellous bone from femoral heads was in great demand (by the Bone Bank), it was not possible to use many femoral heads, and only five heads were used for this experiment.

Fem.Head 1: Mrs R - AVN, Right THR, age 57.

Fem.Head 2: Mr M - O.A., Left THR, age 52.

Fem.Head 3: Mrs G - R.A., Right THR, age 45.

Fem.Head 4: Mr W - O.A., Right THR, age 73.

Fem.Head 5: Mrs G - O.A., Right THR, age 79.

(The parts of femoral heads 2-5 that would be used in the main experiment were not used, but were kept frozen, only cancellous bone which would not have been used in the main experiment was sacrificed for this preliminary experiment. However, all the viable bone from femoral head 1 was used, because this patient had avascular necrosis of her femoral head, a condition not included in the main experiment.)

Bone cubes were fabricated in the normal way (section 4.3). On the following day the BMC of the cubes was measured (section 4.4) with a Hologic QDR 1000 X-Ray Bone Densitometer. The results of these measures were entered into a spreadsheet programme to determine the Bone Mineral Density, since the true volumes of the cubes were determined previously. On the following day the bones were compressed to failure. An Instron Universal Testing Instrument was used. The deformation rate was 0.51 mm/min. The Strength of each cube was calculated from its load deformation curve.

Table C: Results obtained from the preliminary experiment.

Cube No.	BMD (g/cc)	Strength (MPa)	Cube No.	BMD (g/cc)	Strength (MPa)
1	0.25	10.538	26	0.30	9.095
2	0.19	4.481	27	0.24	3.915
3	0.26	9.218	28	0.26	7.416
4	0.11	1.836	29	0.17	5.668
5	0.17	3.572	30	0.28	8.844
6	0.45	14.434	31	0.24	5.368
7	0.22	4.652	32	0.14	2.475
8	0.34	7.227	33	0.06	1.129
9	0.24	5.103	34	0.27	9.294
10	0.16	2.662	35	0.21	6.682
11	0.43	18.279	36	0.27	8.754
12	0.49	20.224	37	0.10	1.989
13	0.53	27.053	38	0.20	5.636
14	0.32	12.978	39	0.25	6.029
15	0.27	10.353	40	0.17	5.469
16	0.39	19.541	41	0.28	6.738
17	0.30	9.607	42	0.22	6.563
18	0.42	11.173	43	0.22	5.868
19	0.24	6.863	44	0.18	2.992
20	0.18	3.082	45	0.22	5.001
21	0.45	12.543	46	0.27	9.345
22	0.24	5.967	47	0.21	5.938
23	0.30	11.975	48	0.21	6.055
24	0.42	18.829	49	0.18	4.335
25	0.27	7.672	50	0.16	2.498

The data was analysed using Statsgraphics version 5 (Statistical Graphics

Corporation), and a power-law relationship was found to have the strongest fit. The equation relating BMD determined by DEXA, to ultimate strength was:

$$\sigma_{ult} = 55.149 \text{ (BMD)}^{1.467}$$

where: BMD is the bone mineral density in (g/cm^3)

($R^2 = 0.88$, Correlation Coefficient = 0.94)

APPENDIX D

METHOD FOR THE PREPARATION OF UNDECALCIFIED CANCELLOUS BONE MICROSCOPE SLIDES

Embedding of the bone

The blocks of cancellous bone were fixed in 100% alchohol for 10 days. The alcohol was renewed daily. After the 10 days, the bone was impregnated with methylmethacrylate (MMA). This step involved placing the bone in a container of MMA under vacuum, this was repeated four times, each time with fresh MMA, and for an increased duration. The containers were then left out in the open overnight, and the next day they were again placed under vacuum for 3 hours. Thereafter the bone blocks were correctly positioned in the containers, and the lids applied. The glass bottles containing the MMA and bone were then incubated at 37°C for 48 hours to allow the MMA to polymerize. The glass bottles were then shattered, leaving small MMA / bone composites which could be sectioned on the Jung Microtome.

Once all the necessary sections had been cut, the next stage of preparing the slides was begun. The 10 μm thick sections were soaked in 70% ethanol and mounted on glass slides using HAUPTS (a gelatine based substance), they were allowed to dry overnight (under compression). The following day the slides were soaked in benzene to disolve away the excess MMA. The slides were then rehydrated, and stained with 0.25% aqueous Toluidine Blue (for 2 minutes) and then soaked in distilled water to remove excess stain (for 2 minutes). The slides were then allowed to air dry. Each slide was then dipped in Xylene and the coverslips were affixed with DPX mountant. This method was used for all the slides used for image analysis.

For the photographs that are included in Chapter 6, the von Kossa Stain was used. This stains mineral salts black and osteoid and soft tissue shades of blue. The following method was found to be very satisfactory.

Modified von Kossa Method (for undecalcified bone sections):

1. Hydrate the sections and thoroughly rinse them in distilled water.
2. Impregnate them in 2% aqueous silver nitrate, in the dark. 30 min
3. Rinse in distilled water (3 changes).
4. Reduce with 0.5% aqueous Hydroquinone. 1/2 - 1min
5. Rinse in distilled water.
6. Tone in 0.02% aqueous Gold Chloride. 10 sec
7. Rinse in distilled water.
8. Fix in 2% aqueous Sodium Thiosulphate. 2 min
9. Rinse in distilled water.
10. Counterstain in 0.1% aqueous Methylene Blue. 25-30 sec
11. Rinse in distilled water.
12. Dehydrate, clear in Xylol, apply coverslip.

APPENDIX E

PROCEDURE USED FOR IMAGE ANALYSIS

This is a list of the steps that were included in the task list followed, using the Joyce Loebl Image Analysis System.

- Load Environment - calibration
  - frame for the reference area
- Capture
- Define Table - Invert the image
- Frame display
- Pointset - determines the area within which measurements will be made
- Threshold - automated histogram
- Binary Operations
- Image based ops - open (2x)
  - close (2x)
- Edit - draw / erase / fill objects
- Measure
  - detected area
  - frame area
  - object measurements - areas and perimeters

Go to the Results program:

- Manipulate data files - select data file
- List data - measures
- Statistics - Get statistics (change expressions as required)
- Run Statistics - to get total values.

Note: "Opening" is an erosion process, followed by a dilation of the same amount. "Closing" is a dilation process followed by an erosion of the same amount.

Erosion results in the removal of small objects, dilation results in the filling of small defects. So these steps are used to "clean" the image.

Table F1 Results for the Female OA Group.

Case Number	Age (yrs)	Mass(kg)	Side	Block	Structure	BMD (g/cc)	App.Dens (g/cc)	Strength (MPa)	Youngs Mod (MPa)	Strain Energy (kJ/m³)
Case 1	74	73	L	1	1	0.36	0.60	12.679	685	206
				2	2	0.36	0.55	13.203	660	232
				3	2	0.34	0.55	12.821	777	162
				4	3	0.31	0.54	13.473	929	187
				5	2	0.36	0.56	7.620	391	82
				6	2	0.30	0.47	6.268	246	93
				7	2	0.22	0.35	4.877	191	76
Case 2	72	76	R	1	1	0.22	0.54	7.717	376	109
				2	1	0.24	0.57	7.879	685	59
				3	2	0.34	0.67	12.855	459	225
				4	3	0.34	0.70	13.576	1181	109
				5	2	0.27	0.65	6.084	369	71
				6	2	0.22	0.50	7.531	837	63
Case 3	79	62	R	1	2	0.34	0.62	10.281	857	123
				2	2	0.24	0.43	9.008	346	161
				3	3	0.22	0.40	9.094	551	122
				5	1	0.24	0.50	7.214	390	94
				6	2	0.12	0.32	5.477	169	95
				7	3	0.18	0.44	7.776	457	113
Case 4	72	64	R	1	2	0.35	0.61	15.208	950	170
				2	2	0.35	0.58	12.815	1282	138
				3	3	0.34	0.59	13.509	675	238
				6	2	0.32	0.60	11.819	563	184
				7	2	0.31	0.54	7.878	525	75
				8	3	0.22	0.41	5.246	238	83
Case 5	65	74	R	1	2	0.45	0.75	17.014	895	280
				2	2	0.42	0.73	19.429	1050	263
				3	3	0.38	0.72	23.237	1499	249
				4	3	0.35	0.74	24.759	1011	354
				5	2	0.35	0.88	16.173	951	282
				6	2	0.32	0.75	16.043	844	263
				7	3	0.33	0.71	16.500	767	254
Case 6	77	57		1	2	0.37	0.82	13.202	1100	97
				2	2	0.28	0.81	12.242	942	132

Table F1 (continued)

Case Number	Age (yrs)	Mass(kg)	Side	Block	Structure	BMD (g/cc)	App.Dens (g/cc)	Strength (MPa)	Youngs Mod (MPa)	Strain Energy (kJ/m³)
				3	2	0.24	0.68	9.195	525	85
				4	2	0.24	0.43	10.873	725	110
				7	2	0.22	0.36	6.911	446	71
Case 7	69	74	R	1	2	0.26	0.55	8.348	439	99
				2	2	0.21	0.41	9.171	459	153
				3	3	0.23	0.47	8.037	731	103
				5	2	0.32	0.69	12.827	583	234
Case 8	57	47	R	2	2	0.18	0.38	5.363	268	60
				3	2	0.18	0.31	4.901	200	82
				4	3	0.22	0.47	7.815	381	124
				5	2	0.18	0.35	5.783	246	65
				6	3	0.20	0.38	4.607	249	51
Case 9	68	61	R	1	2	0.24	0.52	11.345	291	261
				2	2	0.25	0.52	10.356	314	241
				3	2	0.27	0.57	12.716	462	234
				4	3	0.29	0.51	13.765	551	268
				6	2	0.30	0.56	8.930	638	107
				7	2	0.24	0.69	14.604	811	235
Case 10	72	55	L	1	2	0.41	0.77	22.799	1303	347
				2	2	0.37	0.70	21.768	1674	246
				4	3	0.39	0.61	15.982	940	183
				5	2	0.47	0.79	22.185	1849	198
				7	3	0.24	0.50	7.917	360	112
Case 11	58	48	R	1	1	0.37	0.69	17.078	1423	180
				2	1	0.41	0.68	15.415	934	211
				3	2	0.41	0.74	19.292	1072	249
				4	3	0.36	0.62	16.176	558	268
				5	1	0.39	0.80	15.436	718	269
				6	1	0.32	0.70	11.968	584	188
				7	2	0.24	0.47	6.969	436	84
				8	3	0.16	0.34	4.515	148	82
Case 12	60	65	R	1	1	0.3	0.67	10.465	436	199
				2	1	0.31	0.59	13.311	783	173
				3	2	0.32	0.53	12.149	675	153
				4	3	0.3	0.53	11.897	915	125

Table F1 (continued)

Case Number	Age (yrs)	Mass(kg)	Side	Block	Structure	BMD (g/cc)	App.Dens (g/cc)	Strength (MPa)	Youngs Mod (MPa)	Strain Energy (kJ/m^3)
				5	2	0.24	0.68	8.081	317	120
				6	2	0.3	0.50	7.843	327	128
				7	3	0.25	0.43	8.000	314	126

Table F2 Results for the Male OA Group.

Case Number	Age (yrs)	Mass (kg)	Side	Block	Structure	BMD (g/cc)	App.Dens (g/cc)	Strength (MPa)	Youngs Mod (MPa)	Strain Energy (kJ/m^3)
Case 13	74	70	R	1	2	0.58	1.02	26.451	1824	345
				2	2	0.48	0.90	20.594	1525	193
				3	2	0.52	0.92	22.200	1531	223
				4	2	0.51	0.82	19.461	1442	160
				5	2	0.36	0.65	9.660	805	86
				6	2	0.49	0.86	14.368	1026	141
				7	3	0.49	0.82	17.524	2503	99
Case 14	56	113	R	1	2	0.46	0.81	19.117	1738	214
				2	2	0.45	0.82	17.627	1259	221
				3	2	0.37	0.75	18.546	1855	192
				4	3	0.39	0.75	20.904	1493	221
				4+	3	0.31	0.68	17.274	960	218
				5	2	0.3	0.65	8.827	490	109
				6	2	0.33	0.66	9.867	519	128
				7	3	0.26	0.56	9.360	493	120
				8	3	0.33	0.57	12.818	916	134
Case 15	78	89	R	2	2	0.42	0.73	22.892	1761	191
				3	3	0.45	0.73	25.534	2220	172
				4	3	0.45	0.70	27.347	2104	217
				6	2	0.33	0.58	11.567	964	100
				7	2	0.31	0.60	11.009	847	95
				8	2	0.3	0.48	11.010	786	90
Case 16	83	65	R	1	1	0.46	0.91	21.509	1024	391
				2	1	0.32	0.58	13.552	1042	152
				3	2	0.32	0.54	11.027	735	104
				4	3	0.28	0.39	10.362	740	105
				4+	3	0.2	0.40	9.837	492	110
				5	1	0.31	0.69	14.266	984	128
				6	1	0.3	0.50	10.288	686	121
				7	3	0.28	0.47	7.158	421	68
				8	3	0.18	0.37	5.958	238	94
Case 17	58	110	R	1	1	0.36	0.79	16.712	643	516
				2	2	0.38	0.73	23.252	1107	373
				3	3	0.40	0.76	25.619	1314	392

Table F2 (continued)

Case Number	Age (yrs)	Mass (kg)	Side	Block	Structure	BMD (g/cc)	App.Dens (g/cc)	Strength (MPa)	Youngs Mod (MPa)	Strain Energy (kJ/m^3)
Case 18	52	89	L	2	1	0.41	0.87	18.949	1458	179
				3	2	0.45	0.89	24.035	1923	203
				5	1	0.35	0.84	12.312	560	208
				6	1	0.37	0.83	15.490	794	221
				7	2	0.43	0.88	21.699	1447	216
				8	3	0.41	0.78	20.432	1635	173
Case 19	52	92	L	2	2	0.44	0.82	20.990	1999	295
				3	2	0.42	0.71	19.104	1318	200
				4	3	0.45	0.77	20.545	1868	238
				6	2	0.45	0.87	21.851	1150	305
				7	2	0.45	0.89	22.213	1388	315
				8	3	0.36	0.65	16.125	1402	181
Case 20	71	104	L	1	1	0.41	0.71	18.349	941	295
				2	1	0.35	0.61	18.062	1062	219
				3	2	0.34	0.57	18.129	980	217
				4	3	0.38	0.62	18.483	973	231
Case 21	67	94	R	1	1	0.33	0.54	13.693	637	160
				2	1	0.33	0.61	16.374	819	216
				3	2	0.26	0.53	12.651	744	136
				4	3	0.26	0.46	10.230	284	217
				5	1	0.41	0.93	18.210	1012	201
				6	2	0.39	0.71	13.241	679	209
				7	3	0.34	0.62	11.867	742	144
				8	3	0.24	0.43	8.101	463	114
Case 22	73	80	R	1	1	0.25	0.49	10.027	573	127
				2	1	0.31	0.55	12.324	986	132
				3	3	0.34	0.57	17.141	1106	195
				4	3	0.37	0.68	22.976	938	336
				5	1	0.29	0.57	11.323	944	143
				6	2	0.31	0.54	11.731	782	145
				7	3	0.33	0.60	15.039	792	186
				8	3	0.30	0.53	12.678	939	135

Table F3 Results for the Female RA Group.

Case Number	Age	Mass (kg)	Side	Block	Structure	BMD (g/cc)	App.Dens (g/cc)	Strength (MPa)	Youngs Mod (MPa)	Strain Energy (kJ/m^3)
Case 23	45	65	R	2	2	0.37	0.84	13.502	1125	144
				3	2	0.39	0.79	20.238	1349	202
				4	3	0.37	0.74	22.493	1551	198
				6	3	0.43	0.88	22.027	1762	175
				7	3	0.36	0.72	16.449	1567	106
Case 24	45	65	R	1	2	0.43	0.87	16.794	1158	342
				2	2	0.40	0.74	15.646	1304	162
				6	2	0.48	0.78	16.997	1133	278
				7	2	0.45	0.75	15.803	1505	143
Case 25	41	69	L	2	2	0.50	1.11	16.467	1098	366
				3	2	0.48	0.92	21.085	1240	261
				6	2	0.50	1.04	19.068	887	298
				7	2	0.43	0.96	15.401	811	245
Case 26	33	75	L	1	2	0.56	1.28	29.598	1644	339
				2	2	0.35	0.88	17.324	1118	203
				3	2	0.34	0.67	16.168	1244	202
				4	3	0.31	0.59	15.049	752	224
				6	2	0.45	1.13	19.214	1164	251
				7	2	0.32	0.83	15.375	394	374
Case 27	36	35	L	1	2	0.31	0.66	14.088	587	216
				2	2	0.24	0.49	10.065	839	85
				3	3	0.22	0.44	9.228	461	153
				6	2	0.20	0.44	7.799	380	101
				7	2	0.18	0.34	4.368	218	74
Case 28	63	51	L	1	2	0.39	0.71	14.532	765	212
				2	2	0.29	0.64	13.816	564	267
				3	2	0.28	0.57	14.417	534	298
Case 29	59	75	L	2	2	0.32	0.56	15.322	851	206
				3	3	0.28	0.50	16.254	1204	190
				6	2	0.27	0.64	9.693	388	167
				7	3	0.24	0.60	10.544	430	187
Case 30	64	62	L	1	2	0.47	1.00	22.578	1254	289
				2	2	0.32	0.68	20.614	959	254
				3	2	0.34	0.73	22.895	1526	204

Table F3 (continued)

Case Number	Age	Mass (kg)	Side	Block	Structure	BMD (g/cc)	App.Dens (g/cc)	Strength (MPa)	Youngs Mod (MPa)	Strain Energy (kJ/m^3)
				5	2	0.36	0.76	12.645	1012	113
				6	2	0.22	0.43	6.978	297	103
Case 31	78	55	R	4	3	0.54	0.92	28.497	1900	319
				5	2	0.68	1.28	30.788	2123	585
				6	2	0.51	1.01	18.864	1572	189
				7	3	0.38	0.61	14.974	1033	168
Case 32	44	100	R	2	2	0.53	1.04	21.590	1489	301
				3	2	0.4	0.91	16.248	1121	209

APPENDIX G

RESULTS OF THE MORPHOMETRIC ANALYSIS

Table G1 Results for the Female OA Group.

Subchondral Region

Case Number	Trabecular Bone Volume %	Surface Area of Bone-Marrow Interface (mm^2/mm^3)	Mean Trabecular Width (microns)	Mean Trabecular Thickness (microns)
Case 1	29.32	3.51	210	165
Case 2	26.02	4.14	161	127
Case 3	25.3	3.62	177	139
Case 4	28.29	2.91	249	195
Case 5	32.47	3.73	222	174
Case 6	32.11	3.57	228	179
Case 7	16.17	2.58	158	124
Case 9	22.25	3.3	172	135
Case 10	27.23	3.12	223	175
Case 11	34.75	4.61	192	151
Case 12	37.73	5.1	188	148

Compressive Trabeculae

Case Number	Trabecular Bone Volume %	Surface Area of Bone-Marrow Interface (mm^2/mm^3)	Mean Trabecular Width (microns)	Mean Trabecular Thickness (microns)	Marrow Space Width (microns)
Case 1	25.74	2.87	218	182	837
Case 2	26.04	3.48	179	149	671
Case 3	20.19	2.61	181	151	1024
Case 4	28.20	3.03	222	185	765
Case 5	29.01	3.20	218	181	701
Case 6	17.11	2.39	172	143	1111
Case 7	26.28	2.69	236	197	902
Case 9	21.02	2.25	225	188	1123
Case 10	40.60	2.71	361	301	693
Case 11	22.12	2.78	191	159	894
Case 12	28.11	2.86	236	197	800

Table G2 Results for the Male OA Group.

Subchondral Region

Case Number	Trabecular Bone Volume %	Surface Area of Bone-Marrow Interface (mm^2/mm^3)	Mean Trabecular Width (microns)	Mean Trabecular Thickness (microns)
Case 13	53.7	4.44	315	247
Case 14	40.01	4.21	243	190
Case 15	34.51	2.84	313	246
Case 16	36.26	4.38	210	165
Case 18	32.25	3.75	220	173
Case 19	46.96	3.86	332	261
Case 20	32.8	3.58	235	185
Case 21	21.63	4.28	128	101
Case 22	22.52	4.03	143	112

Compressive Trabeculae

Case Number	Trabecular Bone Volume %	Surface Area of Bone-Marrow Interface (mm^2/mm^3)	Mean Trabecular Width (microns)	Mean Trabecular Thickness (microns)	Marrow Space Width (microns)
Case 13	33.06	4.01	198	165	529
Case 14	25.50	2.94	208	173	809
Case 15	23.67	2.60	220	184	950
Case 16	20.93	2.45	207	172	1041
Case 18	28.82	3.11	223	186	727
Case 19	27.04	3.33	193	161	724
Case 20	29.17	3.25	217	181	693
Case 21	23.13	2.64	210	175	1004
Case 22	17.14	2.62	157	131	1018

Table G3 Results for the Female RA group.

Subchondral Region

Case Number	Trabecular Bone Volume %	Surface Area of Bone-Marrow Interface (mm^2/mm^3)	Mean Trabecular Width (microns)	Mean Trabecular Thickness (microns)
Case 24	53.11	3.89	350	274
Case 26	47.07	4.91	244	191
Case 27	31.72	4.22	192	151
Case 28	30.40	3.96	195	153
Case 29	36.54	4.03	232	182
Case 30	44.35	3.49	324	254
Case 32	41.80	5.78	185	145

Compressive Trabeculae

Case Number	Trabecular Bone Volume %	Surface Area of Bone-Marrow Interface (mm^2/mm^3)	Mean Trabecular Width (microns)	Mean Trabecular Thickness (microns)	Marrow Space Width (microns)
Case 23	39.41	3.93	240	200	490
Case 24	48.25	4.18	287	239	393
Case 25	34.72	3.81	219	183	545
Case 26	19.69	3.67	130	108	697
Case 27	18.77	2.80	160	133	920
Case 28	33.26	2.39	335	279	908
Case 29	23.86	2.75	208	173	906
Case 30	25.77	1.87	322	269	1301
Case 31	33.49	3.68	218	181	575
Case 32	25.10	3.95	215	179	518

APPENDIX H

SCATTERPLOTS OF THE RAW DATA

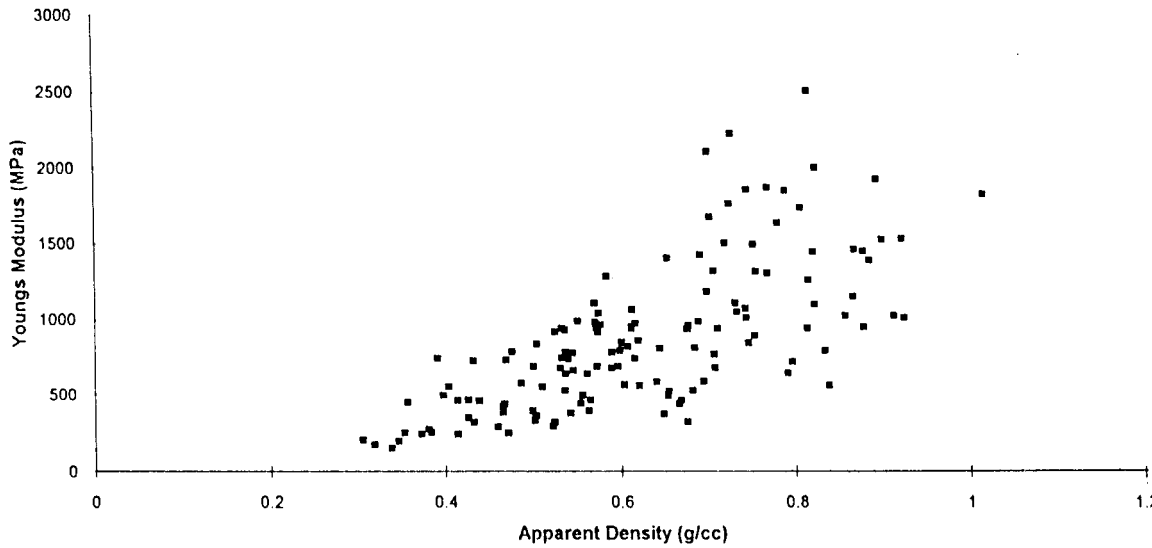

Fig. H1 Young's Modulus vs Apparent Density in OA Bone.

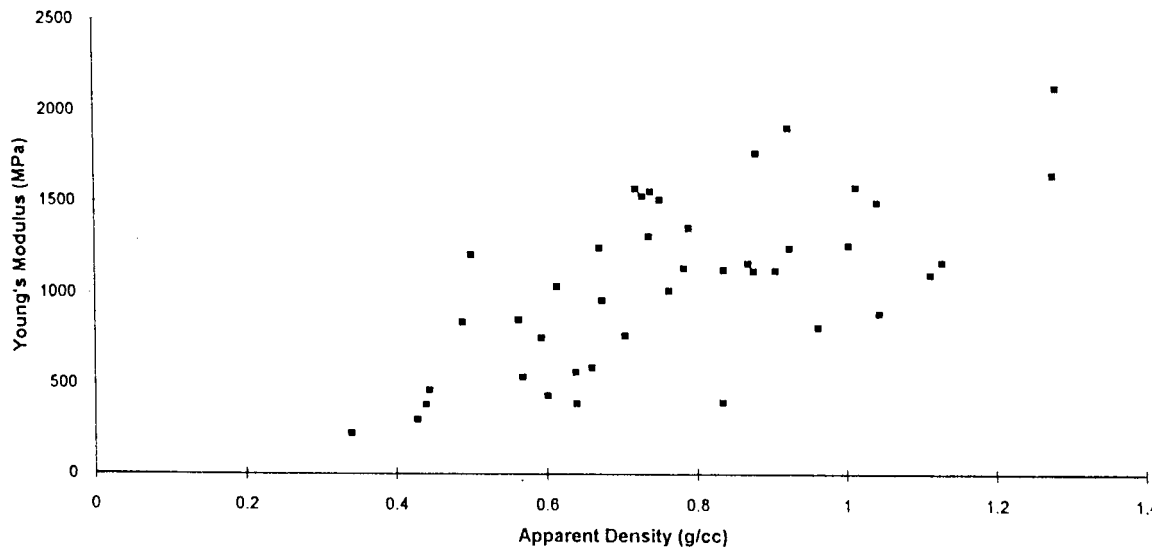

Fig. H2 Young's Modulus vs Apparent Density in RA Bone.

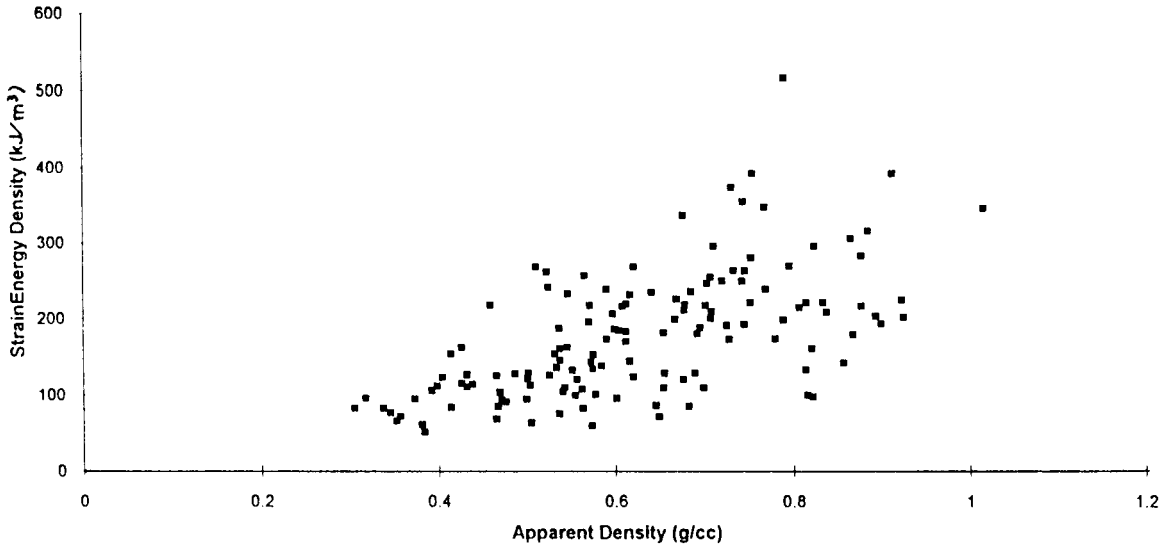

Fig. H3 Strain Energy Density vs Apparent Density in OA Bone.

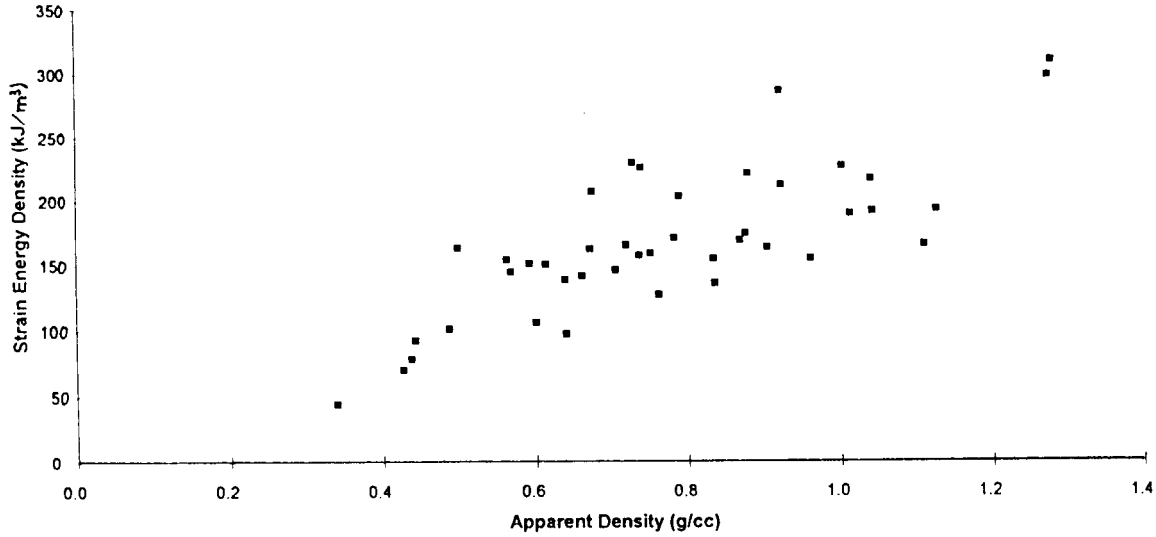

Fig. H4 Strain Energy Density vs Apparent Density in RA Bone.

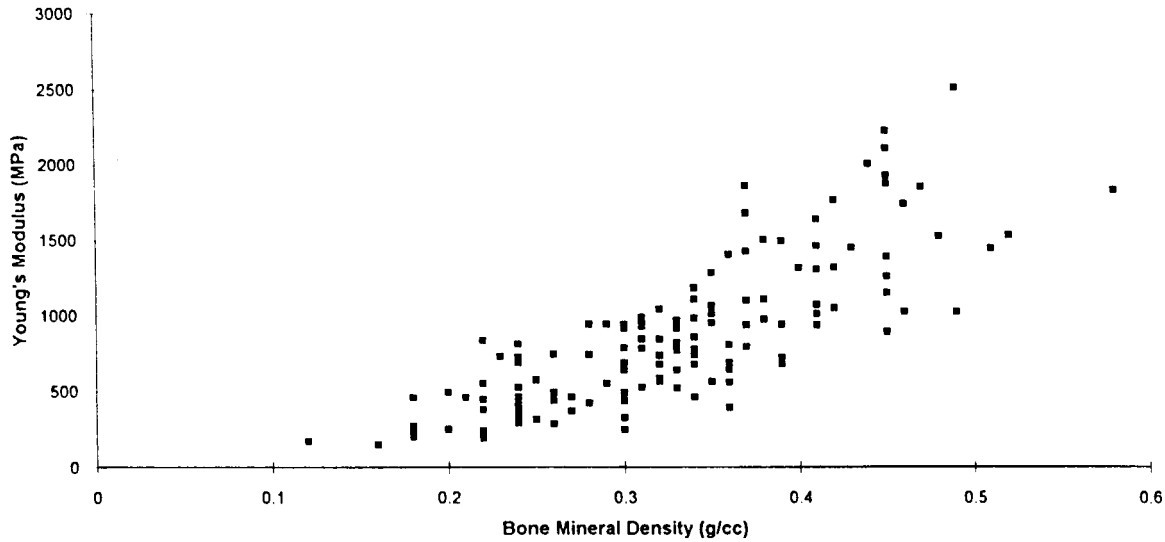

Fig. H5 Young's Modulus vs BMD in OA Bone.

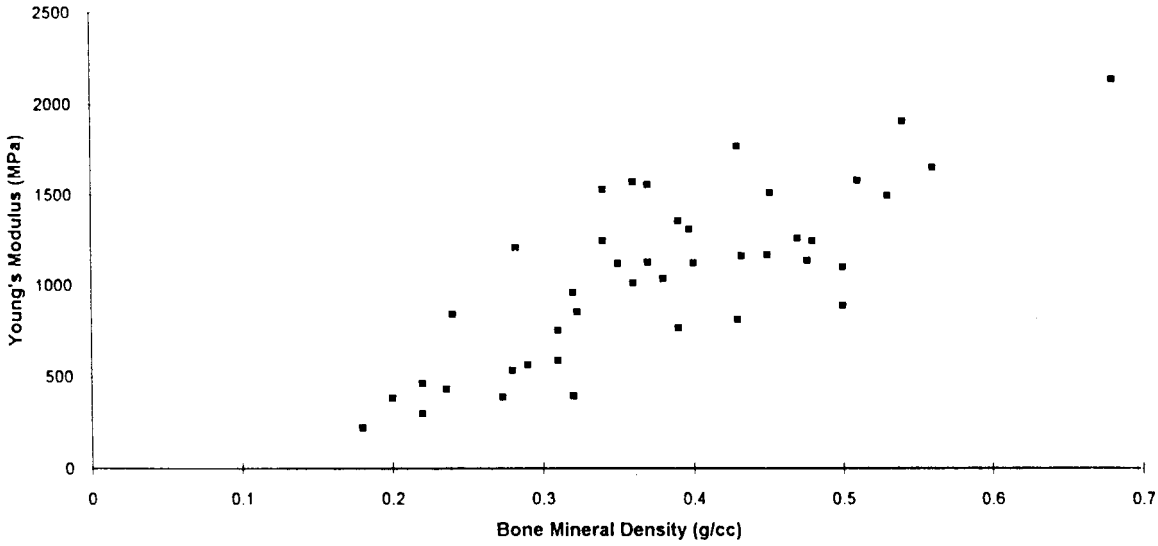

Fig. H6 Young's Modulus vs BMD in RA Bone.

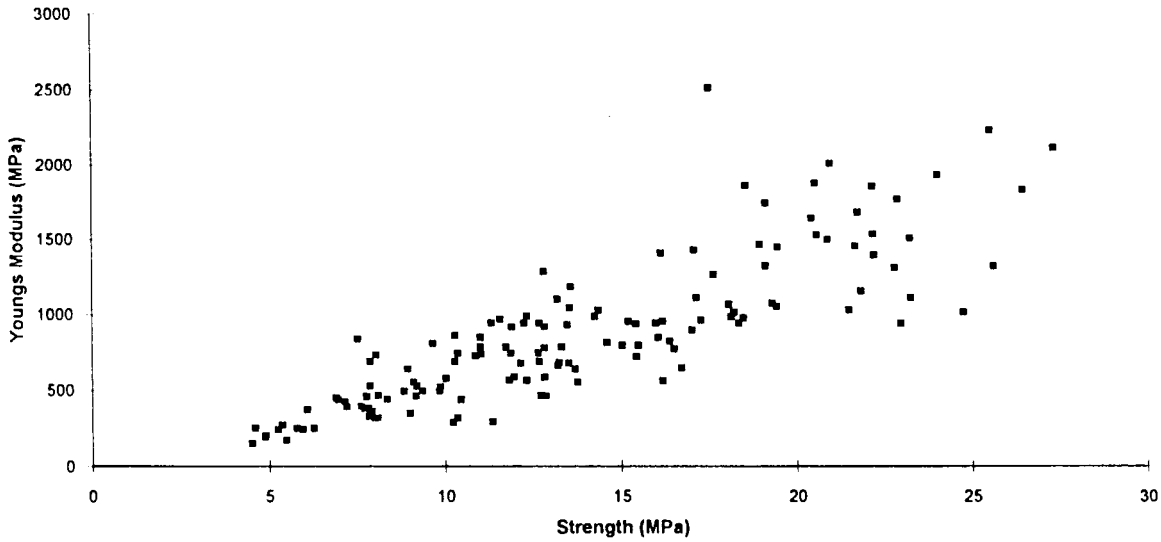

Fig. H7 Young's Modulus vs Strength in OA Bone.

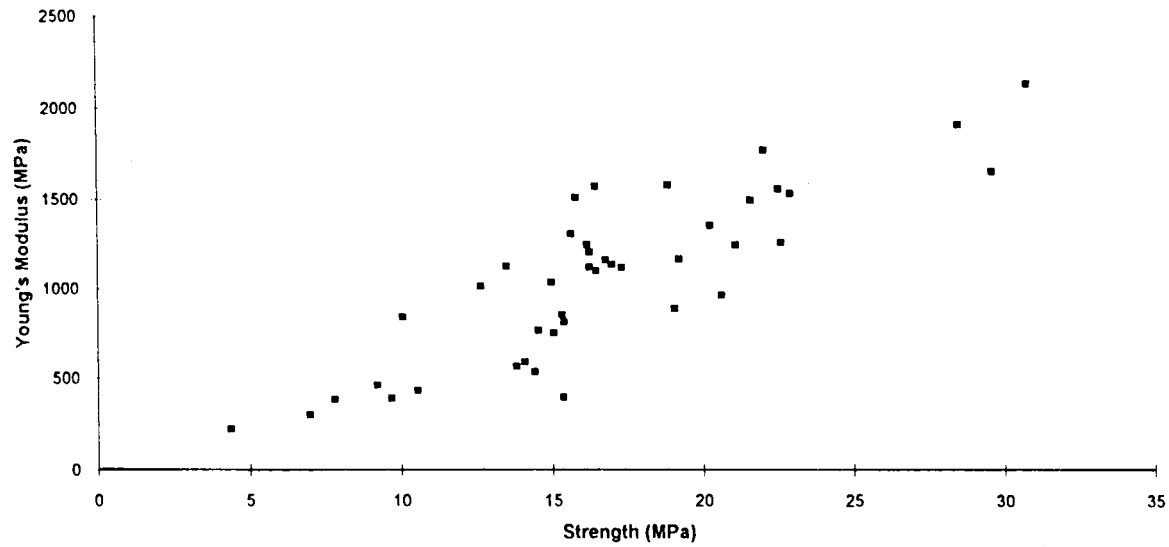

Fig. H8 Young's Modulus vs Strength in RA Bone.

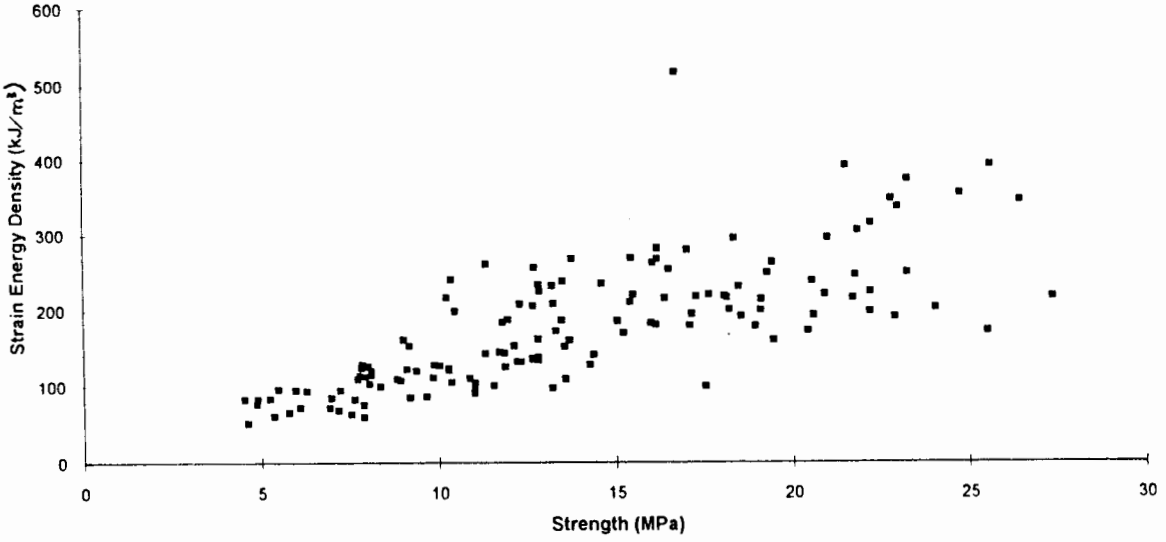

Fig. H9 Strain Energy Density vs Strength in OA Bone.

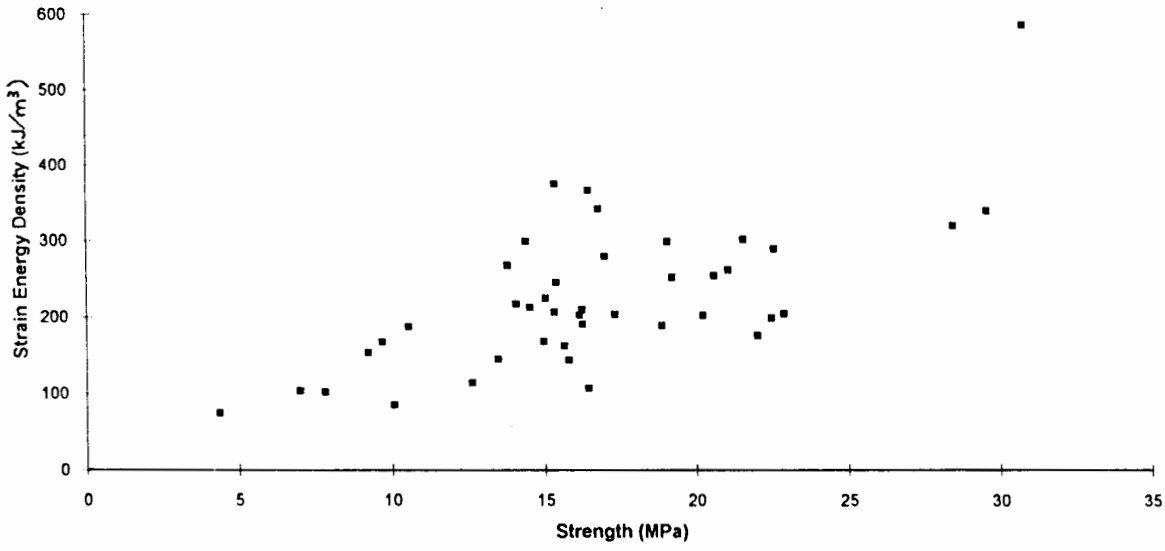

Fig. H10 Srain Energy Density vs Strength in RA Bone.

REFERENCES

AARON JE, MAKINS NB, SAGREIYA K.
1987
The microanatomy of trabecular bone loss in normal aging men and women.
Clin Orthop, 215: 260-271.

ALWAN WH, DIEPPE PA, ELSON CJ, BRADFIELD JW.
1988
Bone resorbing activity in synovial fluids in destructive osteoarthritis and rheumatoid arthritis.
Ann Rheum Dis, 47: 198-205.

AMSTUTZ HC & SISSONS HA.
1969
The structure of the vertebral spongiosa.
J Bone Joint Surg, 51-B: 540 - 550.

ARMSTRONG CG & MOW VC.
1980
Friction, lubrication and wear of synovial joints.
pp.223-232 In: OJ Goodfellow, Bullough P. eds. **Scientific Foundations of Orthopaedics and Traumatology.**
London: William and Heinemann

ASHMAN RB, CORIN JD, TURNER CH.
1987
Elastic properties of cancellous bone: Measurement by an ultrasonic technique.
J Biomech, 20: 979-986.

ASHMAN RB & RHO JY.
1988
Elastic modulus of trabecular bone material.
J Biomech, 21: 177-181.

ASKEW MJ & MOW VC.
1978
The biomechanical function of the collagen ultrastructure of articular cartilage.
J Biomech Eng, 1: 105

BENTLEY G.
1987
Pathogenesis of Osteoarthritis.
pp.93-113 In: Hughes SPF, Benson MK, Colton CL. eds. **The principles and practise of Muskuloskeletal Surgery.**
Edinburgh: Churchill Livingstone

BERGOT C, LAVAL-JEANTET AM, PRETEUX F, MEUNIER A.
1988
Measurement of anisotropic vertebral trabecular bone loss during aging by quantitative image analysis.
Calcif Tiss Int, 43: 143-149.

BOGOCH E, GSCHWEND N, BOGOCH B, RAHN B, PERREN S.
1988
Juxta-articular bone loss in experimental inflammatory arthritis.
J Orthop Res, 6: 648-656.

BREAR K, CURREY JD, RAINES S, SMITH KJ.
1988
Density and temperature effects on some mechanical properties of cancellous bone.
Eng Med 17: 163-167.

BROWN TD & FERGUSON AB.
1980
Mechanical property distributions in the cancellous bone of the human proximal femur.
Acta Orthop Scand, 51: 429-437.

CARTER DR & HAYES WC.
1976
Bone compressive strength: The influence of density and strain rate.
Science, 194: 1174-1175.

CARTER DR, HAYES WC.
1977
The compressive behaviour of bone as a two-phase porous structure.
J Bone Joint Surg, 59-A: 954-962.

CHAYES F.
1965
Determination of relative volume by sectional analysis.
Lab Invest, 14: 249-257.

CIARELLI MJ, GOLDSTEIN SA, KUHN JL, CODY DD, BROWN MB.
1991
Evaluation of orthogonal mechanical properties and density of human trabecular bone from the major metaphyseal regions with materials testing and computed tomography.
J. Orthop. Res, 9: 674-682.

COMPSTON JE, CRAWLEY EO, EVANS C, O'SULLIVAN MM.
1988
Spinal trabecular bone mineral content in patients with non-steroid treated Rheumatoid Arthritis.
Ann Rheum Dis, 47: 660-664

COMPSTON JE, MELLISH RWE, GARRAHAN NJ.
1987
Age-related changes in iliac crest trabecular microanatomic bone structure in man.
Bone, 8: 289-292.

COOPER C, POLL V, MCLAREN M, DAUNT SON, CAWLEY MID.
1988
Alterations in appendicular skeletal mass in patients with rheumatoid, psoriatic and osteoarthropathy.
Ann Rheum Dis, 47: 481-484.

COWIN SC & MEHRABADI MM.
1989
Identification of the elastic symmetry of bone and other materials.
J Biomech, 22: 503-515.

COWIN SC, VAN BUSKIRK WC, ASHMAN RB.
1987
Properties of Bone.
pp.2.1-2.27 In:Skalak R, Chien S, eds. **Handbook of Bioengineering.**
New York: Mc Graw-Hill.

CROWNINSHIELD RD, JOHNSTON RC, ANDREWS JG, BRAND RA.
1978
A biomechanical investigation of the human hip.
J Biomech, 11: 75-85.

CURREY JD.
1969
The mechanical consequences of variation in the mineral content of bone.
J Biomech, 2:1-11.

CURREY JD.
1986
Power law models for the mechanical properties of cancellous bone.
Eng Med,15: 153-154.

CUSH JJ & LIPSKY PE.
1990
Cellular basis for rheumatoid inflammation.
Clin Orthop, 265: 9-22.

DELIGIANNI DD, MISSIRLISS YF, TANNER KE, BONFIELD W.
1991
Mechanical behaviour of trabecular bone of the human femoral head in females.
J Materials Science: Materials in Medicine, 2: 168-175.

DORLAND'S ILLUSTRATED MEDICAL DICTIONARY
1981
Philadelphia: W.B. Saunders Company

EVANS FG & KING AI.
1961
Regional differences in some physical properties of human spongy bone.
pp. 19-67. In: Evans FG (ed). **Biomechanical Studies of the musculo-skeletal system.**
Illinois: Thomas Springfield.

FAZZALARI NL, DARRACOTT J, VERNON-ROBERTS B.
1985
Histomorphometric changes in the trabecular structure of a selected stress region in the femur of patients with osteoarthritis and facture of the femoral neck.
Bone, 6: 125-133.

FAZZALARI NL, VERNON-ROBERTS B, DARRACOTT J.

1987
Osteoarthritis of the hip: possible protective and causative roles of trabecular microfractures in the head of the femur.
Clin Orthop, 216: 224-233.

FELDKAMP LA, GOLDSTEIN SA, PARFITT AM, JESION G, KLEEREKOPER M.
1989
The direct examinations of three-dimensional bone architecture in-vitro by computed tomography.
J Bone Miner Res, 4: 3-11.

FROST HM.
1990
A bone modelling theory.
Anat Rec, 226: 403-413.

GALANTE J, ROSTOKER W, RAY RD.
1970
Physical properties of cancellous bone.
Calcif Tiss Res, 5: 236-246.

GIBSON LJ.
1985
The mechanical behaviour of cancellous bone.
J Biomech, 18: 317-328.

GIBSON LJ & ASHBY MF.
1988
Cancellous Bone.
pp. 316-331. In: Gibson LJ, Ashby MF (eds). **Cellular Solids: Structure and Properties.** New York: Pergamon Press.

GOLDSTEIN SA.
1987
The mechanical properties of trabecular bone: dependence on anatomic location and function.
J Biomech, 20: 1055-1061.

HAYES WC.
1991
Biomechanics of cortical and trabecular bone: Implications for assessment of fracture risk. pp. 93-142 In Van Mow C, Hayes WC. **Basic Orthopaedic Biomechanics.** New York: Raven Press.

HVID I, JENSEN NC, BUNGER C, SOLUND K, DJURHUUS JC.
1985
Bone mineral assay: its relation to the mechanical strength of cancellous bone.
Eng Med, 14: 79-83.

JOHNSTON RC & SMIDT GL.
1969
Measurement of hip joint motion during walking. Evaluation of an electrogoniometric method.
J Bone Joint Surg, 51-A: 1083-1094.

KAWASHIMA T & UHTOFF HK.
1991
Pattern of bone loss of the proximal femur: A radiologic, densitometric and histomorphometric study.
J Orthop Res, 9: 634- 640.

KRAGSTRUP J.
1985
Osteons in trabecular bone.
Danish Medical Bulletin, 32: 287-295.

LINDE F, HVID I, JENSEN N.
1985
Material properties of cancellous bone in repetitive axial loading.
Eng. Med, 14: 173-177.

LINDE F & HVID I.
1987
Stiffness behaviour of trabecular bone specimens.
J Biomech, 20: 83-89.

LINDE F & HVID I.
1989
The effect of constraint on the mechanical behaviour of trabecular bone specimens.
J Biomech, 22: 485-490.

LINDE F, HVID I, PONGSOIPETCH B.
1989
Energy absorptive properties of human trabecular bone specimens during axial compression.
J Orthop Res, 7: 432-439.

LINDE F, NORGAARD P, HVID I, ODGAARD A, SOBALLE K.
1991
Mechanical properties of trabecular bone.
Dependency on strain rate.
J Biomech, 24: 803-809.

LINDE F, HVID I, MADSEN F.
1992
The effect of specimen geometry on the mechanical behaviour of trabecular bone specimens.
J Biomech, 25: 359-368.

LOTZ JC, TOBIN N, GERHART TN, HAYES WC.
1990
Mechanical properties of trabecular bone from the proximal femur: A quantitative CT study.
J Comput Assist Tomogr, 14: 107-114.

MARTENS M, VAN AUDEKERCKE R, DELPORT P, DE MEESTER P, MULIER JC.
1983
Mechanical characteristics of cancellous bone at the upper femoral region.

J Biomech, 16: 971-983.

MELLISH RWE, O'SULLIVAN MM, GARRAHAN NJ, COMPSTON JE.
1987
Iliac crest trabecular bone mass and structure in patients with non-steroid treated rheumatoid arthritis.
Ann Rheum Dis, 46: 830-836.

MERZ WA & SCHENK RK.
1970
Quantitative structural analysis of human cancellous bone.
Acta Anat, 75: 54-66.

MURRAY MP.
1967
Gait as a total pattern of movement.
Am J Phys Med, 46: 290-333.

NORDIN M & FRANKEL VH,
1989
Biomechanics of the hip
pp. 135-151 In: Frankel VH, Nordin M. **Basic Biomechanics of the Skeletal System.**
Philadelphia: Lea and Febiger.

ODGAARD A, HVID I, LINDE F.
1989
Compressive axial strain distributions in cancellous bone specimens.
J Biomech, 22: 829-835.

ODGAARD A & LINDE F.
1991
The underestimation of Young's Modulus in compresssive testing of cancellous bone specimens.
J Biomech, 24: 691-698.

PARFITT AM, MATHEWS CHE, VILLANEUVA AR, KLEEREKOPER M, FRAME B, RAO DS.
1983
Relationships between surface, volume and thickness of iliac trabecular bone in aging and in osteoporosis.
J Clin Invest, 72: 1396-1409.

PAUWELS F.
1980
Concerning the mechanical stressing of the head of the femur and the determination of the forces acting on the regeneration tissue.
pp. 76-96 In: Pauwels F. **Biomechanics of the Locomotor Apparatus.**
Berlin: Springer-Verlag.

PUGH JW, ROSE RM, RADIN EL.
1973
A structural model for the mechanical behaviour of trabecular bone.
J Biomech, 6: 657-670.

PUGH JW, RADIN EL, ROSE RM.
1974
Quantitative studies of human subchondral cancellous bone: its relationship to the overlying cartilage.
J Bone Joint Surg, 56-A: 313-321.

RADIN EL & ROSE RM.
1986
Role of subchondral bone in the initiation and progression of cartilage damage.
Clin Orthop, 213: 34-40.

RAISZ LG & RODAN GA.
1990
Cellular basis for bone turnover.
pp. 1-39 In Avioli LV, Krane SM, eds. **Metabolic Bone Disease.**
Philadelphia: W.B. Saunders Company.

RICE JC, COWIN SC, BOWMAN JA.
1988
On the dependence of the elasticity and strength of cancellous bone on apparent density.
J Biomech, 21: 155-168.

ROH YS, DEQUERKER J, MULIER JC.
1974
Bone mass in osteoarthrosis, measured in-vivo by photon absorption.
J Bone Joint Surg, 56-A: 587-591

RYDELL NW.
1966
Forces acting on the femoral head prosthesis. A study on strain gauge supplied prostheses in living persons.
Acta Orthop Scand, Supp 88: 1-132.

SAMBROOK PN, EISMAN JA, CHAMPION GD, YEATES MG, POCOCK NA, EBERL S.
1987
Determinants of axial bone loss in Rheumatoid Arthritis.
Arthritis Rheum, 30: 721-728.

SAMBROOK PN, SHAWE D, HESP R, et al.
1990
Rapid periarticular bone loss in rheumatoid arthritis.
Arthritis Rheum, 33: 615-622.

SCHWARTZ MP & RECKER R.
1981
Comparison of surface density and volume of human iliac trabecular bone measured directly and by applied stereology.
Calcif Tiss Int, 33: 561-565.

SHARP DJ, TANNER KE, BONFIELD W.
1990
Measurement of the density of trabecular bone.

J Biomech, 23: 853-857.

SMITH JM & JEE WSS.
1983
Automated skeletal histomorphometry
pp.285-295 In: Recker RR. ed. **Bone Histomorphometry: Techniques and Interpretation.**
New York: CRC Press

SOLOMON L.
1984
Geographical and anatomical patterns of osteoarthritis.
Br J Rheum, 23: 177-180.

TOWNSEND PR, RAUX P, ROSE RM, MIEGEL RE, RADIN EL.
1975
The distribution and anisotropy of the stiffness of cancellous bone in the human patella.
J Biomech, 8: 363-367.

WEAVER JK & CHALMERS J.
1966
Cancellous bone: Its strength and changes with aging, and an evaluation of some methods for measuring its mineral content.
J Bone Joint Surg, 48-A: 289-299.

WEISMAN MH, ORTH RW, CATHERWOOD BD, MANOLAGAS SC, DEFTOS LJ.
1986
Measures of bone loss in rheumatoid arthritis.
Arch Intern Med, 146: 701-704.

WILLIAMS JL & LEWIS JL.
1982
Properties and an Anisotropic Model of Cancellous Bone from the Proximal Tibial Epiphysis.
J Biomech Eng 104: 50-56.

WHITEHOUSE WJ.
1974
The quantitative morphology of anisotropic trabecular bone.
J Microsc, 101: 153-168.

WHITEHOUSE WJ & DYSON ED.
1974
Scanning electron microscope studies of trabecular bone in the proximal end of the human femur.
J Anat, 118: 417-444.

WHITEHOUSE WJ, DYSON ED, JACKSON CK.
1971
The Scanning Electron Microscope studies of trabecular bone from a human vertebral body.
J Anat, 108: 481-496.

WILLIAMS JL & LEWIS JL.
1982
Properties and an anisotropic model of cancellous bone from the proximal tibial epiphysis.
J Biomech Eng,104: 50-56

YAMADA H.
1970
Strength tests in biological materials.
pp. 2-18 In: Evans FG. ed. **Strength of Biological Materials.**
Baltimore: Williams and Wilkins Company.